UNIVERSITY OF CALIFORNIA SAN DIEGO
SAN DIEGO STATE UNIVERSITY

Investigating ECoG Signal Acquisition And Transmission in Brain Computer Interface Applications

A dissertation submitted in partial satisfaction of the
requirements for the degree
Doctor of Philosophy

in

Engineering Sciences (Electrical and Computer Engineering)

by

Shams Al Ajrawi

Committee in charge:

University of California San Diego

Professor. Ramesh Rao , Co-Chair
Professor. William Hodgkiss
Professor. Geoff Voelker

San Diego State University

Professor. Mahasweta Sarkar , Co-Chair
Professor. Santosh Nagaraj

2021

The dissertation of Shams Al Ajrawi is approved, and it is acceptable in quality and form for publication on microfilm:

_____

_____

_____

_____
Co-Chair

_____
Co-Chair

University of California, San Diego
San Diego State University

2021

DEDICATION

For my Parents / Dhafir / Sarah / Joseph.

TABLE OF CONTENTS

LIST OF FIGURES

LIST OF TABLES

ACKNOWLEDGEMENTS

First and foremost, my greatest thanks goes to the most merciful **Allah** for all the things for which he has enriched me all my life, and without those blessings, I will not even be here.

I would like to thank those who helped me achieve this stage at the end of my graduate school career and embarked on the journey with me. First of all, my husband, Dhafir, I will not achieve this step for being one of my greatest supporters in every single activity, and for being with me during this whole process and reminding me that there is life beyond the laboratory and for being the strongest backbone of my higher education. I'm very thankful for my awesome parent, my dad, for encouraging me to become an engineer, and for having his daughter tag along to see what technology is all about, my mother thank you so much for your encouragement and inspiring me to fight for my career and my life through all the tough times we have faced together.

Loving sister who believed in me, brothers and amazing friends who made the journey so pleasant!. And certainly my kids, Sarah and Joseph, for the smile they can bring to my face after the most stressful days, as well as their constant sense of awe, amazement, and excitement about the world around them, reminding us of what science is all about and making me a very proud mother.

My sincere gratitude and deepest appreciation goes to my advisor, Dr. Sarkar, for her help, guidance and leadership in starting this generation of ECoG BCI research from the ground up in our laboratory. A great debt of appreciation must go to my co-advisor, Dr. Rao for his observations, and encouragement in getting this study to fruition, And a special thank you to Dr. Hodgkiss, Dr. Nagaraj and Dr. Voelker for their invaluable feedback, support, motivation, and for being on my thesis committee.

For chapter 3, we thank dr. Walid Al Hussaibi for his useful contribution. For chapter 4, Thank you Dr.Syed Hassan, and Hayden Bialek for working with us on this project and for chapter 5, many thanks for Dr. Arafat Al-Dweik contributions.

I am grateful to Center of Neurotechnology (CNT, formerly known as CSNE) and National Science Foundation (NSF) for funding this research work by award number EEC-1028725.The study presented here was funded in part by my fellowship provided by the National Science Foundation (NSF) and San Diego State University (SDSU).

VITA

2021	Ph. D. in Engineering Sciences (Electrical and Computer Engineering), *University of California San Diego/San Diego State University*.
2009	M. S. in Engineering Sciences (Electrical and Computer Engineering) , *New York Institute of Technology*.
2006	B. S. in Engineering Sciences (Computer Engineering) , *University of Technology*.
2012-2018	Associate Core faculty, Coleman University, San Diego.
2016-present	Adjunct faculty, Grossmont College, San Diego.
2017-present	Adjunct faculty, San Diego Miramar College, San Diego.
2018-present	Lecturer, San Diego State University, San Diego.
2018-present	Adjunct faculty, University of San Diego, San Diego.
2018-present	Associate faculty,MiraCosta College, San Diego.
2017-present	Adjunct faculty, San Diego Miramar College, San Diego.
2018-present	Adjunct faculty, University of San Diego, San Diego.
2019-present	Adjunct faculty, Alliant International University, San Diego.
2019-present	Associate faculty, MiraCosta College, San Diego.
2020-present	Adjunct faculty, University of North Texas, Dallas.
2020-present	Lecturer, University of California San Diego, San Diego.

ABSTRACT OF THE DISSERTATION

Investigating ECoG Signal Acquisition And Transmission in Brain Computer Interface Applications

by

Shams Al Ajrawi
Doctor of Philosophy in Engineering Sciences (Electrical and Computer Engineering)

University of California San Diego
San Diego State University, 2021

Professor. Mahasweta Sarkar , Co-Chair
Professor. Ramesh Rao , Co-Chair

Brain-Computer Interface (BCI) can permit individuals to use their thoughts as the sole means to control objects such as smart homes and robots. Although, the main goal of BCI system is to bring back mobility to severely paralyzed people and give them another way to communicate, a way that does not depend on muscle control. While BCI is a promising interdisciplinary tool, researchers are confronting signal acquisition and signal transmission as an obstacle to further development. For signal acquisition, we proposed two approaches to extract and classify brain activities for BCI competition III data-set I, they are Hierarchical recursive feature elimination (HRFE) and Flexible Analytic Wavelet Transformation (FAWT), we evaluated them in terms of accuracy and classification time. This process requires efficient transmission of Electro-

cartographical (ECoG) signal from implanting electrodes inside the brain to an external receiver located outside of the scalp. In particular, the generated artifacts due to in-phase/quadrature (I/Q) imbalance of utilizing down converter, and time interleaved analog-to-digital converters (ADCs) may lead to significant interference to desired signal which affects the detection performance. In this thesis, an efficient, low, complexity, balance technique is proposed for BCI communications to mitigate the interference using the adaptive least mean square (LMS) algorithm. The performance results of the conducted experiments on a phantom human brain model are shown to validate the designed scheme compared with the existing BCI approach. For Signal transmission, investigated the feasibility of passive Ultra High Frequency Radio Frequency Identification (UHF-RFID) for wireless communication between multiple transmitters inside the brain that collect vital data continuously and transmit them to an external controller using Back-scatter technique and we proposed a novel Medium Access Control (MAC) protocols that can be utilized for dependable transmission in BCI applications by altering their control parameters. However, modifying these parameters is another source of concern due to the scarcity in knowledge about the effect of modifications. In this thesis, a hybrid MAC protocol is proposed. Enhancing data gathering in medical records has been considered by proposing SC (Scanner Controller) device which consist of mini-reader, GPS and timer integrated together for every patient.

Chapter 1

Introduction

1.1 Motivation

Brain computer interface (BCI), as a field, has been present in the scientific community for several years, developed as advanced strategies for people with neuron degenerative disorders who have lost the ability to regulate their muscles and are also unable to move, speak, or control their eye movement and the development of robust systems that can differentiate and accurately perform tasks for multiple subjects has yet to be developed. The core of BCI technology is a conversion algorithm that converts brain signals input by users into output control signals or commands. A very important part of BCI research work is to adjust the mutual adaptation relationship between the human brain and the BCI system, that is, to find the appropriate Signal processing and conversion algorithms enable the neural electrical signals to be converted into a command or operation signals that can be recognized by the computer through the BCI system in real time, quickly and accurately.

Sensorimotor neurological disabilities due to stroke and spinal cord injury affect more than a million people in the world each year. Traditional rehabilitation therapies often lead to limited or incomplete recovery of sensorimotor function. Indeed, our lab Wireless Networks and Communication Lab (WINC) at SDSU is one of the labs that working with other institutions like University of Washington and MIT on Brain Computer Interface System as part of the Centre for Sensorimotor Neuro Engineering (CSNE) project. Our goal is to restore mobility in paralyzed limbs in humans and "helping the body heal feel and move again" ——- CSNE mantra.

Work in centre laboratories will advance fundamental knowledge of the mechanisms of sensorimotor information processing and neural plasticity in pursuit of these objectives. More than

one billion individuals worldwide suffer from neurological disorders and injuries (WHO, 2006). A significant number of these individuals have critical sensorimotor impairments due to stroke, spinal cord injury, and neuro-degenerative disorders such as Parkinson's disease. Stroke alone affected more than 25 million people in the world between 1990 and 2013 (Feigin et al., 2015). An estimated 282,000 people in the US have spinal cord injuries, the most common being incomplete tetraplegia (45% of the cases; WHO, 2016). Parkinson's disease has been estimated to affect 6.3 million people worldwide (EPDA, 2017). Bi-directional interfaces can both record and stimulate neural tissues, providing an unprecedented opportunity to radically improve the quality of life of paralyzed and motor-impaired individuals by reanimating paralyzed limbs and inducing plasticity for targeted neuro-rehabilitation. Guided by its transformational vision, CSNE will develop the world's first BBCIs for reanimating paralyzed limbs, directing synaptic plasticity, and restoring sensorimotor function in patient populations with upper extremity sensorimotor impairments. Simultaneously, the centre will engineer and distribute to researchers around the world the Neurochip BBCI research platform to advance fundamental knowledge of neural plasticity, dynamics, and information processing in neuronal networks. To achieve its vision, our lab as part of the centre will leverage its unique strengths in experimental neuro-science, wireless electronics, on board computing and research possibilities of restoring mobility in paralyzed limbs in humans by investigate ways of transmitting neuro signals to paralyzed limbs in wireless manner and developing novel classification algorithms to classify brain activities in accurately and precisely.

We integrate state-of-the-art recording, stimulating, and wireless technologies with a deep computational understanding of sensorimotor processing and plasticity in the nervous system, guided by clinical needs and a responsible neuro-ethical framework.

1.2 Specific Aims

This BCI system aims to bypass the injured spinal cord and build a direct connection between the brain and the associated limb. Many researchers have been working on this field; therefore, different techniques have been proposed to accommodate patients with different disabilities such as incapacitated due to stroke, cerebrum or spinal string wounds. These techniques have advanced this field and have been critical to the development of BCI systems. However, they have been trained and evaluated using only offline signalling.

Fig 1.1 shows how we can design a virtual communication path, this path can bypass the

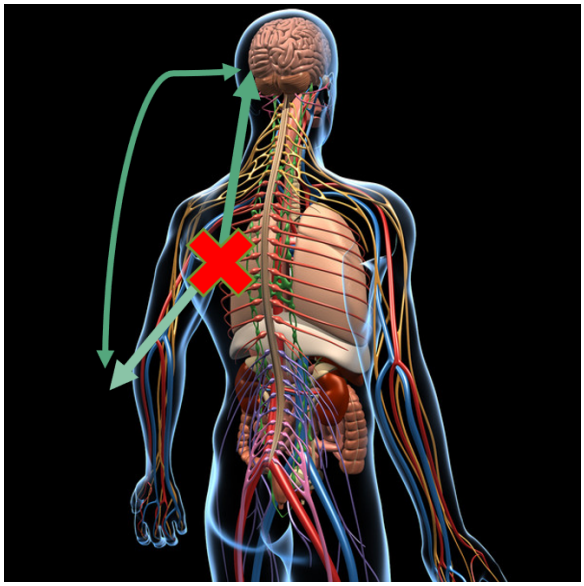

Figure 1.1: BCI System

spinal cord injuries.

In this thesis, we considered the motor imagery as a mental system in which an individual practices or re-enacts a given activity in his/her mind. It is commonly used as a daily mental exercise for individuals recuperating from neurological injuries. It is imagery collection is a psychological procedure where a subject is asked to mentally visualize a physical action. It is generally utilized as a mental routine with regards to activity and neurological recovery, and, has likewise been utilized as a psychological testing technique for neuroscientists to determine the chemical and structural nature of thoughts that drive actions [1, 2]. Brain signals can be obtained through both invasive and non-invasive approaches. The aforementioned methods utilized electrocorticography (ECoG) signals to detect brain activity from electrodes placed under the skull. The most common ways to capture brain signals are through:

- EEG (electroencaphalography) [4, 5].
- ECoG (electrocorticography) [6].
- FMRI (functional magnetic resonance imaging).
- PET (positron emission tomography).
- MEG (magnetoencephalography).

For successful BCI systems, it is essential to obtain clear signals with a maximum signal-to-noise ratio. As EEG data are collected from the surface of the human scalp, it is susceptible to movement of the electrodes and poor signal-to-noise ratio and signal interference. In contrast, using ECoG electrodes, which are implanted into the skull, have better stability of location, allowing the subject to move freely, and better signal-to-noise ratio.

Given the previous motivation, three specific aims were focused upon for examination in this dissertation. Aim 1 represents signal acquisitions which includes feature extraction and classification at the receiver side and noise cancellation. Aim 2 improved signal transmission which includes choice of transmitter and MAC Protocols for Ultra High Frequency - Radio Frequency Identification (UHF-RFID-BCI). Finally, Aim 3 investigates the BCI Cybersecurity challenges and propose a Cybersecurity prototype for BCI applications. Fig 1.2 and 1.3 shows the dissertation contributions.

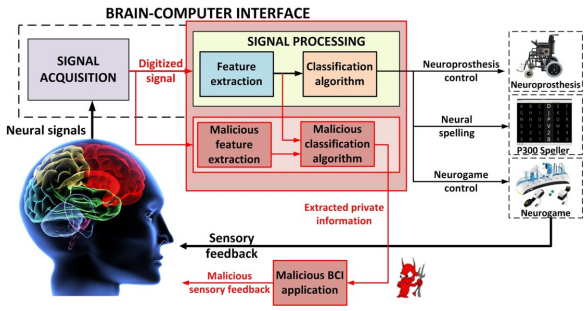

Figure 1.2: BCI Overview

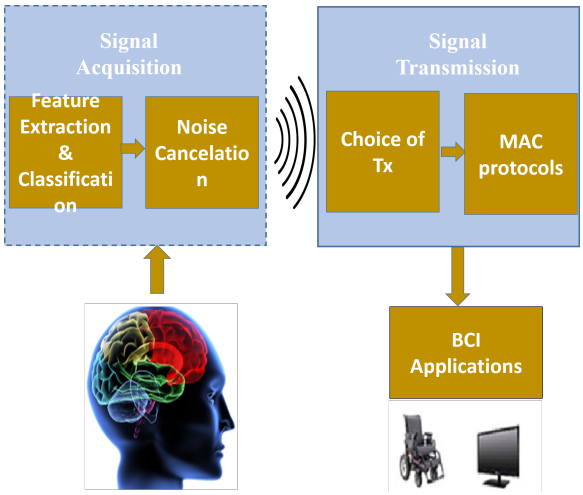

Figure 1.3: BCI Contribution

Specifically, the three aims are:

Aim 1: Improve signal acquisition measurement and calculation of neural signal through implantable electrodes and sensors by using novel machine learning and advanced digital signal processing algorithms.

- BCI systems detect brain signals and use extraction and classification algorithms to convert the detected signals into useful outputs that can be used to control external devices. Designing and developing BCI systems face several challenges, such as session-to-session transfer, subject-to-subject transfer, non-stationary signals required for adaptivity, idle signals for motionless subjects, and continuous data collection that can be used to expand BCI systems for a broad spectrum of subjects. The first goal is to present a novel approach to detect and classify the Electrocorticography (ECoG) brain signals considering time consuming. We proposed two algorithms:
  - Flexible Analytic Wavelet Transformation (FAWT) which is advanced digital signal processing is used to extract entropy features and the Least Square Support-Vector Machines (LS-SVM) is utilized to classify the activities. ECoG signals are obtained by direct recording from the surface of the cerebral cortex. This provides a high resolution data and stability in signals in contrast to Electroencephalography (EEG) signals. Three entropy features were extracted from the ECoG signal, which are log energy entropy, SURE entropy, and cross corr-entropy. Our proposed approach was evaluated by carrying out test-bed experiment and by using the dataset I of the public BCI competition III data. A classification accuracy of 95% was achieved during the testbed evaluation. While a classification accuracy of 93.02% was achieved using the dataset. Our proposed algorithm was implemented in MATLAB.
  - Hierarchical Recursive Feature Elimination algorithm which is a novel machine learning method, HRFE proposes multiple classifiers in a step-wise manner to eliminate bias in detecting BCI signal features. We evaluate the HRFE on the same data sets. We used ECoG signals to select 20 features which are most significant in affecting noise and choice of classifiers. The simulation results confirm that HRFE has significant machine learning improvement, especially for ECoG signal obtains about 93.5% accuracy, compared to related feature selection algorithms in the literature.

The accuracy was around 93% using both of the above methods, but time consuming for FAWT more than HRFE. HRFE time consuming was 3.8 minutes while FAWT time consuming is about 2 hours.

- **An efficient low complexity balance technique is proposed for BCI communications to mitigate the interference using the adaptive least mean square (LMS) algorithm.** Aims and contributions can be summarized as following:
  - An efficient low complexity balance technique is proposed for BCI communications to mitigate the interference caused by I/Q imbalance using the adaptive least mean square (LMS) algorithm. The integration of these cost-effective approaches is very important for feasible BCI applications toward wide adoption of this technology.
  - For the considered technique, we present the time model of I/Q mismatch in BCI and the employed adaptive cancellers to correct the DC offsets and imbalance defects of frequency down converter and QPSK signalling. A balanced model is demonstrated, then to cancel the DC offsets and spectral artifacts produced by the pair of TI-ADCs.

Aim 2: Improve signal transmission in two areas listed bellow:

- Investigate utilizing multiple Implantable UHF-RFID Transceivers in Brain-Computer Interface Applications.
- Develop efficient Medium Access Control protocols (MAC) for BCI system.

Aim 3: Optimize, enhance and provide secure BCI applications by proposing the design of a Radio Frequency Identification RFID-based system having semi− active RFID tags placed outside the brain on the scalp transmit the collected brain activities in wireless format to a device SC (Scanner Controller) consist of mini-reader and timer integrated together for every patient. Additionally, we developed the interface system called BCI Identification System (BCIIS) to assist the patient in the identification process.

1.3 Dissertation Organization

This thesis is divided into eight chapters provides feasibility study for Brain Computer Interface (BCI) main components. The first section in each chapter provides relevant background for that chapter. Chapter 2 presents the general experimental setups and the methodology used

throughout this thesis. Chapter 3 and chapter 4 addresses the goals outlined in Aim 1 through investigating and developing machine learning and advanced digital signal processing algorithms to improve extractions and classification methods in term of accuracy and time consuming, also shows fast convergence of the estimated phase and gain parameters and accurate DC offset cancellation that allows an improved QPSK performance series of open-loop joystick experiments, while chapter 5 and 6 addresses the goals outlined in Aim 2 to improve signal transmissions in term of choice transmitter and propose MAC protocols especially for BCI applications. Chapter 7 meets Aim 3 expectations by investigating the BCI Cybersecurity challenges and propose an enhancing data gathering method in medical records for BCI applications. Finally,chapter 8 summarizes the conclusions and ramifications of these experiments and presents suggestions for directions of future experiments along these lines.

Chapter 2

Signal Acquisitions-Feature Extraction and Classification

2.1 Introduction for Feature Extraction and Classification

BCIs are being created as specialized strategies for individuals with neuron-degenerative disorders who have lost the capacity to control their muscles and hence cannot move, speak, or control eye movement. Current researchers have focused on analyzing signals to fit BCI systems that can be utilized for multiple subjects [3]. Pattern recognition algorithms, when used along with appropriate pre-processing methods, feature engineering and selection techniques that have been seen to produce strong data, particularly in offline scenarios. Using these methods for online situations has been a significant challenge. During this research project, we collected motor imagery data from subjects who were asked to imagine moving their left pinkie finger or tongue [1]. Motor imagery collection is a psychological procedure where a subject is asked to mentally visualize a physical action. It is generally utilized as a mental routine with regards to activity and neurological recovery, and, has likewise been utilized as a psychological testing technique for neuro-scientists to determine the chemical and structural nature of thoughts that drive actions [1, 2]. Brain signals can be obtained through both invasive or non-invasive approaches. The aforementioned methods utilized ECoG signals to detect brain activity from electrodes placed under the skull. The most common ways to capture brain signals are through EEG (electroencephalography) [4, 5], ECoG (electrocorticography) [6], FMRI (functional magnetic resonance imaging), PET (positron emission tomography), and MEG (magnetoencephalography). For successful BCI systems, it is essential to obtain clear signals with a maximum signal-to-noise ratio. As EEG data are collected

from the surface of the human scalp, it is susceptible to movement of the electrodes and poor signal-to-noise ratio and signal interference. In contrast, using ECoG electrodes, which are implanted into the skull, have better stability of location, allowing the subject to move freely, and better signal-to-noise ratio [3, 7].

Motivation. Several theories have been proposed to classify brain activities [1–5], but these studies have almost exclusively focused on just the classification accuracy. Hence, they are lack of joint classification accuracy and classification time. To design any efficient BCI application, we have to consider the classification time. For example, consider a patient that has a spinal cord injury and is unable to use his hand. To help him, we can design a robotic arm for him. To do so, in the first step, we need to collect his brain activities, classify them and translate them into actions. If the classification accuracy is 100%, but it needs hours to do this simple task, then we cannot consider it as the best solution. If the time is 10 seconds and accuracy is around 50%, this is also not acceptable. Motivated by this, in this thesis, we proposed an algorithm called HRFE consider both classification accuracy and classification time factors. In order to come up with a novel classification algorithm, we have evaluated all the most commonly used machine learning methods such as ECoGNet, main component analysis (PCA), independent component analysis (ICA), linear discriminant analysis (LDA), Autoregressive (AR) coefficients, moving-average (MA), and shallow convolutional neural networks (ConvNets) [12–15]. We will show that we could reach reliable and acceptable results around 93% as accuracy in less than 4 minutes.

Contribution. In this dissertation, we propose two novel approaches for feature extraction, and elimination allows for optimal use with BCI correspondence. The first approach is *Hierarchical Recursive Feature Elimination (HRFE)*, while the second approach is Flexible Analytic Wavelet Transformation.

For HRFE, the primary steps using an ensemble of L2 regularized logistic regressions on AR values extracted from each sample, followed by feature selection. It should be noted that regularization is a widely used technique to help a learning machine algorithm reduce its generalization errors. Regularized logistic regression has found wide adoption in many fields.

While FAWT is used to extract three entropy features (i.e. cross corr-entropy, log energy entropy, and SURE entropy). After the three features are extracted, the LS-SVM is used for classifying the extracted features.

This work utilizes a wrapper strategy for dimensional reduction by picking a selected number of significant features. Hence, the contribution of this chapter summarizes as below:

- We proposed a novel machine learning algorithm hierarchical recursive feature elimination named *HRFE* adopting noise addition and extract and classify the brain activities.

- We give a detailed mathematical analysis for HRFE and explore the adopted L1 and L2 regularization and support vector machine solutions.

- We proposed another novel advanced digital signal processing algorithm Flexible Analytic Wavelet Transformation named *FAWT* to extract entropy features and the Least-squares Support-Vector Machines (LS-SVM) is utilized to classify the activities. Three entropy features were extracted from the ECoG signal, which are log energy entropy, SURE entropy, and cross corr-entropy.

- We validate the HRFE and FAWT on two datasets. First one, real-world BCI signal dataset, which is BCI competition III dataset I. Second one is the experimental setup dataset collected from the Testbed experiment. In the first dataset, we tested our proposed algorithms and many other exciting algorithms and we compared between them in term of accuracy and classification time like deep convolution network classification algorithms, ECoGNet, main component analysis (PCA), independent component analysis (ICA), linear discriminant analysis (LDA), Autoregressive (AR) coefficients, moving-average (MA), and shallow convolutional neural networks (ConvNets).

- We conclude the achievements of both FAWT and HRFE on two datasets and various ML metrics like precision, recall, accuracy and f-measure and confirm that we could reach reliable and acceptable results around 93% as accuracy in less than 4 minutes for HRFE and around 2 hours for FAWT. Based on that we designed our evaluation table that mainly considering two parameters, accuracy and classification time and recommending HRFE as it giving us high accuracy with less classification time.

2.2 Related Work

The objective of this investigation is to demonstrate the practicality of a movement/imagery prediction for a (BCI) system and to determine which electrocorticography (ECoG) neural activity would be best for controlling such a device. We used ECoG signal detection for optimal data collection. Over one million people suffer from movement impairments due to stroke or spinal string wounds [16–18]. A significant number of these individuals experience hand movement

Table 2.1: Comparison of related works.

Num	Classification Method	Features	Accuracy
1	linear SVM	CSSD, Combination of Bandpower, Fisher Discriminant Analysis	91%
2	Regularized Logistic Regression	ICA, spectral power (0-45Hz),combination of AR coefficients, wavelet coefficients	87%
3	Logistic Regression	Spectral Power of Selected Channels and Offset	86%
4	Mahalanobis Distance Between classes	Selected 7 Channels and Standard deviation of Hilbert-Huang Transform for time-frequency windows (5Hz*0.2S	86%
5	Non classical Algorithms Models	Selected 7 Channels	86%
6	LDA	CWT, correlation between trials, Bandpass (2.5Hz to 25Hz), CSP	86%
7	LDA	AR coefficients and band power (10-12 Hz and 16-24 Hz) from 10 channels	84%
8	LDA	CSP, Bandpass (5-30Hz) , CWT with Coefficients Corr. to 4-24Hz, 12 Channels, Weighting of Coefficients by T-Test	84%
9	semi-supervised learning (self training) based on a quadratic classifier	CSP feature and the coefficients of AR mode	83%
10	via cluster mean	bandpass (8-12Hz), Gaussian Mixture Model for channel selection and clustering	82%
11	SVM	correlation and covariance matrix coefficients	81%
12	leave-one-out cross-validation on the whole training set	AR coefficients and bandpower (7-10,1 0-12, 16-24 Hz), 11 channels chosen	81%
13	ensemble of neural networks and fisher discriminant functions	bandpower	79%
14	Robust Discriminant Analysis	phase, PSD, and Empirical Mode Decomposition	79%
15	FDA	band power of 4 channels, selected by Fisher ratio, multi-variate AR coefficients	69%
16	Bayesian classifier and SVM	bandpass (0.5-45Hz), statistical and parametric models, various transforming functions	67%
17	sparse model from 'finite prediction error'	bandpass (8-40Hz), AR coefficients and 'coupled fits'	66%
18	SVM	channel reduction via feature subset selection, correlation coefficients of all trials	65%
19	probabilistic classification	cross-spectrum in alpha frequency range	65%
20	discriminative biorthogonal bases	discriminative biorthogonal bases	59%
21	linear model with Tikhonov regularization	downsampling, subset of 30 channels	58%
22	Attribute Clustering Network via Nearest Neighbors	time-frequency coefficients chosen by Rayleigh Coefficients	54%
23	neural network (single layer FF) with ELM training	AR coefficients for overlapping windows	50%
24	SVM	2 CSP components, AR coefficients	48%
25	1-nearest neighbor AR coefficients	cross-correlation between test and training trials	44%
26	Nearest neighbor, SVM	AR coefficients	22%

disability [31–33]. Recent studies demonstrate that a BCI serves as a potential intervention in treating people with spinal cord injuries. Research has proposed hand movement classifications using the support vector machine (SVM), adaptive Gaussian coefficients, and C-SVM. Despite the recent study proposals, computation and low power output complications have prevented most substantial advancements [34–38].

BCIs are valuable medical devices for patients who have lost control of their limbs. A BCI empowers these patients to control a smart device with their cerebrum activity, allowing mobility. A BCI serves as a unique intervention, as it can be tailored to individuals and their characteristic needs. Movement controlled BCI's enable the patient to show a decision by making or envisioning one of a few predefined movements[10,11].

Current movements controlled by BCIs have two substantial disadvantages. These devices quickly exhaust subjects by requiring continued movement imagery for several seconds. Neural signals related to non-continued movement/imagery dies down rapidly, and a more extended sample of information is required for characterization. After the neural signals are received, the smart device can require a few seconds to order it, mainly whenever complex actions are included. This causes a latent period between the patient's neural order for action and the BCI's reaction, diminishing ease of use and comfort of the BCI. To address these issues, a BCI proposed that utilized the cerebrum activities proceeding movement execution. This empowered the extraction of over one moment of preliminary neural data from a solitary non-supported movement/imagery and could diminish the delay between the patient's activities and BCI action of the BCI by utilizing prior neural signals [19–21].

Many algorithms were implemented on this data set. Twelve approaches achieved 80% accuracy. Michal Sapinski, Mao Dawei, and Alexander D'yakonov [25–28] achieved 86% accuracy, using different approaches to extract features, such as selecting channels and applying spectral power on it, a standard deviation of Hilbert transform for time-frequency window, along with Mahalanobis distance, and logistic regression as a classification method. Paul Hammon [24] achieved 87% accuracy by applying ICA, AR coefficients, spectral power (0-45 HZ), and wavelet coefficient as features, along with regularized logistic regression. Qingguo Wei and his research group used Fisher discriminant analysis to extract features such as band-power, together with CSSD, and they applied linear SVM to achieve 91% as the highest accuracy [23]. Different extraction methods, along with different classification algorithms, have been used to achieve better performance. Table 2.1 shows the related work on this data set and how the accuracy ratio increased from around 50% to approximately 91%.

2.3 HRFE: The Proposed Approach

In this chapter, we introduce a new classification algorithm, called *Hierarchical Recursive Feature Elimination (HRFE)*. The core idea behind HRFE is that, instead of just using one classifier to pick the important features, multiple classifiers are used in a step-wise manner, in order to eliminate bias in detecting features.

We used Dataset I of BCI Competition III [1] which was recorded from one subject performing the same task in two sessions separated by one week interval. The subject performed motor imagery without feedback which comprised of two actions: left pinkie finger movement and tongue movement. A typical assignment in BCI is to apply a classifier that was prepared from past session for a later session without retraining it [6–9]. To test this assignment, electrical signals are compared for each subject, often presenting unique changes in activity in each trial. This inconsistency can be caused by various underlying reasons, for instance, varying levels of inspiration, excitement, and exhaustion. The recording system cannot be set up in the exact same way between sessions. Therefore, there might have been slight differences between electrode position and impedance between the two sessions.

As Electrocorticography (ECoG) was utilized and not EEG, the variety of terminal positions and impedance is minimal. The objective of this data set is to train a classifier on the labeled training data from the first session and apply it to the unlabeled test data from the second session. The execution criteria utilized for assessment was the accuracy of effectively characterizing the test preliminaries. The subject selected experienced epilepsy. The given data set comprises of 278 preliminaries performed during the main session (training data) and 100 preliminaries from the second session (test data). Electrical cerebrum movement was picked up using a 8×8 ECoG platinum electrode grid that was set on the contralateral (right) motor cortex. All recordings were performed with an examining rates of 1000 Hz. The preliminary span was three seconds. To keep away from outwardly evoked possibilities being reflected by the information, the chronicle interim began 0.5 seconds after the visual signal had finished [22]. Data is provided in Matlab format, containing continuous signals from 64 ECoG channels. Our proposed approach for extracting and classifying the features of brain activities is depicted in Fig. 2.1. As shown in the figure, frequency filtering is applied to process the Dataset I of BCI competition III. The idea of adding minor noise is that real life data innately include noise. Therefore, features which are the most resistant to this ecological noise could be selected. This is a form of regularization and a way to make the final model more robust by assuming a particular feature has a large coefficient in logistic regression.

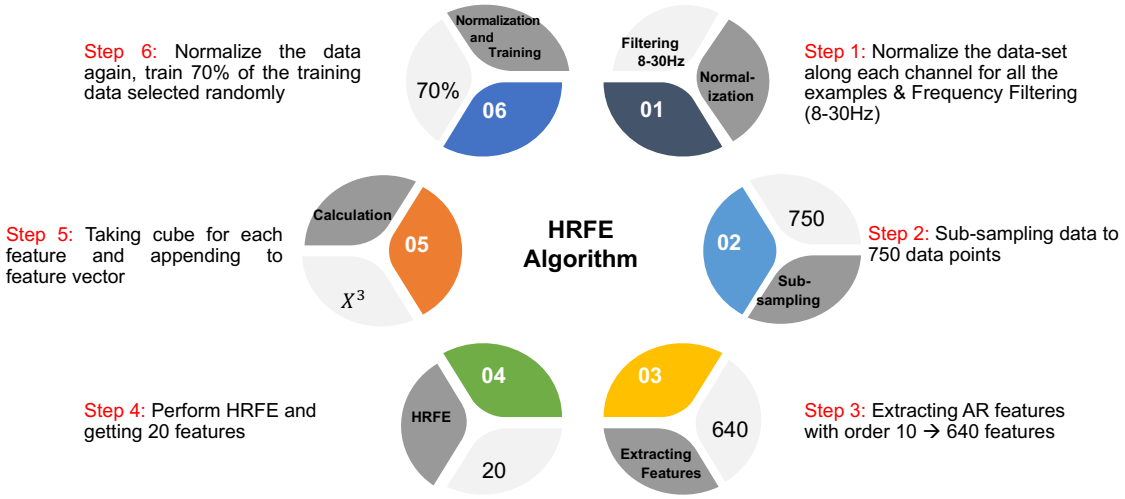

Figure 2.1: HRFE steps applied to the dataset.

If a bit of noise occurs in the feature, then, because the coefficient is large, it may change the output drastically, since the noise also gets multiplied. Therefore, we selected large coefficients. Normally, a linear classifier is used. However, we transformed the data set to get a non-linear classifier. We selected and added the cube of each input as a feature. For example, if a sample has 11 features, it will have 22 features (original + cube of each value). With this approach, we achieved 93% accuracy. A normalization followed this procedure. With the above analysis, 93% was determined as the maximum test accuracy.

2.3.1 HRFE Mathematical Analysis

In this part, we adopt the following mathematical equations on HRFE method to produce the HRFE model. For a given Dataset (Y_i, X_i) where $i = 1, \ldots, N$, X_i is the feature set and Y_i is the label set. The general decision function for a linear classifier is defined as:

$$D(X) = W^T \cdot (X)B \tag{2.1}$$

where B is the bias term and W is the weight vector. As B was not impacting the authors' results, they omitted the bias term, because linear classifier is used for data with many features [11, 12]. They defined their decision function as:

$$D(X) = W^T \cdot (X). \tag{2.2}$$

In this chapter, we applied three types of classifications: SVMs, L1 regularization, and L2 regularization. The risk minimization equation is as follows:

$$Min_W \cdot F(W) = R(W)C \cdot \sum_{i=1}^{N} \xi(W, X_i, Y_i). \tag{2.3}$$

2.3.2 Support Vector Machines

For SVMs there are *three* different loss functions to penalize the wrong-classification, they are: (1) L1-loss, (2) L2-loss, and (3) LR (logistic regression). All of the loss functions are convex and positive functions. In this study, the authors used the logistic regression as defined below:

$$\varepsilon(W, X, Y) = log(1e)^{(-YW^T X)} \tag{2.4}$$

we have used equation(13) logistic regression with equation (12) because it is twice differential [13].

2.3.3 L1 and L2 Regularization

For a given Dataset X, it is possible to predict the Y label using L1 and L2 classifier, in order to reduce or prevent over-fitting problems; this method which is used to eliminate the training loss. L1 and L2 regularization can be defined as:

$$R_{L1}(W) = ||W_1|| = \sum_{i=1}^{N} |W_i| \tag{2.5}$$

$$R_{L2}(W) = \frac{1}{2} \cdot ||W_2||^2 = \frac{1}{2} \cdot \sum_{i=1}^{N} W_i^2. \tag{2.6}$$

The purpose of R_{L1} and R_{L2} is to avoid over-fitting in the search space(W) by pushing it toward zero. A sparse model can be generated by L_1 regularized case, while L_2 causes intensive (W), although some elements can be pushed to be close to zero because of $\frac{W^2}{2}$ that can go flat and close to zero. For L_1 regularized scenario, $|W|$ is uniformly steep and easier to be zero. In algorithm 1, we explain instantiating a new classifier (L1LR, L2LR, SVM). To so so, we are adding minor noise to the vectors of samples. Then, we select n-th features, check whether feature is biased or not, if it is not biased, we will consider and use this feature set.

Algorithm 1 HRFE algorithm

Requirements: ECoG Dataset

Step 1:Initialization

F_s :Set of ranked features which = ϕ.

R_f :Remaining feature set = 1,2,3,...,N.

A :The accuracy of K-fold cross validation. At the beginning the remaining feature, K=N.

Step 2: Training L_1, L_2 regularization and SVM, calculating the accuracy as:

A_1 = A $(X_i(R_f)Y_i)$.

Step 3: Calculating W_i and ranked feature set based on W_i values (from the least significant values to the highest significant values).

$\eta = F_1, F_2, F_3, ..., F_k$.

Step 4: Letting K = K 1 and m = 1.

Step 5: Creating a new set for the remaining feature set R_1 by eliminating the features F_m from R_f.

Step 6: Training L_1,L_2 regularization and SVM on the set of the remaining features and finding:

A_2 = A $(X_i(R_f)Y_i)$.

Step 7: If$(A_1 < A_2)$

$F_s = F_s \cup F_m$

go to step 8.

else if $(m == K)$

Remove the first feature set from η and update the remaining feature set as:

$F_s = F_s \cup F_m$,

$R_f = R_f - F1$

go to step 8.

else

$m = m + 1$

go to step 5.

Step 8: Looping step 2-7 until $R_f = \phi$.

2.3.4 Performance Evaluation

To evaluate our proposed approach, we used Dataset I of BCI competition III and by carrying out testbed experiment.

Dataset-based Evaluation

This thesis aims to develop an approach with high accuracy ratio for extracting and classification brain signals. We used three main classifiers to select and switch between them. The

classifiers are L1 logistic regression, L2 logistic regression, and linear support vector classifier. We added minor noise to each value in the data set to make a most random feature, and we repeated the process by selecting n-features from the feature pool and updating the feature set, as shown in Fig. 2.1 and Algorithm 1. The test data consists of 100 samples, where 93% accuracy was the highest determined. The authors analyzed the failed samples by repeating the experiment over 1000 times, where each time involved 5 models in being trained and tested over the said 100 examples. The researchers took an intersection of all the incorrectly predicted samples. Given the random 70% selection of samples and the selected classifier's general high performance, it is reasonable to expect that each sample might get correctly classified in at least one of the 1000 trials. The authors determined that samples 13, 16, 53, 56, and 58 were not classified correctly. Sample 97 was classified correctly only once in over 1500+ repetitions. This suggested a significant error. Potentially, the subject imagined moving the tongue instead of the finger. When the authors removed these trials, they determined a 99.35% test accuracy with 5-fold-cross validation was determined.

Testbed-based Evaluation

In order to evaluate our proposed HRFE algorithm, we introduced another evaluation by using a testbed experiment.

Experimental Components

To generalize the algorithm for ECoG signals, we modelled the brain environment by using a chemical solution that represents the dielectric tissue [31] to study the transmission characteristics of ECoG signals through the brain environment and classify the activities. RFID quickly expanded for remote observing of the people by methods for low-power and low-cost UHF (860-960 MHz). We used a channel model with invasive passive RFID tags through experimental setups and measurements. Numerous advantages of RFID would prove to be an effective and an efficient technological device in the health care domain. As it is not conventionally plausible to provide power to implantable sensors by batteries for a longer duration, we also used a programmable passive RFID implantable tag (wireless identification and sensing platform) (WISP), which is battery-free and uses a back-scatter mechanism to excite its circuitry, overactive RFID which has batteries. Moreover, the implantable chip should be an ultra-low power device to avoid any effect on high power neurons or brain cells. Back-scatter RFID in the UHF range is a promising communica-

tion technology for WBAN. Back-scatter sensor tags have a low power consumption and are thus appropriate for WBANs that require small, lightweight, low maintenance sensor devices. RFID technology has shown great promise for real-time monitoring of fully implantable sensors in the human body. In the case of passive RFID systems, sensors or passive tags are powered by inductive or electromagnetic coupling, as it receives power externally from the reader and sends back-reflected signals containing data. RF power decomposition in the tissue for these kinds of passive systems can be made concerning the brain. For communication with the implanted RFID sensor in the human body, the read range is approximately 12 cm. For security and confidentiality constraints, RFID sensors may serve as a good fit for its short read range. The parameters of specific channels are presented, including SNR, received signal strength (RSS), and channel capacity for ECoG signals when it traverses through tissue fluid (i.e., blood).

WISP The Wireless Identification and Sensing Platform (WISP) adheres to the requirements of the stage of experimentation, which is low computation, sensing of power, and communication. It is an open and transparent source and is not dependent on any alternative sources of energy. Instead, it runs on the power of UHF RFID readers. WISP micro-controllers yield a network consisting of no wires (wireless) and no batteries and create a sensing device. WISP5 is an ultra-low power fully-passive UHF RFID tag that uses an ultra-low-power micro-controller MSP430FR5969 by Texas Instruments. It is an energy harvesting circuits, where it harvests energy after receiving from the reader to power up its circuits, and then uses the backscatter technique to send data back to the reader by reflecting the same carrier signal received from the reader. It has forced duty cycling and burns around 1 mW of power when operating. The WISP5 designs are based on the electronic product code (EPC) C1G2 protocol, which can be Reader-to-tag signalling and include Amplitude shift keyed (ASK) modulation, Pulse interval encoding (PIE), and Timing parameters sent in Preamble. The protocol of WISP5 also be formed based on Tag-to-reader signalling consisting of Backscatter modulation: load shift keying, Bi-phase space encoding (FM0), and Medium access control (MAC) are Slotted Aloha.

RFID Reader and Antenna

The WISP is powered by an RFID reader which emits RF signal continuously in the UHF range (908-928 MHz). It is connected to the network and sends RF signals to tags consisting of data and used for generating power. An RFID reader manufactured by Impinj supports the WISP. We used the R420 model of Impinj's reader.

Experimental Setup

In order to mimic the brain environment, we used glycerin to replicate the tissue fluid because the dielectric properties of tissue fluid and the glycerin are close to room temperature [28, 30]. We added saltwater (sodium chloride (NaCl) solution to the glycerin, which resembles blood, as the medium through which UHF RFID signals traverse. We studied the propagation effects of the signal, and we used a plastic beaker which shows a strong resistance to radio frequency waves, mimics the human skull with the specific measurements as 44.95 cm $\times$ 32.7 cm $\times$ 19 cm. In order to create the virtual environment of the brain, we used plastic beaker along with glycerin and saltwater. This served to model the surrounding of cerebellum with blood. For this experiment, we used a single wireless sensor to transmit the collected signals in wireless format to a receiver located on the scalp outside the brain.

Fig. 2.2 and 2.3 show the experimental set up where the WISP (passive RFID tag) is placed in a Ziploc bag over the solution of the glycerin and the saltwater barely touching it. The RFID antenna was placed below the beaker, which would replicate the real-world scenario where the RFID antenna would be outside the brain, the WISP would be implanted inside the brain surrounded by blood and tissue fluid, and the RFID reader is connected to the controller (laptop) through an Ethernet cable. A cable from RFID antenna was connected to the Impinj's RFID reader. The WISP contains the microcontroller MSP430FR5969, which is manufactured by Texas Instruments; it needs to be programmed to read the RF signal from the reader. This was done by connecting the WISP to the laptop through a USB FET debugger and coding it through Code Composer Studio IDE of Texas Instruments as the interface. The WISP operates in the UHF range. The reader is receiving the signals and sending them to the controller, which store them in an Excel sheet to process them in MATLAB for various results.

To imitate the real surrounding scenario for the implanted transmitter inside the human brain, and stable the behavioural implications, we used a plastic beaker more than double the size of the human brain. With varied measurements of glycerin and salt water from 1 cm to 4 cm, on the analyzed the depth requirement of the sensor implantation. At different implant depths, we recorded the RSS (received signal strength) values, found out the log files at each depth level, and then analyzed in MATLAB to generate results. The transmitting power from the reader to the WISP is varied from 25 dBm to 30 dBm. WISP is forced duty-cycled, RF power device, and burns around 2 mW of power, when operating. As per the FCC regulations, frequency hopping can be used to make the system more reliable. Therefore, it is used in RFID systems to increase reliability

and to avoid a collision when multiple tags operate simultaneously (as in Bluetooth). Then, we divided the UHF band into 50 channels, as highlighted in Table 2.2. This figure shows the received signal strength, the signal to noise ratio, and the channel capacity at different implant depths. At 0 cm, the data are considered to be an EEG signal. At 1, 2, 3, and 4 cm, the data are those that of an ECoG signal. We collected the data from a single sensor at different implant depths and considered

Table 2.2: Network Simulation Parameters.

Frequency of Operation	925MHZ
Channel Bandwidth	250KHZ
Receiver Sensitivity	-84dBm
Data Rate	2Mbps
T_X **and** R_X **Power**	0.175mW
Number of Tags	1×1

just the received signals at 4 cm as ECoG signals collected from 99 electrodes.

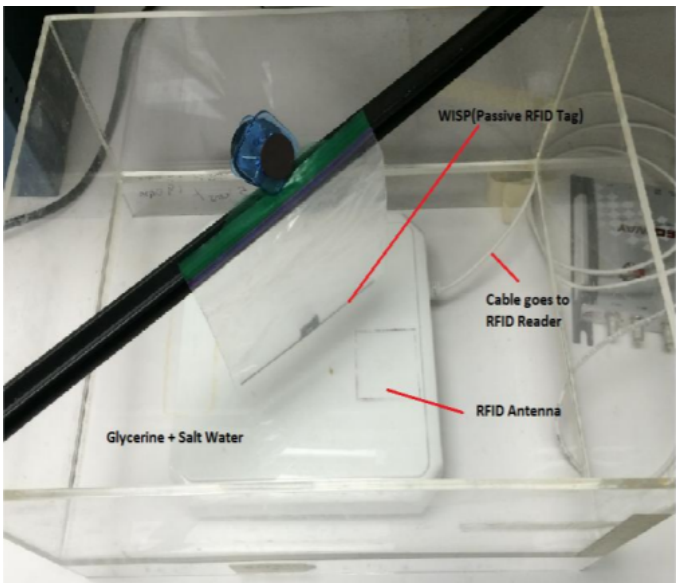

Figure 2.2: The Mimicked Brain Environment

We built a wireless network based on the experimental setup to mimic the brain environment using the NS2 simulator. Because the Dataset collected from 64 channels, we have to feed the data 64 times using the NS2 simulator by building a small network consisting of a single transmitter and a single receiver in order to classify received and not received signals as two classes.

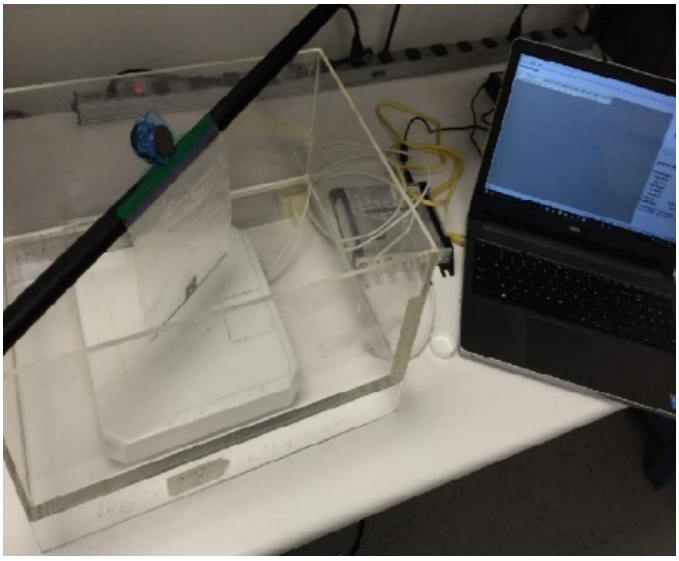

Figure 2.3: Lab setup snapshot.

For this network, we used RFID technique with specific parameters explained in Table 2.3, and we run our proposed algorithm and the accuracy to classify two classes were 94%.

Table 2.3: Network parameters for one sensor.

Implant Depth	**Received Signal Strength**	**Signal to Noise Ratio**	**Channel Capacity**
4 Cm	-15.918 dBm	18.232	2.93E+06
3 Cm	-15.23 dBm	19.012	3.23E+06
2 Cm	-14.718 dBm	20.125	3.43E+06
1 Cm	-13.418 dBm	21.45	3.52E+06
0 Cm	-10.918 dBm	25.203	4.34E+06

2.4 Flexible Analytic Wavelet Transformation

Our proposed approach for extracting and classifying the features of brain activities is depicted in Figure 2.4. As shown in the figure, sub-sampling and frequency filtering are applied to process the dataset I of BCI competition III, which includes samples of ECoG signals. Then, the FAWT is used to extract three entropy features (i.e. cross corr-entropy, log energy entropy, and SURE entropy) [39-43, 48-50]. After the three features are extracted, the LS-SVM is used

for classifying the extracted features. The following sections explain the steps of our proposed approach in details.

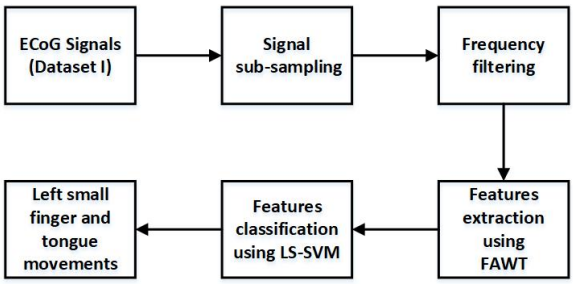

Figure 2.4: Our Proposed Extraction and Classification Approach

2.4.1 Signal Sub-Sampling

In order to reduce the memory overhead and the processing time, we have sub-sampled the ECoG signals using 250 Hz frequency. This is below the Nyquist rate, which is the minimum rate that must be used to sample a bandwidth signal in order to sustain all of its information [57].

2.4.2 Frequency Filtering

The frequency band used in this work is between 8-30 Hz. This band was chosen as 8 Hz is the frequency where the unclear direct current level of some individual channels could be eliminated and 30 Hz is the frequency which could pick up maximum power.

2.4.3 Features Extraction

The FAWT was used for ECoG signal decomposition. Dataset I was collected using 64 channels; it contains the total of 3000 samples. We applied the FAWT with J levels, where we had the approximate and detailed signal at each level [20,24,29]. These J+1 level's details were brought back to the time domain separately, leading to J+2 signals for each channel, where each channel corresponded to different details. For each of the corresponding J+2 levels, we computed correlation and wavelet entropy features [13, 24]. Above correlations and entropy were concatenated for all levels leading to a 2016*(J+2)*3 length feature vector for each channel [51–59].

The FAWT utilizes the Hilbert transform pairs of atoms and provides flexibility in order to control the redundancy, quality factor (QF), and dilation factor. It also helps in analyzing signals

with easily adjustable parameters, which are: up sampling factor for low pass channel (s), down sampling factor for low pass channel (t), up sampling factor for high pass channel (u), down sampling factor for high pass channel (v), and parameters that controls the QF (β). By applying the iterative filter bank structure, we obtained J^{th} level of FAWT. At each level, two channels are obtained from the decomposition. One channel corresponds to low pass filters and the other channel corresponds to high pass filters. The frequency response of low pass filter is expressed as:

$$f(w) = \begin{cases} (st)^{\frac{1}{2}} & |w| < |w_p| \\ (st)^{\frac{1}{2}}\theta(\frac{w-w_p}{w_s-w_p}) & w_p \leq w \leq w_s \\ (st)^{\frac{1}{2}}\theta(\frac{\pi-(w-w_p)}{w_s-w_p}) & -w_s \leq w \leq -w_p \\ 0 & |w| \geq |w_s| \end{cases} \tag{2.7}$$

While, the frequency response of high pass filter is expressed as:

$$R(w) = \begin{cases} (2uv)^{\frac{1}{2}}\theta(\frac{\pi-(w-w_0)}{w_1-w_0}) & w_0 \leq w < w_1 \\ (2uv)^{\frac{1}{2}} & w_1 \leq w \leq w_2 \\ (2uv)^{\frac{1}{2}}\theta(\frac{\pi-(w-w_2)}{w_3-w_2}) & w_2 \leq w \leq -w_3 \\ 0 & w \in [0, w_0) \cup (w_3, 2\pi) \end{cases} \tag{2.8}$$

For proper signal reconstruction, the following two conditions must be satisfied:

$$\theta|(\pi - w)|^2 + \theta(w)^2 = 1 \tag{2.9}$$

$$(1 - \frac{s}{t}) \leq \beta \leq \frac{u}{v} \tag{2.10}$$

The parameters of FAWT are deduced based on the above conditions, where s = 2, J = 16, u = 1, t = 4, and v = 2. Based on these values, the values of Q_F and β were 4 and 0.4, respectively. The QF was calculated using the following equation:

$$Q_F = \frac{(2-\beta)}{\beta} \tag{2.11}$$

We were able to produce the reconstructed ECoG signal and its 15 sub-band signals. The 16 signals are depicted in Figure 2.5. As shown in the figure, signals a - o are the sub-band signals. While, signal p is the reconstructed signal. Our feature extraction algorithm was implemented

in MATLAB [25]. Entropy MATLAB functions were used to extract entropy features from the reconstructed signal (i.e. signal p), the extracted features are as follows [16, 19, 20]:

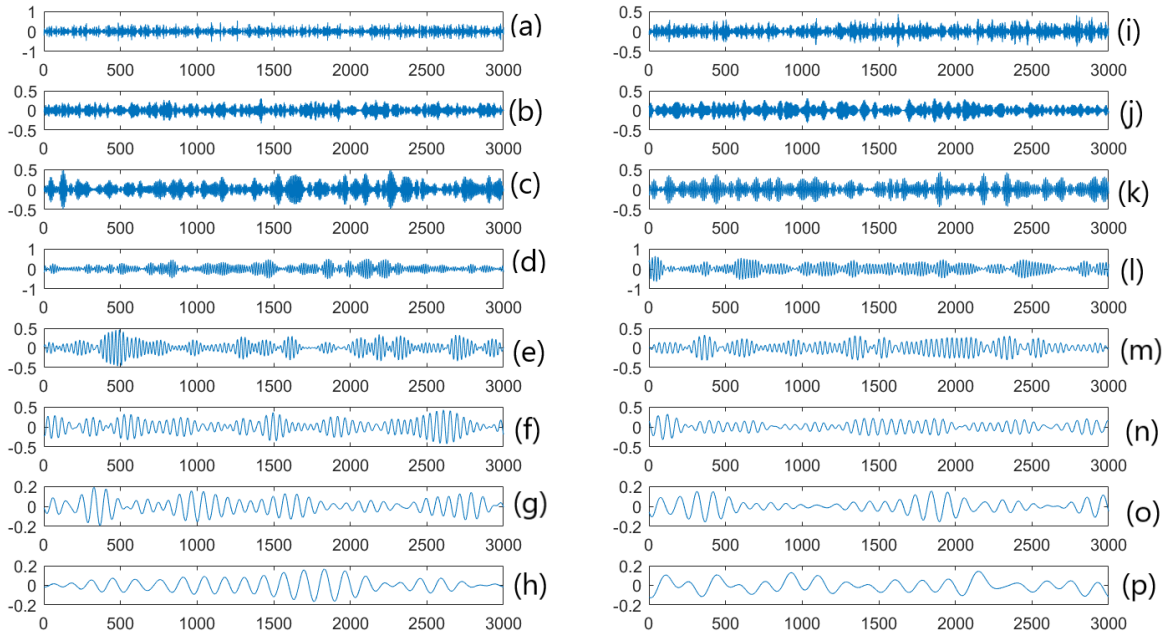

Figure 2.5: The 15 sub-band signals (a-o), and the reconstructed ECoG signal (p)

- **Cross Corr-entropy:** It is a generalized correlation of arbitrary processes that determines the similarity between two random variables [27–29]. With the help of cross corr-entropy, information can be captured from higher order moments. The cross corr-entropy was calculated as follows:

$$V_{N,\sigma}(x,y) = \frac{1}{N}\sum_{i=1}^{N} K_{\sigma}(X_i - Y_i) \tag{2.12}$$

  Where X and Y are the two random variables with N data samples, denoted by $(X_i, Y_i)_{(i=1)}^{N}$.

- **Log energy entropy:** To evaluate the degree of complexity in ECoG signals, the computation of log energy entropy is performed [26]. It is expressed in the following equation:

$$E_{LogEn} = \sum_{i=1}^{N} log(a_i^2) \tag{2.13}$$

Where N denotes to the length of the signal, and xi represents the i^{th} sample of the signal. To compute the log energy entropy, sub-band signals from 'X' and 'Y' channels of bi-variate ECoG signals have been used [12, 18].

- **SURE entropy:** The SURE energy is based on SURE [33], which is an accurate representation of a signal; it is the common measuring tool to quantify the properties that are related to the information. It can be expressed as:

$$E_{SEn} = N - \#\{\text{i such that} |x_i| \leq \varepsilon\} + \sum_i min(x_i^2, \varepsilon^2) \tag{2.14}$$

Where ε is a positive threshold value, x_i is the i^{th} sample of the signal, and X_i is sample observation.

2.4.4 Features Classification

Support vector machines have been widely used for pattern recognition [18]. To discriminate the dissimilar sets of patterns, this approach maps the data into a higher dimensional input space, which allows for a hyper-plane to be constructed. SVM classifier has the fewest square formulation known as an LS-SVM classifier. We have applied the LS-SVM to classify the brain activities. The discrimination function for the two class classification problem can be expressed as:

$$u(x) = sign[\sum_{i=1}^{N} \alpha_i u_i \phi(x, x_i) + b] \tag{2.15}$$

Here x_i, u_i, b, α_i, and $\phi(x, x_i)$, shows the i^{th} output vector and i^{th} input vector, bias, Lagrange multiplier and mapping function, respectively.

Different kernel functions can be used with LS-SVM (e.g. RBF and polynomial). The RBF kernel function is used in this thesis. The RBF non-linear maps examples into a larger dimensional space. It manages the status when there are nonlinear relations between labels of class and the attributes. After extracting the features in the previous step, we have implemented LS-SVM with RBF kernel. The bandwidth of RBF kernel was chosen using cross validation. By Using the corr-entropy, log entropy, and SURE entropy, and the RBF kernel, we obtained about 7% miss-classification error on the validation set.

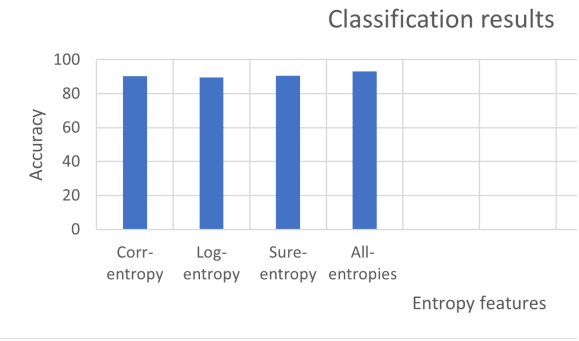

Figure 2.6: Classification Results

2.4.5 Evaluation and Results

Our proposed approach was evaluated by also using both the data set I of BCI competition III, and by carrying out test-bed experiment. The following sections elaborate the evaluation of our proposed system.

Dataset Based Evaluation

The aim of this study is to develop an accurate algorithm for extracting and classifying brain activities. Three entropy features were extracted from the ECoG signals. The FAWT was used to extract the features, and the LS-SVM with RBF kernel was used to classify the extracted features.

The performance of our classifier was evaluated using the data set I of BCI competition III data. Our classifier achieved 93.02% classification accuracy. This is considered as a significant improvement as compared to the approaches that are explained in Table 2.1. The evaluation results of classifying the left pinkie finger and tongue movements using our proposed classifier are explained in Figure 2.6. As shown in the figure, using the corr-entropy, a classification accuracy of 90.29% was achieved. A classification accuracy of 89.57% was achieved using the log entropy. Using the SURE entropy, the classification accuracy was 90.7%. While, using the three entropy features achieved a classification accuracy of 93.02%.

The data set I consists of 100 test preliminaries and our maximum accuracy throughout all trials (1000 times) was 93%. When we selected 70% of the available test data for each ensemble and used 5 ensembles, the highest accuracy on average is determined. Throughout each of our repeated experiments, 5 models were trained and tested, receiving 100 samples per trial. It is reasonable to expect that each example might get correctly classified in at least one of the 1000

trials. We found that trials 13, 16, 53, 56, 58 were not classified correctly at any point. Sample 97 was classified correctly only once in over 1500+ repetitions. Potential sources of error include erroneous samples from divergence in subject motor imagery (imagined moving the tongue instead of the finger, or vice versa). When these samples were removed, we obtained 99.35% classification accuracy with 5 fold cross-validation.

Test-bed Based Evaluation

This section introduces the evaluation of our proposed FAWT approach, using a test experiment. In order to evaluate our proposed extraction and classification approach, we replicated the brain environment in the lab. We used a chemical solution that duplicates the dielectric tissue [31, 32]. We used the same experiment for HRFE to mimic the brain environment and collect the brain signal.

We built wireless network based on the above experimental set up to mimic the brain environment using the NS2 simulator. Also because the data set I was collected from 64 channels, we have fed the data that we collected from the test-bed 64 times using the NS2 simulator by building a small network that consists of single transmitter and a single receiver in order to classify the received and not received signals as two classes. For our network, we used the WISP with specific parameters explained in Table 2.3. We have run our proposed extraction and classification algorithm and the accuracy to classify two classes (i.e. left pinkie finger and tongue) is 95%.

2.5 Various Classification Approaches

We have implemented many extraction and classification algorithms on the Data set I of BCI competition III data, and we evaluated them based on accuracy and time-consuming.

The following parameters were used to evaluate our classification models:

i) **Accuracy** Which is the sum of right forecasts divided by the total number of forecasts.

ii) **Precision** is the portion of important cases among the recovered occurrences.

iii) **recall** is the portion of applicable cases that have been recovered over the aggregate sum of significant cases. Both precision and recall are thus founded on comprehension and proportion of pertinence.

iv) **F-measure** in a statistical examination of parallel grouping, the $F1$ score (likewise F-score) is a proportion of a test's precision. It considers both the precision p and the recall r are on the test to figure the score.

Table 2.4: The baseline classification.

Classifier	ACC	Precision	Recall	F-measure
L1LR	0.564	0.592	0.5598	0.57463
L2LR	0.55	0.616	0.545	0.57768
Linear SVC	0.58	0.632	0.573	0.5995
LDA	0.542	0.568	0.539	0.5526
Shrinkage LDA	0.542	0.616	0.53711443	0.5711

2.5.1 Baseline

The baseline model is a learning algorithm that can be quickly implemented and offers a comparison for the prediction task at hand. The data set was pre-processed, followed by a 5 fold cross-validation using methods like Linear SVC, LDA, and Shrinkage LDA, L1 Logistic regression and L2 logistic regression. Default parameters were used (in Scikit learn) for all the models. Table 2.4 shows that LinearSVC is the best model, with an accuracy of 58%.

2.5.2 ECoGNet

In this deep ConvNet, there are four convolution-max-pool blocks. The first block deals with ECoG inputs, followed by three standard convolution max-pool blocks. A dense layer with softmax follows this. The softmax yields/classifies a signal and categorizes it amongst the K classes.

Determining the representation of input x_j^2 is necessary when applying ConvNets for decoding. We represent the ECoG signal as a timing chain of images organized topographically as voltage division across the surface of the flattened scalp. The data is also normalized before passing it to the ConvNet. The loss function used for improving the training accuracy is represented in equation (2.16).

$$\theta = min_\theta \sum_{j=1}^{N} loss \cdot (y^i, P(l_k| \int_k (X^i; \theta)). \tag{2.16}$$

Commonly, the negative log probability of labels is used for training a ConvNet. The parameters are optimized using mini-batches of stochastic gradient descent during back-propagation. Both Linear and Elu activation functions were used to compute the performance of the model. This method did not obtain high accuracy compared to other networks. The results for ECoGNET with Elu are summarized in Table 2.5.

Table 2.5: The ECoGNet classification.

Classifier	**ACC**	**Precision**	**Recall**	**F-measure**
ECoGNet	0.652	0.70624	0.6678	0.63662
ShallowConvnet	0.816	0.8984	0.7798	0.82803889

2.5.3 Shallow ConvNet

Shallow ConvNet is simplified to compose of one advantage layer, convolution filtering and the average pooling. The Network architecture is as proposed in Fig. 2.7. S2 follows the convolution layer C1, a pooling layer, followed by C3 (convolution), S4 (pooling) and C5 (convolution) layers. Convolution layer C1 has eight feature maps, with each feature map having 24×24 neurons. Similarly, pooling layer, S2 has eight feature maps and 12×12 neurons for every feature map.

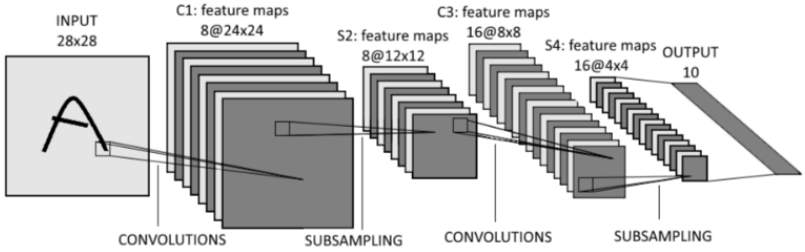

Figure 2.7: Simple Shallow Convolution Neural Network.

Gradient descent is used to reduce the Mean Square Error (MSE) between the desired output and Neural network's output. MSE uses the last layer's output as follows:

$$E_S = \frac{1}{2}\sum_{k=1}^{l}\sum_{j=1}^{m}(y_i^k - e_j^k)^2 \tag{2.17}$$

where y_j^k and e_j^k are desired output and neural network's output respectively. After that, by using a gradient descent approach, we can write learning of mini-batch as below:

$$W_{Cij}(t+1) = w_{Cij}(t) - \alpha \cdot \frac{\varpi \cdot E(r)}{\varpi \cdot w_{Cij}(t)} \tag{2.18}$$

where α is the learning rate, $\mathbb{E}(r)$ is the expectation error for r samples. Since the units of each feature mapping in a convolutional layer contain the sets of the same weight:

$$\frac{\varpi \cdot \mathbb{E}(r)}{\varpi \cdot w_{Cij}(t)} = \sum_{i,j} \frac{\varpi \cdot \mathbb{E}(r)}{\varpi \cdot w_{Cij}(t)} \tag{2.19}$$

As a result of batch learning case, we can get delta for updating weights:

$$w_{Cij}(t+1) = w_{Cij}(t) - \alpha(t) \sum_{i,j} \sum_{k} \gamma_{i,j}^k \cdot (S_{ij}^k) \tag{2.20}$$

The results for ShallowConvNet are better than that for ECoGNet. In general, it was between 75-81% accuracy as shown in Table 2.5.

2.5.4 PCA + LDA and ICA + LDA

We also statistically analyze Principal Component Analysis (PCA), Linear Discriminant Analysis (LDA), and Independent Component Analysis (ICA). PCA concentrates on Gaussian and uncorrelated components. Also, it is a second-order statistics, and the transformation is orthogonal (Algorithm 2).

Algorithm 2 Principal Components Steps

Step 1: Collect data points X_i of N dimensions, where $i = 1, 2, ..., m$

Step 2: Calculate the Co-variance matrix (C) as:

C= (X_i m· X)·(X_i m · X)· T

Step 3: Find eigen vectors and eigen values

Step 4: Sort the previous values in descending order

Step 5: Chose the first d that are less than or equal the number of vectors then generate new data set representation

Step 6: Compare every projected training data with projected test data using similarity measure

2.5.5 Independent Component Analysis(ICA)

A statistical procedure transforms the observed vector that is random and multi-dimensional into many statistically independent components. For a non-Gaussian distribution with considerable variation, PCA cannot be used. ICA can decrease both the higher and second-order data and helps to find statistically independent data. ICA is considered as a particular case of the redundant technique. When compared with many statistical methods, we found ICA to be more powerful than PCA. ICA concentrates on non-Gaussian and independent components, higher-order statistics, and non-orthogonal transformation (see Algorithm 3).

Algorithm 3 Independent Components Steps

Step 1: Collect X_i from m dimensional Dataset X, where $i = 1, 2, ..., m$

Step 2: Calculate Co-variance matrix C as defined below: C = (X_i m·X)·(X_i m·X)·T

Step 3: x factorize to the covariance matrix C

class $S1$ and the matrix of the second class $S2$

Step 4: Transform data X into Z that the components are independent

Linear Discriminant Analysis (LDA) is a reliable technique for dimensionality reduction for classification problems. The underlying space vectors are used to discriminate among classes. The primary goal of LDA is to maximize the measure of class scatter matrix (see Algorithm 4).

Algorithm 4 LDA Steps

Step 1: Samples for Class1 and Class2

Step 2: Calculate the mean of class1 as $\mu 1$ and class2 as $\mu 2$

Step 3: Calculate Co-variance matrix of the first class S1 and the matrix of the second class S2

Step 4: Calculate class scatter matrix using (in-between-class and within-class scatter matrix) using :

SW = S1 S2

$SB = (\mu 1 \mu 2) \cdot (\mu 1 \mu 2)$

Step 6: Compute the LDA projection, then LDA projection is obtained as a solution of generalized eigen value problem

Step 7: Compare the matrix of the test data projection with matrix of projection of every training data using similarity measure

The PCA method was revised and used for reducing dimensionality of the ECoG data. It was followed by using LDA for classification to see if it works better. This is proved to be ineffective. With 100 ICA components, performance was lost. The results are presented in Table 2.6.

Table 2.6: PCA + LDA for reducing dimentionality.

Classifier	ACC	Precision	Recall	F-measure
L1LR	0.716	0.752	0.70351074	0.72613061
L2LR	0.682	0.64	0.70021887	0.66784365
Linear SVM	0.698	0.656	0.71577985	0.68417538
LDA	0.612	0.516	0.64203995	0.57052355

We then combined PCA, ICA, and ShallowConvNet and found an accuracy of 80.6%.

2.5.6 Auto-regressive coefficients

Auto-regressive (AR) models are representative of a random process. They can be used for describing a specific process which is time-varying in nature. In Machine Learning, the Auto-regressive model learn from the chains of steps which are timed. It takes measures from past procedures as an input to the regression model, to get the next step's value. It is a type of a Vector Auto-regressive model (VAR), containing a system of one or more than one interlocking stochastic variation equations. We were inspired to use AR coefficients from [2] which states that AR coefficients are successful in ECoG motor imagery. The notation AR (p) suggests an Auto-regressive model of order p. There are many ways to estimate the coefficients, for example, least squares or Yule-Walker equations. Table 2.7 presents the results for p=8. Data was subsampled to 300 time points, followed by feature selection using RFE, where in 25 features were selected.

Table 2.7: AR coefficients model.

Classifier	ACC	Precision	Recall	F-measure
L1LR	0.85	0.752	0.94664741	0.82961039
L2LR	0.86	0.76	0.94987436	0.84387322
Linear SVM	0.856	0.828	0.87865646	0.85185753
RBF and SVM	0.814	0.9	0.77022101	0.82933132
LDA	0.824	0.832	0.8244533	0.82587714

The results obtained in Table 2.5 are not a significant improvement over our previous methods. However, after changing the data sub-sampling to 750 time points, AR coefficients to 10, and

allowing feature selection only up to 20 features, we got 91% accuracy as shown in Table 2.8.

Table 2.8: AR coefficients with feature selection.

Classifier	ACC	Precision	Recall	F-measure
L1LR	0.91	0.872	0.94391557	0.90638663
L2LR	0.86	0.828	0.88618377	0.85471281
Linear SVM	0.826	0.832	0.82261554	0.82659695
LDA	0.794	0.776	0.80940077	0.78933053

2.5.7 MA coefficients with feature selection

Moving Average Model (MA) model: The time series model is the ARIMA model, which may include auto-regressive term with or without moving average terms. Moving the average term in a time series model involves multiplying an old error by a coefficient. The first order MA model, is defined as MA (1), where:

$$X_t = \mu w_t \theta_1 \cdot w_t - 1 \tag{2.21}$$

The second order MA model, defined by MA (2), where:

$$X_i = \mu w_t \theta_1 \cdot w_t - 1 \theta_2 \cdot w_t - 2 \tag{2.22}$$

the qth order MA model is defined as:

$$X_i = \mu w_t \theta_1 \cdot w_t - 1 \theta_2 \cdot w_t - 2 \cdot \theta_q w_t - q. \tag{2.23}$$

For time series prediction relies heavily on both AR and MA features, MA coefficients up to order 10 was used, for data with 300 time points. Accuracy obtained was lesser than previous trials, as seen in Table 2.9.

Table 2.9: AR coefficients and MA features.

Classifier	ACC	Precision	Recall	F-measure
L1LR	0.812	0.9	0.76805299	0.82791475
L2LR	0.846	0.868	0.83161614	0.84918393]
Linear SVM	0.828	0.74	0.90035816	0.81103429
LDA	0.768	0.604	0.90088739	0.72186571

2.6 Discussion of Analysis

This study aims to develop a fast and efficient algorithm for extracting and classifying brain activities. In this part, we are evaluating all the proposed algorithms based on accuracy and time classification. Table 2.10, shows FAWT has a competitive accuracy, but it is very slow, so it is not suitable for the lifetime brain data. Nevertheless, HRFE has higher accuracy, which is 93%, and the classification time is 5 minutes, which make it is a better approach than all the other approaches.

Table 2.10: Evaluation of proposed algorithms.

Algorithm	**Accuracy**	**Classification Time**
L1LR	56%	50 seconds
L2LR	55%	100 seconds
SVM	58%	150 seconds
ECoGNet	65%	98 seconds
L1LR + AR	85%	130 seconds
L2LR + AR	86%	145 seconds
SVM + AR	85.6%	170 seconds
LDA + AR	81.4%	220 seconds
L1LR + MA	91%	6 minutes
L2LR + MA	86%	6.3 minutes
SVM + MA	82.6%	7.8 minutes
LDA + MA	79.4%	8.2 minutes
HRFE + AR	93.05%	3.8 minutes
FAWT	92%	2 hours

In this thesis, many techniques have been investigated to reach these performances, as explained in Table 2.10. Machine learning techniques are widely used to classify the possible ECoG brain signals collected from inside the brain using implantable passive wireless sensors at different implant depths [29, 30]. Therefore, the novel hierarchical recursive feature elimination (HRFE) along with noise addition techniques are used in this research to overcome the problem of classification's accuracy in conventional BCI communication schemes which significantly affects the system performance.

Chapter 3

Signal Acquisitions-Noise Cancellation

3.1 Noise Cancellation

During the last decade, intensive research efforts have been performed on the promising brain-computer interface (BCI) technology for various health applications. It is used mainly to facilitate direct communication links between the central nervous system of human beings with the external electronic devices. This approach can be considered as a novel extension to the initial objective of BCI, represented by the realization of immediate communication environment between the brain and embedded devices, to help patients suffering from spinal cord injuries, paralysis situations, and amyotrophic lateral sclerosis [70–73] . In practice, BCI schemes have the effects to reduce the need for typical information delivery methods and then improve the lifestyle of disabled persons. On the other hand, massive number of devices/machines can be connected to the Internet, usually referred as the Internet of things (IoT), allowing a fundamental shift in the way that individuals can interact with the surrounding objects [25]. Therefore, the integration of IoT and BCI schemes represents an emerging technology to control varied personal phones and computers, electronic and wearable devices, smart machines, and other modern smart home applications. This will make the home/office environment more accessible and comfortable for disabled persons as well as normal users by simply employing their neuronal signals (i.e. brain reactions and thoughts) [74–77].

3.2 Technical Background

Most of the persons with tetraplegia have flawless cerebrum work, but cannot move due to some damage/infection that influences the spinal cord. Therefore, different BCI schemes are developed to sidestep the harmed nerves and build up an alternative connection between brain signals and embedded devices to re-establish muscles' development or co-appointment of paralyzed muscles [7, 11]. For instance, Fig. 3.1 (a) shows how the bypass wireless channel can handle the wireless transmission of brain messages as encoded data through BCI to activate and control the movement of paralyzed arm through external controller (brain spine interface, BSI) or implanted device. The implementation of utilizing BCI requires bio-compatible electrodes for signal interface with neurons in the brain's cortex and an external transceiver device on the scalp to receive the electro-corticographical (ECoG) signals and re-transmit them to the intended controller on the defective part of the disabled person's body [30].

On the other side, BCI can be considered as an emerging alternative for supporting interaction between IoT objects and individuals as shown in Fig 3.1 (b). In this scenario, the ECoG signals of wheelchair user are transmitted with high data rate to the implanted external transceiver on the scalp and then to the analyzer device (such as computer, tablet, and smart phone) for data analysis and examinations with pre-portrayed examples. The determined person's order is then sent through IoT network to the intended smart devices/applications for desired actions.

In any of the aforesaid BCI applications, information messages are transmitted with high data rate using one of the well-known signal modulation methods such as quadrature phase shift keying (QPSK) to the receiver side [29] [78, 79]. Besides, the efficient BCI communication system can be determined typically when a distortion free transmission from the wireless transmitter in the brain to the receiving end on the scalp is achieved. However, realization of this target is difficult owing to the effect of in-phase/quadrature (I/Q) imbalance in the employed frequency down converter and time interleaved analog-to-digital converters (TI-ADCs) at the receiver processor. In particular, the gain and phase imbalance in the two paths of analog processor can cause undesired coupling between the positive and negative frequency components of the signal carried by these paths [80–88]. This may potentially lead to a considerable interference level to desired signal which affects the detection performance, and hence the required response. Therefore, controlling this kind of mismatch is very important in the utilized receivers that detect signals spanning a wide range of levels as might be found when extracting one or more channels in multi-channel filter banks. This will have a direct impact to improve the performance of the BCI system significantly.

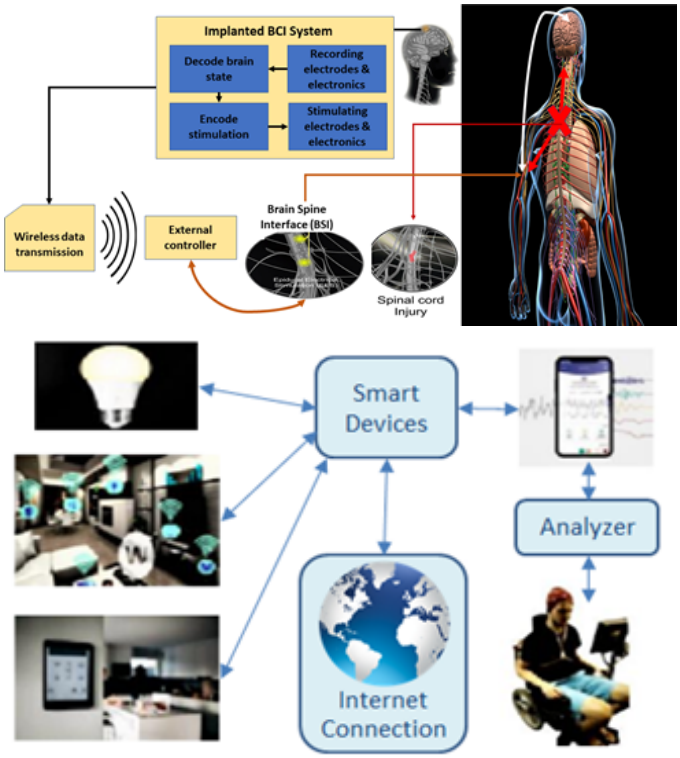

Figure 3.1: BCI applications: (a) Spinal cord using by-pass wireless channel; (b) Brain control for smart devices and IoT network

3.3 Aims and Contributions

The employment of signal processing techniques to undo the signal degradation caused by the analog I/Q imbalance is adopted as an efficient solution in varied electrical, electronic, and communication systems [81–86]. This comes against the common idea that this kind of distortion is challenging and irreversible [80]. In this thesis, we aim to mitigate the inherited I/Q imbalance in BCI communication systems using low complexity balance technique to achieve the target performance and exploit this important technology. The main contributions of this work are summarized as follows:

- An efficient low complexity balance technique is proposed for BCI communications to mitigate the interference caused by I/Q imbalance using the adaptive least mean square (LMS) algorithm. The integration of these cost-effective approaches is very important for feasible BCI applications towards the wide adoption of this technology.

- For the considered technique, we present the time model of I/Q mismatch in BCI and the

employed adaptive cancellers to correct the DC offsets and imbalance defects of frequency down converter and QPSK signalling. A balanced model is demonstrated then to cancel the DC offsets and spectral artifacts produced by the pair of TI-ADCs.

- Performance outcomes of conducted tests on a near-realistic phantom model of human brain demonstrate the effectiveness of designing balanced BCI (BBCI) scheme compared with the generic BCI [29, 30].

3.4 System Model of BCI Communications

In this work, we consider a wireless BCI communication system for health applications as shown in Fig.3.2. It consists of an implanted BCI transmitter unit, wireless channel, and receiver device. The brain ECoG signals from implanting electrodes are modulated using QPSK technique, and the generated radio frequency (RF) signals are transmitted, then over wireless channel through brain tissues to the fixed receiver on the scalp. The received RF signal with an additive white Gaussian noise component is pre-filtered as in the typical communications systems to eliminate the noise effects [89]. Then, it will be down converted and sampled using the ADC unit for signal demodulation. The demodulated brain signals are processed to prepare the information and control messages for the response/analyzer device, while a parameter estimation and balance unit is used to solve the problem of I/Q imbalance in BCI system.

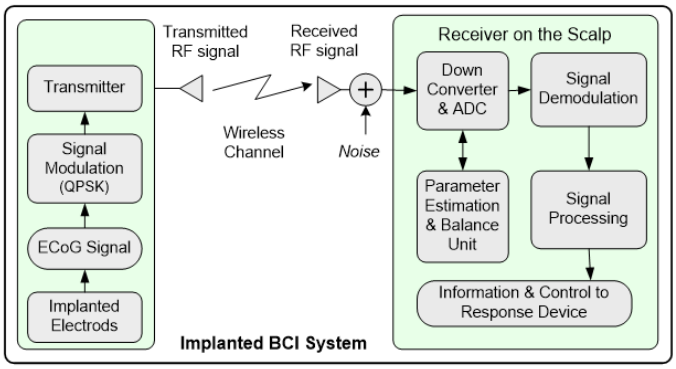

Figure 3.2: System model of a general wireless BCI communications.

Note that the propagation delay due to wireless signal propagation between the implanted electrodes and the reader on the scalp through human tissues can be mitigated using multiple in-

brain transmitters and relevant multiple access technique as in [30]. This has a direct impact to satisfy the required user experience. But, the signal propagation delay between mounted device on the scalp and computer/smart devices through indoor wireless channel has no significant impact on the performance of BCI as in the existing wireless systems [90]. Moreover, other signal processing delays can be ignored based on the advancement in digital signal processing chips [72].
As in our previous work [30], a wireless identification sensing platform 5 (WISP5) is used for the adopted BCI system. It is based on a passive RF identification (RFID) tag that works for an ultra-low power and micro-controller for sensing, processing, and communication [91]. The receiver on the scalp is implemented using an RFID reader such as Impinj's Speedway model [92–94]. This RFID model is used to detect the WISP signals and also emits RF signals (in the frequency range 908–928 MHz) to send commands and power to the implanted WISP tags. The reader is supported with an antenna and Ethernet connection for data transmission to intended controllers such as laptops/smartphones.

3.5 Proposed Balance Technique for BCI

For QPSK signalling, a balanced modulator is required, which can be comprised of two matched amplitude modulation modules. However, maintaining perfect balance between these modulation modules over RF carrier is not an easy process in the BCI communication system. This kind of imbalance between I/Q channels may result in a signal distortion leading to undesired inter channel interference (ICI) and increased error rate performance [78]. For instance, when a target bit error rate of 10^{-6} is desired, the required levels of amplitude imbalance and phase imbalance should not exceed 1 dB and 5o, respectively [81, 82]. Therefore, an efficient low complexity balance method is proposed in the following.

3.5.1 IQ Down Converter

The received QPSK ECoG signal in BCI is processed using IQ down converter which consists of two branches of multipliers, low pass filters (LPFs), and ADCs as shown in Fig. 3.3 (a). The in-phase and quadrature components for down conversion are represented by I=cos(ωt) and Q=sin(ωt), respectively, where $= 2\pi$f, and f denotes the carrier frequency. The mismatch in IQ down converter which leads to ICI is shown in the second path due to phase distortion (α) and gain

distortion $(1+\varepsilon)$ elements. The time-domain model of I/Q mismatch is demonstrated in Fig.3.3 (b). This model shows also the insertion of DC components in both of in-phase and quadrature paths due to the utilized ADCs.

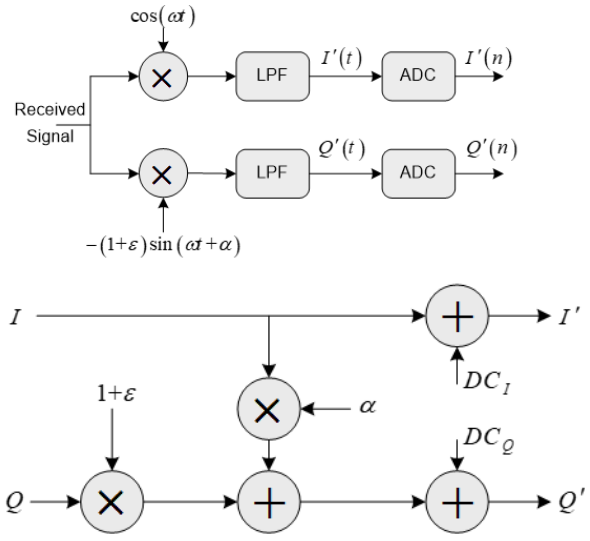

Figure 3.3: IQ down converter: (a) I/Q mismatch representation;
(b) Time-domain model of I/Q mismatch.

This can be explained mathematically without showing the time index n as

$$\hat{I} = I + DC_I \tag{3.1}$$

$$\hat{Q} = Q(1+\varepsilon) + \alpha I + DC_Q \tag{3.2}$$

where $\alpha = \eta sin(\phi)$; $\varepsilon = \eta cos(\phi) - 1$; and ϕ represent the amplitude and phase elements of distortion signal, respectively. So, the quadrature component can be simplified and rewritten as

$$\hat{Q} = \eta sin(\omega t + \phi) + DC_Q \tag{3.3}$$

It can be seen that the I and Q signal components are not orthogonal due to gain and phase imbalance as well as a DC insertion in both signal paths. Therefore, and elements should be estimated, as and , for possible signal correction with DC cancellation.

3.5.2 TI-ADCs

In the utilized receiver, ADCs are used to convert the modulated RF signal into digital form. This is followed by signal detection using digital signal processing unit to extract the transmitted ECoG messages. In this case, the ADCs need to convert analog signals of large bandwidth to digital forms with high processing speed and sufficient conversion accuracy. To avoid the aliasing effects, the sampling rate f_s must fulfil the Nyquist rate at least (i.e. $f_s \geq 2f$).

In general, the sampling rate can be increased using parallel ADCs with different sampling points of time, and higher digitization rate can be obtained by interleaving the outputs of each ADC using TI-ADC approach. However, time interleaving in ADCs may produce unwanted artifacts in the signal's spectrum (due to $DC_I and DC_Q$ components) and ultimately leads to performance loss and accuracy degradation. Therefore, removal/correction of the unwanted artifacts in TI-ADCs is very essential to achieve high system performance [82].

3.5.3 Adaptive Canceller Model for BBCI

To mitigate the drawbacks of down converter and TI-ADCs, an adaptive canceller model based on the well-known LMS algorithm [93, 94] is designed for BBCI scheme as shown in Fig. 3.4 The DC cancellation units are used to remove the DC_I and DC_Q components from desired I and Q signals, respectively. Besides, and estimation units with LMS technique are used to provide and elements, respectively, for desired signals' correction.

The LMS algorithm is one of the adaptive filter approaches typically used to estimate the desired filter coefficients which have the effect to produce the least mean of a squared error signal (i.e. the difference between desired and actual signals). This method is based on a stochastic gradient-descent where the filter coefficients are adapted based on the realized error at the current time instant (more details can be found in [93, 94]). Therefore, to mitigate the ICI, the adaptive LMS algorithm is used in our model to estimate the phase and gain parameters, $\hat{\alpha}$ (n) and $\hat{\varepsilon}$ (n), at current time sample n from actual values by minimizing the following cost functions

$$C_\alpha(n) = E\{|e_\alpha(n)^2|\} = E\{|\hat{\alpha}(n)\alpha(n)|^2\} \tag{3.4}$$

$$C_\varepsilon(n) = E\{|e_\varepsilon(n)^2|\} = E\{|\hat{\varepsilon}(n)\varepsilon(n)|^2\} \tag{3.5}$$

where E{.} is the expectation (mean) operator while $e_\alpha(n)$ and $e_\varepsilon(n)$ denote the errors at the current time sample n. The parameters $\hat{\alpha}$ (n) and $\hat{\varepsilon}$ (n)) are used then to find $\hat{I(n)}$ and $\hat{Q(n)}$ signals, respectively.

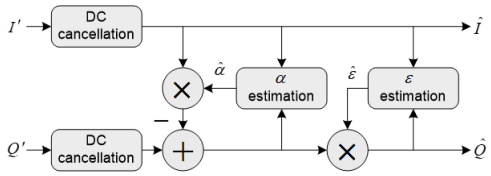

Figure 3.4: Adaptive canceller Model for BBCI scheme.

3.6 Experimental Setup of BBCI and Results

To show the effectiveness of BBCI, we have conducted different experiments on phantom brain model. We replicate the near-realistic brain environment using salt water as blood, glycerine to mimic tissues, and plastic beaker to mimic the skull. These adopted materials are used due to their close dielectric properties with the brain. A single wireless sensor (WISP5) is used to transmit the collected signals from the implanted electrodes at a depth of 2 cm in the brain tissue to the BBCI receiver on the scalp.

The considered experimental setup for this work is explained in chapter 2 and 4. To the best of our knowledge, this work is the first of its kind and there is no close reference for fair comparisons. Therefore, we have compared the achieved results with that generated from the generic BCI scheme without balance technique in [29, 30] to validate the proposed BBCI design.

Performance of the DC canceller in BBCI is demonstrated in Fig. 3.5 which shows how fast the trajectory curve can learn as a function of time samples (for both in-phase and quadrature components) and then efficient cancellation process for the system DC offset. Similarly, Fig.3.6 demonstrates the fast convergence of phase and gain estimates based on LMS algorithm to detect the signals without distortion.

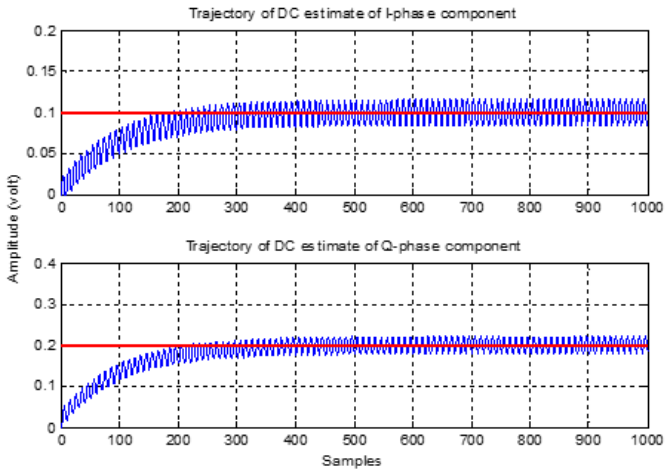

Figure 3.5: Learning curves of the in-phase and quadrature DC components (amplitude in volts) of BBCI as a function of time samples.

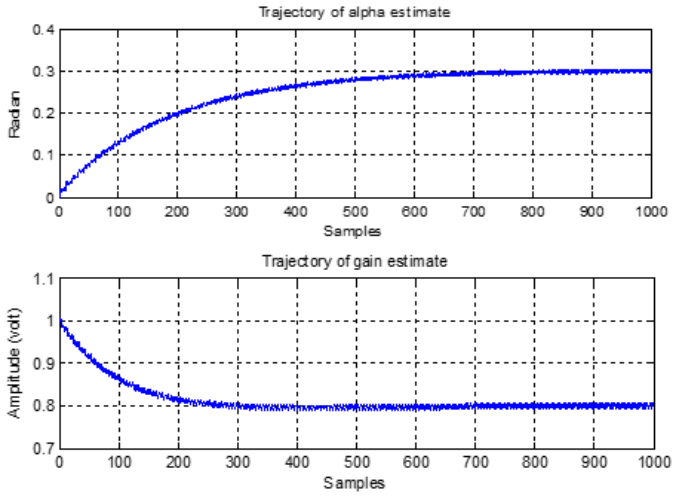

Figure 3.6: Parameter estimation based on LMS algorithm:
(a) Phase estimate in radian as a function of samples;
(b) Gain estimate in volts as a function of samples.

The impact of ICI in BBCI scheme with QPSK signalling is shown in Fig. 3.7 through Lissajous patterns and constellation diagrams of the detected signals. From Fig. 3.7 (a) of Lissajous patterns, it can be seen clearly that both of phase and gain components (distorted BCI signals) are corrected by the end of balancing process using BBCI scheme. This is shown also in Fig. 3.7 (b) where a clear QPSK constellation is achieved in BBCI system after cancellation of the DC offset, phase error, and gain imbalance.

The spectrum (in log magnitude) of the TI-ADCs are shown in Fig. 3.8 after the DC can-

cellation as a function of the number of received time instance of: (a) first 2000 samples and (b) last 2000 samples. The spectrum of the output signal of balanced model is demonstrated also in (c) for the first 2000 samples and (d) for the last 2000 samples. These figures demonstrate that the first samples will suffer from possible signal distortion due to the imperfect estimation of the system parameters. But, the system will converge to best estimate and produce reliable performance as the time samples grow.

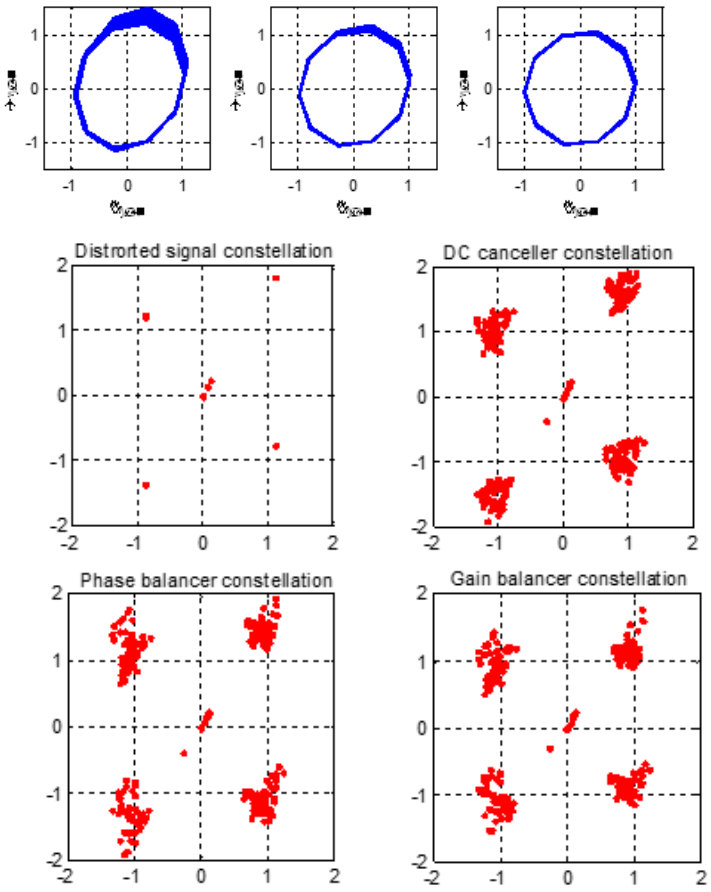

Figure 3.7: QPSK of distorted (BCI signals) and non-distorted signal components (BBCI signals): (a) Lisasajous patterns; (b) Signal constellation.

3.7 Discussion

Signal processing techniques are widely used to considerably alleviate the possible signal degradation produced by the I/Q imbalance in diverse electrical, electronic, and communication

systems [81–86]. Therefore, the existing I/Q down converters and LMS techniques are used in this research to overcome the problem of I/Q imbalance in conventional BCI communication schemes that greatly affects the system performance.

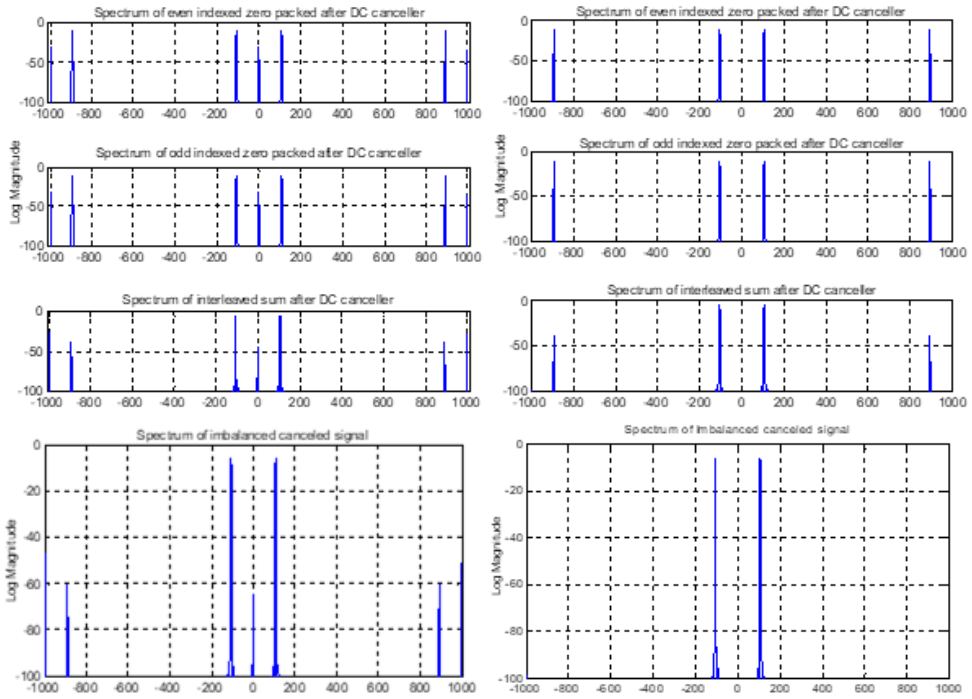

Figure 3.8: Spectrum (log magnitude) of TI-ADCs after dc cancelling as a function of time instance for: (a) first 2000 samples and (b) last 2000 samples. Spectrum of output signal of balanced model for (c) first 2000 samples and (d) last 2000 samples.

To the best of our knowledge, the integration of these existing methods into the BCI system is the first of its kind and demonstrated a cost-effective solution for feasible wireless BCI applications.

The achieved results of proposed balance technique over near-realistic environment demonstrate the effectiveness of designing BBCI communication system with approximately distortion free QPSK transmission. This has been validated through different performance measures such as trajectories of parameter estimation, Lissajous patterns of the I/Q components, and signal constellation diagrams. It is shown that the inherited effects of I/Q imbalance in the employed down converter and TI-ADCs (i.e. DC offsets and spectral artifacts), as in the existing BCI system [29, 30], can be mitigated using low complexity and cost-effective balance technique which includes parameter estimation and balance circuits. In this case, the unwanted coupling between frequency components of I/Q signals is removed in an effective manner. This is reflected on the received signal constellation and hence the performance of the BBCI system for modern and future special

purpose wireless applications.

3.8 Conclusion

In this thesis, an adaptive low complexity balance technique based on LMS algorithm is designed for wireless BCI communications to mitigate the inherent interference due to I/Q imbalance of utilized down converter and TI-ADCs. The achieved performance results of conducted experiments on a near-realistic phantom human brain model demonstrate the effectiveness of proposed scheme compared with the existing BCI. It shows fast convergence of estimated phase and gain parameters and accurate DC offset cancellation that allow an improved QPSK performance. In future work, the blind equalization technique will be used to demonstrate the complexity-performance trade-off. Besides, performance analysis and evaluation over the actual human brain environment will be considered.

Acknowledgment

We thank Dr. Walid Al-Hussaibi for his useful contribution.

Chapter 4

Signal Transmission-Choice of Transmitter Overview

4.1 Choice of Transmitter Overview

Bi-Directional Brain Computer interfacing(BBCI) is a developing technology that has many potential applications for restoring motor control for paralyzed patients as well as providing tactile feedback to the brain. However, current technology uses a wired connection between implanted electrodes and an external device which processes and transmits the information. This wired connection makes creates a great risk of infection, making it significantly less viable for use in human subjects. Additionally the implant being wireless allows the operative field to fully heal post-surgery. The early studies were targeting battery-free sensors with arrange of 1 meter or more which sensing a simple quantities such as temperature or light intensity [36], or neural signals [95] or specific motion [96].The new electronic neural or the efficacy of electronic neural implant, which developed later has been enabled previously impossible brain-research experiments [97], and main improvement has been made toward neutrally controlled Prosthesis [98]. Near-field inductive link to transmit power and data has been introduced and achieved wireless operation [97, 99]. However, this technique required the external coil be placed within a few centimeters of the internal coil.

In this thesis, we present a wireless Identification sensing platform (WISP5) which is a fully-passive UHF RFID tag that uses an ultra-low power, micro-controller for sensing and RFID communication by harvesting power from RF energy provided by a radio frequency identification (RFID) reader.WISP5 technology based on back-scatter modulation, each tag responds with

a unique identification number by reflecting energy back to the reader, the more power that is transmitted the longer the read range of the tag.

To insure safety [64, 100], The Federal Communication Commission(FCC) in the United States limits the power transmitted in the Industrial, Scientific, and Medical (ISM) radio band (902 MHz-928 MHz) to 4 W (EIRP) [100].

UHF-RFID is one of the best options for wireless communication inside of the human body due to its extremely low transmission power requirements. If the transmission power requirements are too high then the system cannot be charged in wireless format requiring repeated surgeries to replace batteries. There are no real-time UHF-RFID communication channel models designed to examine the transmission of signals using multiple transmitters. Implementation of multiple transmitters in the brain requires a suitable medium access control(MAC) protocol to support maximum throughput [101–103]. The purpose of this study was to investigate the feasibility and application of multiple implantable UHF Passive RFID transmitters inside the brain for capturing multi-channel ECoG signals at high data transfer rates.

4.2 Related Works

Channel characteristics for BCI applications is very important in biological channel design. It is crucial to maintain or restore the integrity of the transmitted signals as they travel through skin, muscle, blood, bones, and other tissues.The basic foundation of the BCI application will be destroyed if the receiver fails to receive and interpret a signal exactly the way the signal was generated. For this to happen , the transmission characteristics of the ECoG signals have to be studied when it propagates through the brain to the outside world. Mainly to make sure it is received at the receiver sitting outside the brain on the scalp with enough power level and information to decode the signals. Literature for the channel model in biological communication is less as compared to channel models in mobile communication. Knowledge of channel characteristics such as path loss, received signal strength, signal to noise ratio, channel capacity etc, is imperative when discussing the theme of BCI. The IEEE 802.15.6 didn't focus on a particular part of the human body or human tissue [121] which used in [122] and the results show it didn't fit well with the measured data. [123–125] described the Channel modelling for body communication. The edge cut product that we have today on the market based on using implanted electrodes to capture the data and transmits to a transmitter located on the scalp through wires which creates infection in the brain due to scar tissue which might lead to neural injuries. Fig 4.1 shows our contribution by

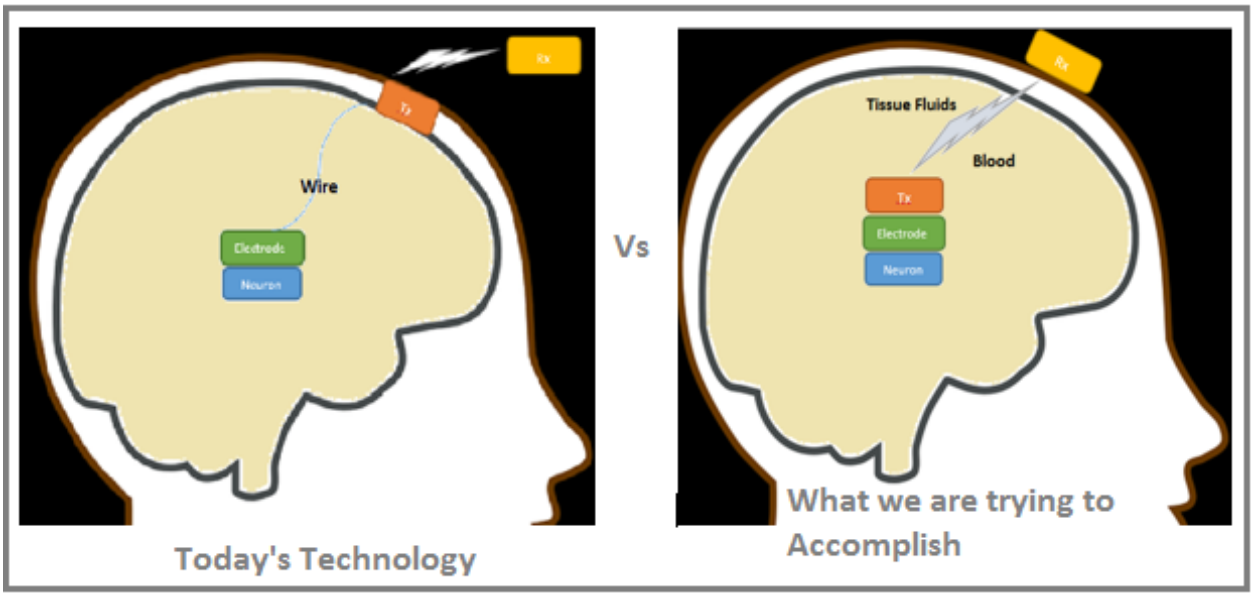

Figure 4.1: Multiple implantable transmitters in brain

replacing wired technology with a transmitter sitting on the electrode and transmit to a reader set on the scalp in wireless format.

4.3 BCI Applications

Smart, Interactive devises plays an important role in the modern age. BCI has been involved in many applications. For health care, there are many issues have been considered in order to develop a complete health care framework [116] such as low-cost modelling and designing, investigating signal transmission characteristics, and system scalability. Moreover to develop smart bio-medical devices such as Mammograms [117, 118] sophisticated digital signal processing, machine learning, and data science are considered along with a deep understanding of BCI underlying processing [120]. Forensic applications such as lie detection, brain fingerprinting, and trust assessment, BCI plays a core role to detect and extract specific information from the neural signals. Entertainment like mood assessment [119], “thought control”, fast response detection considered one of the best BCI applications. Additionally multivariate pattern analysis / brain imaging has been considered as one of the most important BCI applications.

4.4 Need Of Multiple transmitters

It is very imperative to understand the need of multiple transmitters in human brain to transmit wireless signals to a controller placed outside the brain as advancements in BCI technology are made. Previous investigations have considered single transmitters but none with multiple transmitters as it induces complexity with the introduction of simultaneous multiple access [101–103].

The focus of our work is to implement multiple transmitters, which would, potentially help, in restoring the upper limb movements for paralytic patients using BCI. It is well understood that the area of the Cerebrum is responsible for upper limb movement generation. An arm movement using a BCI system requires a significantly large number of cortical neurons for signal generation. It has been shown that an array of 512 electrodes can be used to generate meaningful arm movement [108, 109]. In terms of packet/data loss and delay single transmitter would be insufficient to transmit multiple signals. The small size of the BCI can cause This kind of loss and delay to perform such rapid acquisition and transmission of signals. Moreover, the deficiencies in the transmitter would cause system failure. To capture more data, the consideration of complexity and density of neural signals transmitted in wireless form is needed. Although using multiple tags increases the quality and quantity of the ECoG signals by capturing more signals, it would also increase the probability of collision between the multiple tags. To solve this issue Time division multiple access TDMA algorithm has been developed to eliminate the probability of signal collision.

Previous work [115] states how the throughput decreases and the delay increases as the number of transmitters increases for transmitting data. OPNET has been used to examine how multiple transmitters work in term of delay and throughput.Three scenarios have been used; first scenario 2 transmitters with one receiver, second scenario 3 transmitters with one receiver, and Third scenario 4 transmitters with one receiver.

The study [115] shows that the patients who are severing from Tetraplegia the delay is an average from 90 ms to 100 ms in a human body. Also, it states that we can use up to three transmitters to transmit simultaneously because more than 3 transmitters the delay will be nearly 100ms which exceed the threshold for such application so in this thesis we examined the transmitting ECog signals transmitted by three transmitters [126–129, 132].

Using multiple transmitters has a great potential in term of Bi-directional Brain Computer Interface. We can place multiple transmitters to cover multiple areas in the brain and connect

them via RFID readers (controller) placed outside the brain to analyze the receiving signals and send other instructions to another transmitter covers the different Brain area. Fig 4.2 shows Bi-directional transmission.

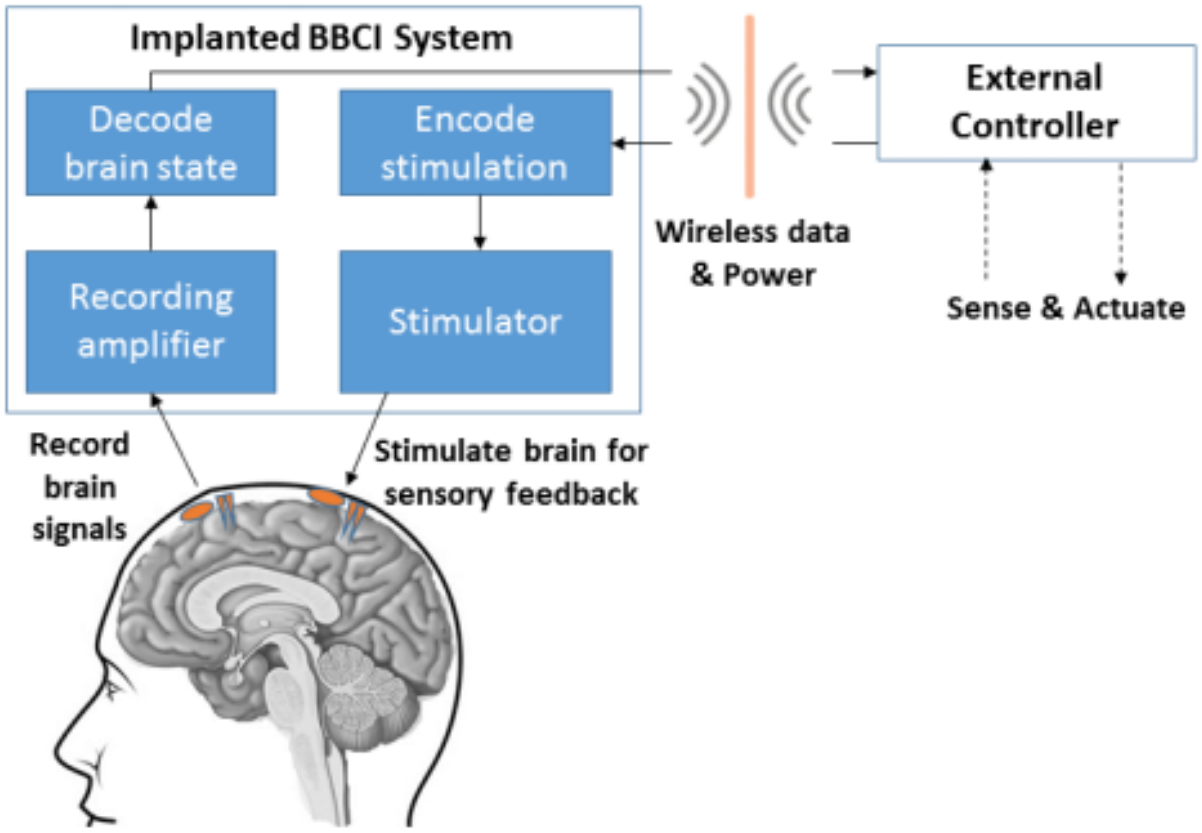

Figure 4.2:
Multiple implantable transmitters in brain

Moreover, In order to determine the amount of energy required for data transmission in terms of the amount of data transmitted we measured the voltage value across the capacitor that stores the energy for the system. When the WISP turns on to transmit the voltage across the capacitor will drop with the use of the stored energy. This creates an oscillating waveform where the capacitor is constantly charging and discharging as the WISP receives commands with incoming RF waves and transmits commands through back-scattering. In a simple acknowledgment protocol where no other operation besides transmission is performed the average energy consumed for a single transmission over thirty samples is 1.97 J with a standard deviation of .038 J. EPC values contain 96 bits thus the average energy required per bit of data transmitted is 20.5 nJ which achieve

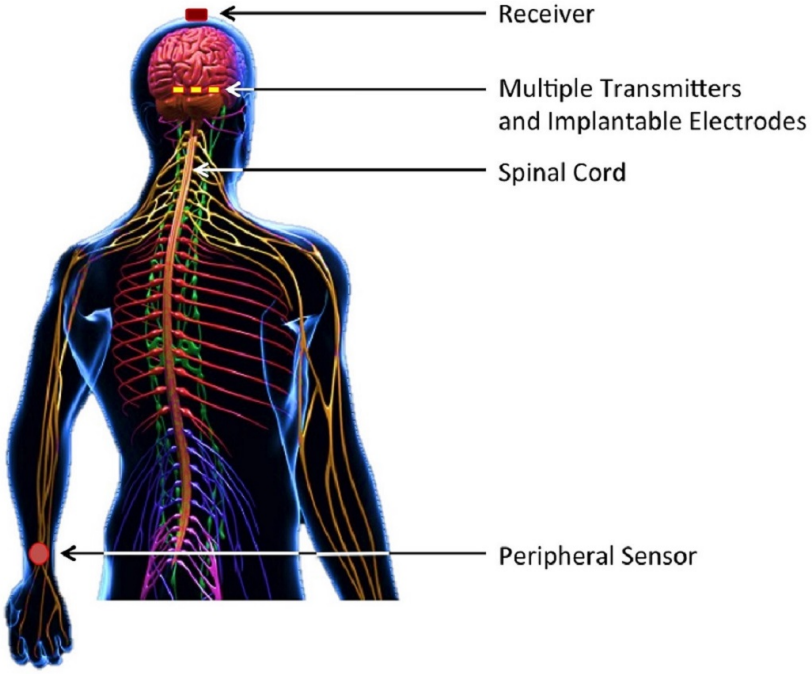

Figure 4.3: Design of a brain computer interface (BCI) system

the FCC power transmitting limit [131, 134].

Fig 4.3 shows a hypothetical scenario where multiple transmitters are implanted within simulated brain matter. This then transmits signals in wireless format to a receiver placed in the simulated skull. Using multiple implantable transmitters in the brain would enhance the bandwidth though the transmission data rate is reduced [101–103].

WISP5 an open source and a battery free platform (Wireless Identification Sensing Platform) as implantable transmitter which supports Slotted Aloha [105, 111] as an anti-collision algorithm has been used. This improves the amount of the capture signals. Multiple transmitters can be used for implementing many channels responsible for moving or connecting many different body parts. Passive RFID transmitters (tag) can't communicate with each other as each tag requires -20 dBm to operate for transmitting a signal to the receiver. These transmitters employ low sensitivity

diode detector receivers, and low back-scatter signal strength from the tag (-20 dBm) and prevent any tag-to-tag path loss between tags [112]. Also Implanted transmitters do not transmit data all the time as it depends on the neural signal generations and the distribution of the signals. Therefore, an enhanced MAC protocol considering the low power consumption of transmitters, bandwidth utilization, throughput enhancement and minimizing the transmission delay was designed for our BCI applications [62].

4.5 Experimental Components

4.5.1 WISP

An open source and a battery free platform wireless identification and sensing platform (WISP) has been used in this experiment. Its applications are seen in low power sensors, measurement and computation, and, communication experimentation. WISP is powered by the carrier signal emitted by the reader. As per FCC standards, the maximum allowed power emitted from reader is 30 dBm. In this study, WISP5 [106] is used with software-defined implementation of a UHF RFID tag, and EPC class1 generation 2 (EPC C1G2) standard for UHF RFID tags [111] as shown in Fig 4.4. WISP 5 uses energy-optimized firmware to support FM0 modulation and, read

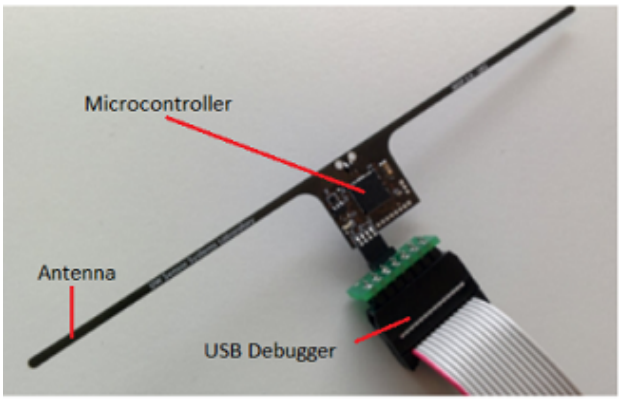

Figure 4.4: WISP (Wireless Identification and Sensing Platform)

and write command. MSP 430FR5969 micro-controller is used to work as an ultra-low power data storage suitable for BCI application and retrieval provided by Texas instruments. Also, ADXL362 accelerometer with low power consumption and Slotted Aloha as Medium Access Control [106].

4.5.2 RFID Reader

Impinj's Speedway reader has been used for robust RFID-based information expected measurements which gives the performance, quality, and the necessary reliability. Speedway RFID reader supports a maximum of 32 ports for the antenna [110]. The RFID reader continuously emits an RF signal in the UHF range (908 - 928 MHz) to power the implanted WISP that is supported by RFID reader manufactured by Impinj. WISP along with the RFID reader form a network, along with an antenna used to send data and commands to the tags. An antenna and an ethernet cable were used with the R420 model of Impini's Reader to connect the RFID reader to the controller (portable computer; Fig4.5 [110]. The main function of a reader is to provide power to the RFID tag in the form of an RF carrier wave and to decode and detect the back-scatter signal from the WISP.

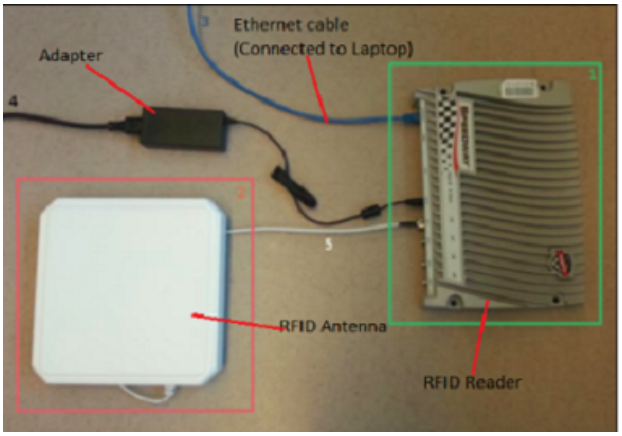

Figure 4.5: RFID Reader and Antenna

4.6 Experiment SETUP

Fig4.7 and 4.6 show the full experimental setup. To replicate the human brain environment, we have used glycerin to mimic cerebellum [104], to mimic human blood we have used salt water (Sodium Chloride (NaCl), whose dielectric properties resemble the human blood as the medium through which UHF RFID signals traverse [29, 64, 112–115], and plastic beaker to mimic skull. Glycerin, salt water and plastic beaker they are similar in electro-conductivity properties to blood, tissue fluid and human skull under room temperature. To study the characteristic of multiple UHF passive RFID radios that would be implanted within, we surrounded the backer by four plates to

avoid multi-path propagation reflected by the wall and to isolate the solution from outside RF, the transmitters are placed inside the glycerin and salt water solution held in a beaker. The plastic beaker dimensions are (44.95 cm x 32.7 cm x 19cm), which shows resistance to radio frequency waves [60-66].

The separated ziploc bag has been used for each WISP (passive RFID tag). This set up is placed over the chemical solution of the glycerin and saltwater barely touching it, mimicking implantable electrodes. In reality, the WISP would be implanted inside the human brain surrounded by blood and tissue fluid and the RFID antenna is placed outside the brain located on top of the skull. To replicate this, the RFID antenna is placed below the beaker. Fig4.5 also shows the experimental set up in which an Ethernet cable connects the controller (laptop) to the RFID reader and RFID antenna is connected to the Impini RFID reader through cable. The plastic beaker with various titrations of glycerin and salt water from 1 cm to 4 cm helps perform the analysis of the depth requirement of the sensor implantation. At different implant depth UHF RFID signals from multiple tags have been captured and analyzed on MATLAB. WISP contains a power harvester circuit to generate power from the RF signals received from the reader and, a modulator circuit to back-scatter information to the reader [111].WISP is a programmable device, and to work multiple tags simultaneously, Code Composer Studio IDE (Texas Instruments) was used. This reprograms the EPC tags to use multiple sensors simultaneously to capture more signals from a specific area. To reprogram the tags, a USB FET debugger is used to connect the WISP to the laptop. Code Composer Studio IDE is used to change the EPC for enabling multiple passive RFID transmitters to be used simultaneously. The EPC code sent by WISP is captured by the reader and stored for post hoc signal processing [67-69]. WISP divides the whole channel into 50 subchannels and is used for frequency-hopping to transmit data the reader.

4.7 Results

To analyse the transmission of backscattered RFID signals a prototype for cerebral tissue fluid and blood has been used as glycerin and salt water. For a patient with a severe neural injury deeper implant depths might be needed. Therefore to capture signals with greater spectral resolution, we examined various depths from 1cm to 4cm within the glycerin and salt-water. Through the medium different parameters such as received signal strength, SNR, Path Loss, Maximum number of electrodes, and channel capacity were quantified at every depth step of the implant. Brain signals (ECoG) characteristics have been analyzed when it propagates through the chemical solution

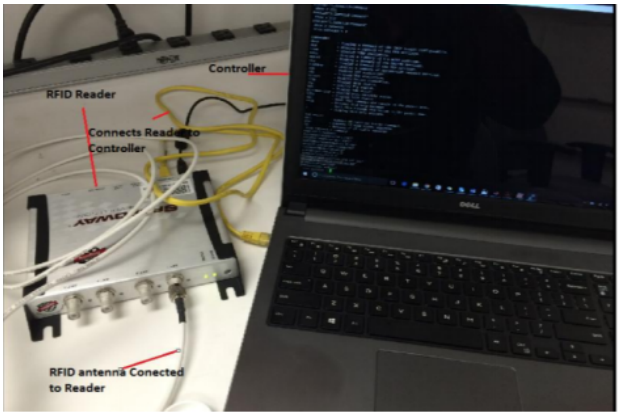

Figure 4.6: Experimental Setup

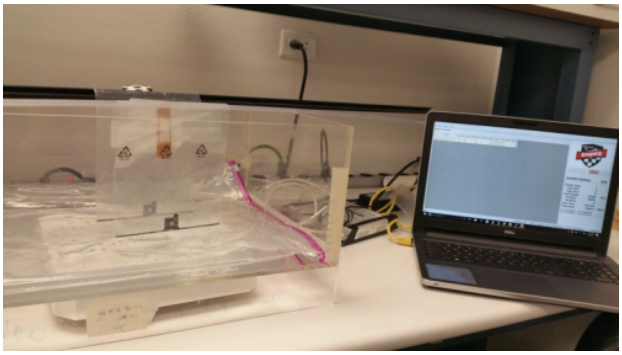

Figure 4.7: Full Experimental Setup

that mimic human brain fluids.

4.7.1 Received Signal Strength

RSSI is a measurement of how well the receiver is communicating with the transmitter, or it is the measurement that reflects the nature and characteristic of the location in a radio map [107]. RSSI values are useful for determining if the signal is transmitted at the receiver properly. It plays a vital role in designing the receiver side of the communication system for demodulating and decoding the received signal. In this experiment we have used Wisp5 as a transmitter that uses a BLE module programmed as slaves and the BLE is periodically woken by the Wisp5 to receive a new data [111]. The BLE radio has native support for RSSI on the received side, so the RFID reader can detect and measure the RSS values back from the tags by measuring the amount of the energy harvested by the CRFID (computational RFID). Fig4.8 shows the RSS values for the multiple tags are gradually decreased with increasing the implant depth of the passive RFID

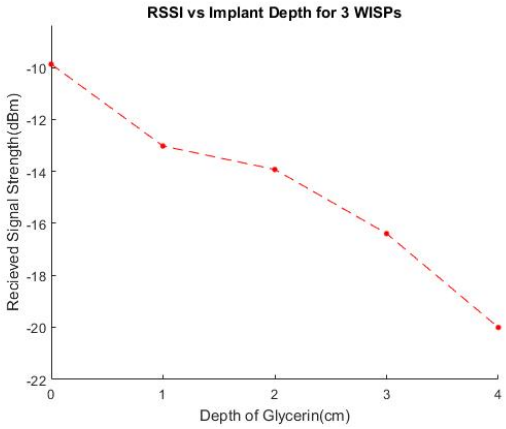

Figure 4.8: Received Signal Strength for 3 WISPs at reader VS different implant depth in centimeter

transmitter from 1cm to 4 cm, 4cm being maximum implant depth [113, 114]. Because Wisp5 using Slotted Aloha as Medium Access Control (MAC) protocol and gets the whole channel to transmit when free to transmit data continuously at full rate, the average value of Received signal strength for multiple transmitters, three transmitters in our experiment at varied implant depth is similar to the case where we used single transmitter also Slotted Aloha minimizes control overhead in turn minimizing the delay which is very critical in BCI systems. So the comparison between multiple transmitters and single transmitter scenario shows there is no significant change. From Fig4.8, the average value of received signal strength for multiple transmitters at an implant depth of 1cm is approximately -13 dBm and it gradually decreased with the increase in implant depth to 4 cm where the value is around -20dBm by setting The RFID reader power to 30dBm. We recorded the ECoG signals from different depths to simulate severity of neural injury [112].The received signal strength decays with an increase in the implant depth due to decrease in the signal power received at the reader. We explored the received signal strength from 1 cm to 4 cm due to exposure of high frequency neural activity.0cm has been considered to show how the human fluids impact the power received at reader side.

4.7.2 Signal-to-Noise ratio

One of the most important factors in communication design is the signal strength relative to background noise, known as signal to noise ratio (SNR). The default value of WISP noise level which is equal to -34.25 dBm and RFID reader transmitted RF signal power as 30 dBm have been used.

Fig4.9 shows that of 1 cm to 4 cm SNR is approximately ranged between 21dBm to 14dBm. Table 4.2 states that the SNR characteristics are similar to that of the signal strength as the signal to noise ratio depends on the signal power. Using higher order modulation scheme, more data can be captured for an implant depth of 1cm to 3cm because SNR values are much better compared at 4cm implant depth. No fluid scenario with 0cm has been considered to show how the SNR value when there is no fluid to propagate through.

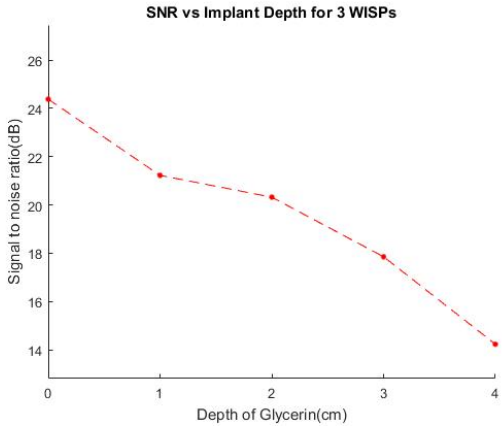

Figure 4.9: Signal to noise ratio for 3 WISPs VS implant depth in centimeter

4.7.3 Channel Capacity

One of the major parameters of a communication system is channel capacity. We designed our wireless communication system using the channel capacity theorem of Shannon- Hartley which enables us to calculate the maximum amount of data that a channel can carry. This is accomplished by calculating the additive white gaussian noise in the channel to find the channel capacity of the wireless link. We are using Shannon Hartley's Channel Capacity theorem to predict maximum data transmission rate:

Capacity = Bandwidth * log2(1 + Signal / Noise)

Channel capacity refers to the channel not each tag, thus for multiple tags each tag has a maximum data rate of a proportion of the Channel Capacity given in the Fig 4.10.

Fig 4.10shows the capacity of the channel decreased with the increase of the implant depth from 1 cm to 4 cm. At 1 cm the average channel capacity was more than 3.5 mbps for three transmitters that gradually decreased to around 2.3mbps at 4 cm. However, the use of multiple tags will achieve the needed high data rate at an implant depth of 3 cm as well.

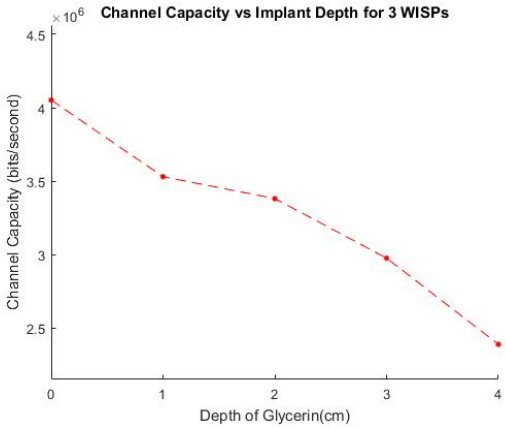

Figure 4.10: Channel capacity vs. implant depth in centimeters

4.7.4 Path Loss

The transmission of a signal through a medium is often characterized by its path loss. The path loss indicates the amount of power that is lost as a ratio of the power transmitted to the power received. In this case we use the received signal strength as well as the transmitted power to calculate the round trip path loss from initial transmission to reception of the back-scattered signal at the reader. The path loss is typically characterized using a logarithmic curve, in this case we also observe that general trend.

Fig 4.11, shows the path loss for three transmitters at 1cm is around 43 dBm and at 4 cm is around 50 dBm.

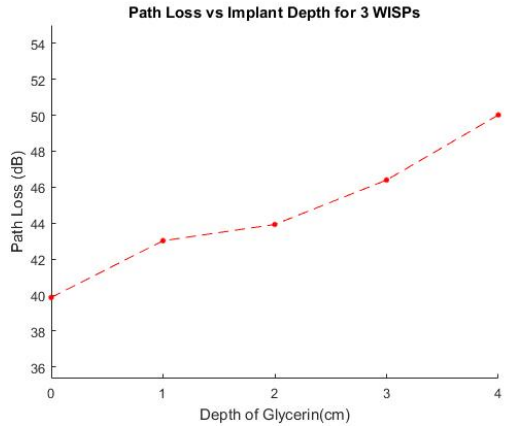

Figure 4.11: Path loss for 3 WISPs vs implant depth in centimeters

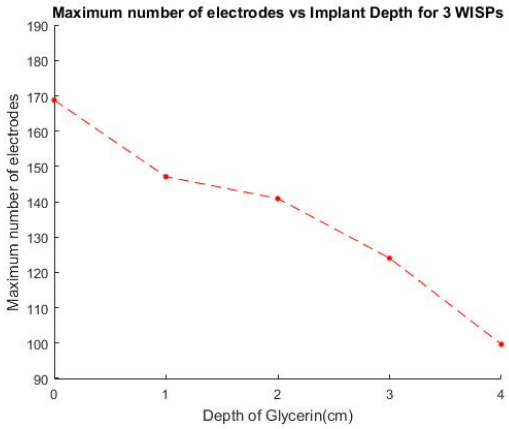

Figure 4.12: Example calculated maximum number of electrodes vs implant depth in centimeters

4.7.5 Visualizing results

To help better visualize what these results mean we calculated the maximum number of electrodes that could be constantly transmitting with example precision and sampling rate values. For this calculation we used a sampling rate of 1 kHz and a precision of 16 bits. An additional 50 percent data per transmission was used to account for headers and error correction protocols. Fig 4.12, shows the number of electrodes for three transmitters varying from 147 electrodes at 1 cm to 99 electrodes at 4 cm.

4.8 Comparative Between Single and Multiple WISPs

Number of passive RFID systems play an important role in designing implantable sensors at different depths in terms of network lifetime, the size of the communication channel, power consumption, data rate, maximum number of electrodes versus a different implant depths, channel capacity, throughput for BCI applications. Multiple WISP5's has been used as transceivers placed at different implant depth inside the human brain which receive signals from the electrodes and re-transmit them to RFID reader outside the brain on the scalp. Using Slotted Aloha as MAC protocol for multiple passive tags to lower power consumption, maximize network throughput, and improve Network lifetime. This kind of transmission is collision free transmission. To get better understanding on how increasing numbers of transmitters can impact the receiving signals, three scenarios have been considered at different implant depths varies from 1cm to 4cm the scenarios are; single transmitter with single RFID receiver, two transmitters with one receiver, finally three

transmitters with single RFID reader(receiver).

4.8.1 Received Signal Strength For Single And Multiple WISPs

Table 4.1: RSS at different Implant Depth for three transmitters

Implant Depth(cm)	0cm	1cm	2cm	3cm	4cm
1 WISP	-9.3337	-13.028	-14.22	-15.502	-16.395
2 WISPS	-9.2931	-13.828	-14.545	-15.12	-17.747
3 WISPS	-9.8718	-13.025	-13.929	-16.399	-20.018

RSS is the measurement that reflects the nature and characteristic of the location in a radio map [109]. The three scenarios have been examined.

Fig 4.13 shows the average value for three transmitters at varying implant depth are approximately similar to the case where a single transmitter has been used because WISP5 uses Slotted Aloha as Medium Access Control (MAC) protocol and gets the whole channel to transmit when free to transmit data continuously at full rate which minimizes control overhead in turn minimizing the delay which is very critical in BCI systems.So there is no significant change in the signal strength values at the receiver side when compared with a single transmitter scenario.

Table 4.1, shows the received signal strength at different implant depth for three transmitters. The average value of RSS recorded by RFID decreases from -13.028dBm for single WISP to -16.395dBm at 3cm, and for three WISPs from -13.025dBm at 1cm to -20.018dBm at 4cm. Also 0cm has been considered to show how the human fluids impact the power received at reader side.

4.8.2 Signal To Noise Ratio For Single And Multiple WISPs

From lab measurements, The three scenarios have been considered as well. We calculated signal to noise ratio for all of them. Fig 4.14 shows the characteristics of SNR are similar to that of RSS as the signal to noise ratio depends on the signal power.

Table 2, shows the values With respect of the transmission medium, the average SNR value for single transmitter at 1 cm implant depth is around 21dBm and at 4cm is around 17 dBm ,SNR

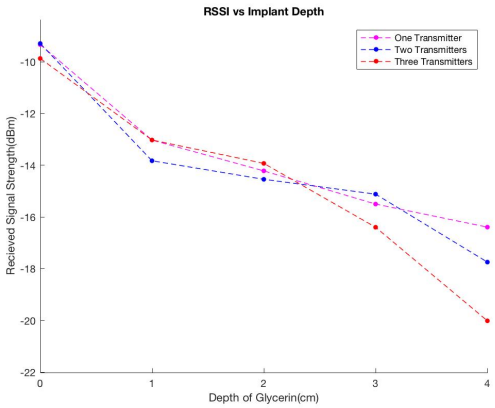

Figure 4.13: Received signal strength at reader VS implant depth in centimeter

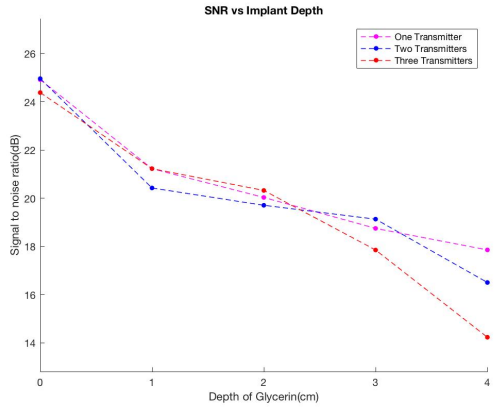

Figure 4.14: Signal to noise ratio for VS implant depth in centimeter

Table 4.2: SNR (dBm) at different Implant Depth for three transmitters

Implant Depth(cm)	0cm	1cm	2cm	3cm	4cm
1 WISP	24.916	21.222	20.03	18.748	17.855
2 WISPS	24.957	20.422	19.705	19.13	16.503
3 WISPS	24.378	21.225	20.321	17.851	14.232

for two transmitters at 1cm depth is around 20dBm and at 4cm is around 17dBm, finally SNR for three transmitters at 1cm is approximately 21dBm and at 4cm is around 14dBm. the average SNR values for multiple transmitters at 3cm are much better than the values measured at 4 cm implant depth. Also 0cm has been measured to show the impact of the human brain fluid on SNR, which is definitely higher than within fluid measurements.

4.8.3 Channel Capacity For Single And Multiple WISPs

Channel capacity indicates the total amount of data that can be transmitted from tags to the reader. Fig 4.15 shows how the average value of Channel capacity decreased gradually with increasing number of transmitters and increasing the implant depth. To find the channel capacity of the wireless link we need to calculate the Additive White Gaussian noise in the channel which is -34 dBm for WISP. Using Shannon Hartley's Channel Capacity theorem to predict the maximum data transmission rate:

Capacity = Bandwidth * log2(1 + Signal / Noise)

In order to increase channel capacity we have to increase either the bandwidth which is a constant value and not optional for RFID technology or we have to increase SNR which is also depend on RSS and cannot be increased.

Table 4.3 shows the channel capacity for a single transmitter at 1cm is 3.5 Mbps and at 4cm is around 2.98 Mbps. For two transmitters at 1cm is around 3.4 Mbps and around 2.7 Mbps at 4cm. Finally, for three transmitters at 1cm is 3.53 Mbps and 2.39 Mbps at 4cm. also 0cm considered to show full capacity is around 4 Mbps for all the above cases.

4.8.4 Path Loss For Single And Multiple WISPs

Path loss in Fig 4.16refers to the amount of power lost round trip from the signal being to transmit to receiving the back-scattered signal back from the tag. Table 4.4, shows three scenarios based on number of transmitters. First case single transmitter at different implant depths from 1 cm to 4 cm the values for path loss are approximately ranged from 43 dBm to 46 dBm. Second case, two transmitters at 1cm the path loss is around 43 while at 4 cm it's around 45 dBm. Third case for three transmitters at 1 cm is around 43dBm and at 4 cm around 50 dBm. The path loss when there is no medium 0cm is around 39dBm for all the three cases.

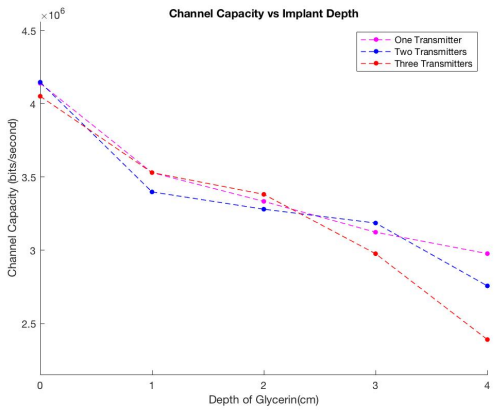

Figure 4.15: Channel capacity vs. implant depth in centimeters

Table 4.3: Channel Capacity (bits/second) at different Implant Depth for three transmitters

Implant Depth(cm)	0cm	1cm	2cm	3cm	4cm
1WISP	4.14E+06	3.53E+06	3.33E+06	3.12E+06	2.98E+06
2WISPS	4.15E+06	3.40E+06	3.28E+06	3.19E+06	2.76E+06
3WISPS	4.05E+06	3.53E+06	3.38E+06	2.98E+06	2.39E+06

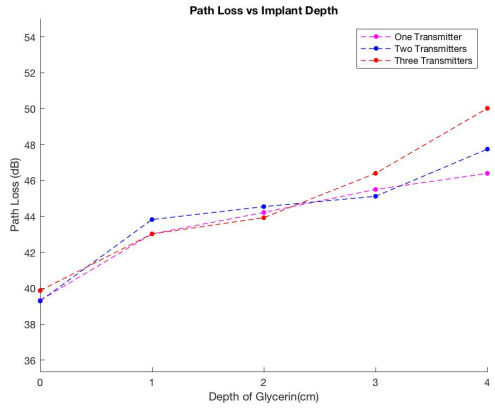

Figure 4.16: Path loss for vs implant depth in centimeters

Table 4.4: Path Loss at different Implant Depth for three transmitters

Implant Depth(cm)	0cm	1cm	2cm	3cm	4cm
1 WISP	39.334	43.028	44.22	45.502	46.395
2 WISPS	39.293	43.828	44.545	45.12	47.747
3 WISPS	39.872	43.025	43.929	46.399	50.018

4.8.5 Maximum Number Of Electrodes And Multiple WISPs

By using channel capacity, we have calculated an approximation for the maximum number of electrodes that would be viable. For this calculation we assumed a sampling rate of 1kHz, a precision of 16 bits as well as an additional 8 bits for headers, error correction and synchronization bits [29].

Fig 4.17 shows the maximum number of electrodes decreased by increasing number of transmit-

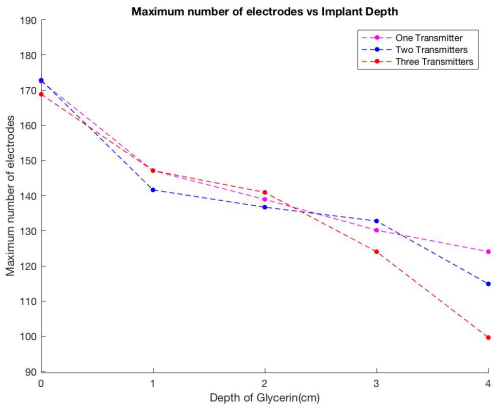

Figure 4.17: Maximum number of electrodes vs implant depth in centimeters

ters and the implant depth. Table 4.5states the maximum number of electrodes that the transmitters can collect the data from and organize them in three scenarios as well. The first scenario, single transmitter, the maximum number of electrodes for single transmitter at 1 cm is 147 and 124 at 4cm . A second scenario, two transmitters at 1 cm is 141 electrodes while at 4 cm the maximum number of electrodes is 114 electrodes. The third scenario for three transmitters at 1 cm it is 147

electrodes and at 4 cm it is 99 electrodes.For 0cm no human fluid the maximum is around 170 for the three scenarios.

Table 4.5: Calculated Maximum Number of Electrodes at different Implant Depth for three transmitters

Implant Depth(cm)	0cm	1cm	2cm	3cm	4cm
1 WISP	172	147	138	130	124
2 WISPS	172	141	136	132	114
3 WISPS	168	147	140	124	99

4.9 Summary

In the current thesis, we have found that passive UHF-RFID is a viable wireless technology for many BCI applications. This technology can support stable transmissions for at least a hundred electrodes in the depths and configurations we have measured. We studied the impact of tissue fluid, blood viscosity and implant depth on signal transmission (e.g. ECoG signals) using multiple UHF passive RFID transmitters. Also, we present a comparative study between single, two and three transmitters at different implant depth. Our study is the first step in modelling multiple channels for BCI applications. We specifically studied system parameters, which are imperative to the design of any wireless communication system. These were received signal strength, channel capacity, path loss, Maximum number of electrodes, power delay and frequency response for varying implant depths from 1cm to 4 cm. These results have been showcased in tables and graphical representation for varying implant depth. We find that passive UHF RFID does not work accurately when the implant depth of the transmitter is greater than 3 cm. Using multiple transmitters can improve the bandwidth transmission even though the transmission data rate could be reduced. Furthermore, implantable chips should be ultra-low power devices to avoid any deleterious effects of high power on the neural tissue within the cranium and on the spinal cord. In conclusion, the appropriate requirements for WBAN sensor devices are small, lightweight and low maintenance. These devices are achieved by using a promising communication technology which is back-scatter

RFID in the UHF range. Back-scatter sensor tags have low power consumption and thus makes it suitable for WBAN systems.

Acknowledgment

We thank Sidhant Mohanty, Dr. Albena Mihovski, Dr. Harsimran Baweja, Hayden Bialek and Dr. Syed Hassan Ahmedis for their useful contribution.

Chapter 5

Signal Transmission-MAC Protocols for UHF-RFID-BCI

5.1 MAC Protocols for UHF-RFID-BCI

5.1.1 Basic MAC protocols

MAC protocols are generally needed to manage the communications of multiple users by allocating each user a certain transmission resources such as time or frequency. Broadly speaking, MAC protocols can be classified into three categories:

1. Channelization protocols:
    (a) Frequency division multiple access (FDMA)
    (b) Time division multiple access (TDMA)
    (c) Code division multiple access (CDMA)
2. Random access protocols:
    (a) Aloha:
        i. Pure Aloha
        ii. Slotted Aloha
    (b) Carrier sense multiple access (CSMA)
        i. CSMA with collision detection (CSMA-CD)

ii. CSMA with collision avoidance (CSMA-CA)

3. Controlled access protocols:

   (a) Reservation

   (b) Polling

   (c) Token Passing

Each protocol has certain advantages and disadvantages in terms of spectral efficiency, delay, reliability, overhead and complexity. For example, FDMA has low complexity and overhead because it does not require synchronization among the users. However, it has a low spectral efficiency due to the frequency guard bands. Unlike TDMA, FDMA is immune to system timing issues since the frequency band is reserved for the user for the entire duration of the transmission session. Therefore, timing adjustment is not critical and fewer number of bits are required for synchronization and framing [142]. In FDMA, it is rare for the receiver to get information from more than one transmission source. One of the key limitations for FDMA is the maximum data rate, which is minimal. FDMA can be attractive for BCI systems due to its simplicity, however, power consumption should be reduced.

5.1.2 Related Work

BCI systems can be generally classified as wireless sensor networks (WSNs), wireless body area network (WBANs), or wireless personal area networks (WPANs). Therefore, the MAC for such networks can be adopted for BCI. Examples for these MACs are the IEEE 802.15.1 and IEEE 802.15.4. However, the characteristics of the brain environment are different from such networks [136, 137], which leads to a modest performance when WSNs, WBANs or WPANs protocols are adopted for BCI [115, 138]. Such local area networks are typically based on the IEEE 802.15.1 and IEEE 802.15.4 standards. Such protocols relatively offer low-cost, low power consumption, and does not require underlying infrastructure. Nevertheless, these protocols are designed to support low data rates. More specifically, The 802.15.4 can support very long battery life and has very low complexity.

In spite of the 802.15.4 advantages, it may have poor performance in terms of power consumption, reliability, and delay, if the MAC parameters such as the back-off window size and the maximum number of re-transmissions are properly selected. In [139], the authors investigated this

problem and proposed an adaptive MAC algorithm for minimizing the power consumption while guaranteeing reliability and delay constraints. The data traffic is considered unsaturated which allowed to use sleep/wake-up modes to minimize the power consumption.

Periodic listening, idle listening, additional control overhead, and collision are the main drivers of power consumption. To manage these issues, the authors in [140] consider the out-of-band wake up radio. Nodes switch into sleep mode when there is no information for transmission. When a tag has data, the wake-up radio transmits the control signal to the fundamental circuit for the wake-up and information transmission. Further, the tag remains in sleep mode to save power. The authors do not provide any system for crisis occasions. A review of various MAC protocols and the IEEE 802.15.4 for WBANs can be found in [141] where a diagnostic model is presented using delay and throughput, which affects low power tuning and vitality minimization. Moreover, path loss analysis is given for in-body, on-body, and off-body correspondence. MAC parameters for different networks are summarized in Table 5.1.

5.1.3 Motivation and Main Contributions

As can be noted from the literature survey, very little work has been devoted to design an efficient MAC for BCI applications. In such applications where the sensors are embedded inside the skull, some constraints such as limited power and end-to-end delay is critical. The limited power constraint is mostly due the small size of the embedded sensors, and time constraint is imposed by the maximum tolerated delay between the brain activity and neuro-prosthetic device response [138]. The throughput, received data rate and delay are essential to extract sufficient information in order to translate the neural signals into a desired movement. Therefore, this study proposes a new protocol for BCI applications that mitigates such problems and enhance the network performance. The new protocol combines the benefits of FDMA that allows using multiple channels without interference and with high throughput, TDMA can avoid collisions using a scheduling algorithm based on Breath First Search (BFS) approach, and CSMA-CA to improve the throughput and reduce the power consumption by reducing the idle listening state introduced by the TDMA [143]. Therefore, the proposed MAC is hybrid.

Although the data rates for certain BCI applications such as the P300-based BCI can be very low [144], there are other applications that is currently being investigated were much higher data rates might be required. For example, Kaplan *et al.* [145] considered adapting the P300-BCI for the gaming applications. Furthermore, it is shown in [146] that an EEG signal might require

Table 5.1: MAC parameters for WBAN, BCI and WSNs where Bluetooth and Zigbee are abbreviated as (BT) and (ZB), respectively.

Attribute	**WBAN**	**BCI**	**WSN**
power Source	Low	Ultra-Low	Low
Architecture	Star	Star	Mesh
Traffic	Burst	Regular	Burst
Applications	Healthcare	Prosthetic	Various
Form Factor	Wearable	Implantable	Medium
Transceiver	m-range	Cm range	m-range
Power	Ultra-Low	Ultra-Low	Low
MAC	CSMA/TDMA	TDMA	CSMA
Protocol	BT/Custom	Custom	BT/ZB
Link Establish	One-by-one	All-at-once	One-by-one
Sync	Periodic	Periodic	Algorithmic
Spatial Resolution	Several mm	A few mm	Several mm
Covered Area	Head	Cortex	On Body
Invasion	Medium	Medium	No
Freely Motion	No	Yes	No
Electrode type	Surface Scalp	MEA	-
Electrode Position	Over Scalp	Intra-cortical	-

about 85 kbps in particular scenarios. Therefore, the need for high data rate support for BCI systems is a key enabler for future BCI applications [197-203].

Moreover, to the best of the authors' knowledge, there is no research in the ope literature that investigates different transmission technologies and mechanisms for BCI-MAC protocols. Therefore, the goal of this work is to determine the suitable technology for developing BCI systems among UHF-RFID, UWB, and Ultrasonic, as well as to develop a MAC protocol that addresses previous concerns of network delay, data dropped, and traffic send/receive.

The performance of the proposed system is evaluated in terms of throughput, data rate and time delay. The hybrid system is evaluated using three different combinations FDMA+TDMA, FDMA+CSMA, and FDMA+TDMA+CSMA, for three technologies, which are UHF-RFID, UWB,

and ultrasonic. The obtained results show that the proposed hybrid MAC outperforms all the individual MACs and can satisfy the requirements of BCI applications. The results are presented for several cases of using 12 and 100 tags. The results are obtained using Opent [147], which is a highly reliable simulation tool that is used by several industrial giants such as Cisco and AT&T. Nevertheless, developing a test-bed will be targeted in our future work to capture all practical aspects. The main obstacle in developing a test-bed in the time-being is the lack of reliable development kits that can support such a system.

5.2 BCI System Model

This work considers a BCI system where N_T transceivers on the brain surface to collect and transmit the electroencephalogram (EEG) brain signals, and N_R transceivers are placed on the scalp to acquire the transmitted signals. The sensors used are semi-active, and they remain idle until they receive brain signals to transmit. The wireless network parameters for BCI are investigated using the MAC protocols of three different technologies, which are ultra-high frequency (UHF) radio-frequency identification (RFID) [109, 133], ultra-wide band RFID (UWB-RFID) [29, 30], and Ultrasonic technology mimicking the Neural Dusts by modifying the super-frame structure [136, 149, 150].

To select the appropriate frequency bands, The FDMA is tested using four distinctive frequency channels with RFID parameters, which mimics the realistic circumstance of multiple transmitters placed on the human brain to transmit the neural signals captured from the implanted electrodes to a receiver placed on the scalp. Since the frequency scope of passive RFID is from 860-960 MHz and center frequency is 915 MHz, the four frequency channels utilized are 915, 920, and 930 MHz. The receiver analog-to-digital converter (ADC) sampling rate is 200 KHz and the channels are inspected at rate of 50 KHz per channel. Initially, 103 samples are used to generate the modulating signal, which is considered as a sinusoidal signal to represent the brain reaction and behaviour of each signal at various frequency slots. The information signal is modulated using amplitude shift keying (ASK) and passed through the channel. At the receiver, the received signal passes through limited band filters to reduce the interference. The lag of the signal from the transmitter to the receiver is computed as shown in Table 5.2 for four different frequencies. Because the lag of the 940 MHz band is much larger than 2 ms, it will not be considered suitable for BCI applications.

Table 5.2: Lags at different frequencies.

Frequency (MHz)	915	920	930	940
Lag (ms)	1.5	2.0	2.2	3.3

5.3 Proposed Hybrid Protocol 1

The hybrid protocol is designed by dividing the N_T sensors into a number of clusters, three in this work, where FDMA is used to assign a frequency band for each cluster. Within each cluster, TDMA is used to multiplex the users to avoid interference between the sensors of that cluster. Finally, CSMA-CA is used to reduce the waiting time for the sensors in each cluster, and hence, reduce the delay and increase the throughput. This design allows the use of multi-channels to transmit and receive in full duplex mode [**?**]. Each tag wakes up upon receiving a brain signal, communicates with its neighbors in the cluster and goes to sleep until the next signal arrives. The communication between the tags is through Request-To-Send (RTS) and Clear-To-Send (CTS) ACK. Fig. 5.1 shows the general design of the hybrid MAC protocol in which the brain signals collected by bio-sensors are divided into three clusters and delivered to one receiver. The frequency and band slot assignment is performed using the BFS algorithm described in Sec. 5.3.1.

5.3.1 Scheduling Algorithm

In this work it is assumed that one of the tags has sufficient computational capability, and it is called the main tag, which is used to construct the schedule for all the tags and implement the network connectivity graph that maximizes the network data rate and reduces the delay. Fig. 5.2 shows an example of the scheduling algorithm outcome using 12 sensing tags. In the figure, the circles represent the sensing tags, the first and second numbers represent the time slot and frequency band, respectively. The starting point is represented by a circle labeled with an *R*.

BFS algorithm is used to assign a specific time slot and frequency band for each tag. Using BFS to implement the tree, the main tag serves as the root as we traverse through the tags. Therefore, the default time slot and frequency are assigned for each tag in the first level and then interference probability between one and two hops is checked. If there is a conflict between the N_j neighbour tags for N_i, we check the siblings. If they are in fact siblings, the algorithm assigns different time slots for N_i. The multi-channel is used to send data to the same root tag (parent) at the same time slot using different assigned frequencies [148, 153–155]. In the beginning, the

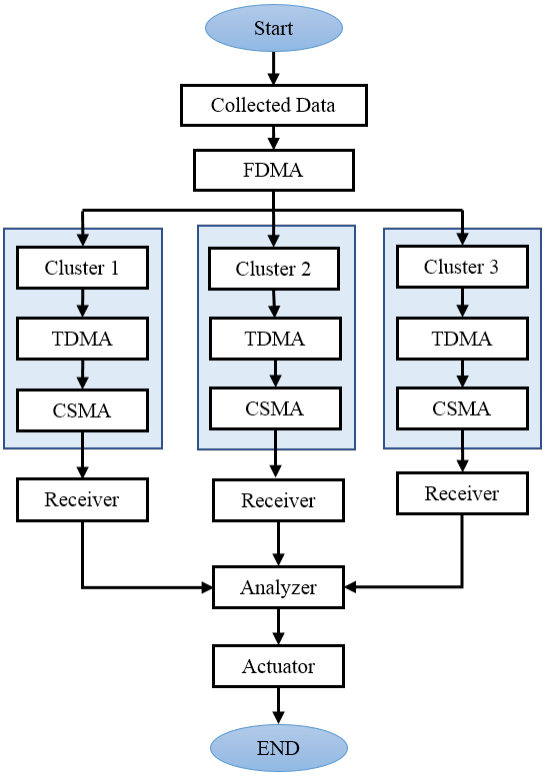

Figure 5.1: Example of the hybrid MAC protocol using three FDMA channels and one receiver.

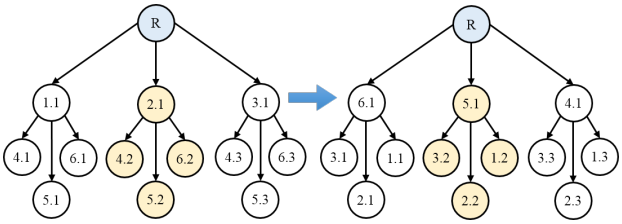

Figure 5.2: The outcome of the first and second iterations of the scheduling algorithm using 12 tags, $T_{Max} = 6$.

default time slot is increased by one for the initial levels. Then the time slots are updated to ensure that the time slot for the child tags is less than their parents. Therefore,

$$T_{New} = T_{Max} - T_{Current+1} \tag{5.1}$$

where T_{New} represents the updated time slot, T_{Max} represents the total number of slots, and $T_{Current}$ represents the currently assigned time slot. The scheduling algorithm is described in **Algorithm 1**.

Algorithm 5 Scheduling algorithm.

Requirements: Bio-sensor Network Topology Graph

Graph : G=(N,E)

N = set of 12 sensors

1: initialization

2: N'= u

3: **for** all tags N_i loop

4: $Time\_Slot[u] \leftarrow current\_Time\_Slot$

5: $Cluster\_Channel[u] \leftarrow 1$

6: **for** all the same level visited 1-2-hop n of u **do**

7: **if** ((Sub_Tree_parent[n] == Sub_Tree_parent[u]) OR(Number_of_Channels >= current_channels)) **then**

8: **if** (Time_Slot[u] = Time_Slot[n]) **then**

9: $Time\_Slot[u] \leftarrow Time\_Slot[n] + 1$

10: **end if**

11: **else**

12: **if** ((Time_Slot[u]=Time_Slot[n])AND (channel[u]=channel[n])**then**

13: $channel[u] \leftarrow channel[n] + 1$

14: **end if**

15: **end if**

16: **end for**

17: **for** all not visited edge e of u **do**

18: let L be the other not visited endpoint of edge e

19: $Parent[L] \leftarrow u$

20: $Height[u] \leftarrow Height[L] + 1$

21: **end for**

22: **end for**

The complexity of the scheduling algorithm as described in [42]. Let $G(V,E)$ be a graph with $|V|$ number of vertices and $|E|$ number of edges. The BFS algorithm visits every vertex in the

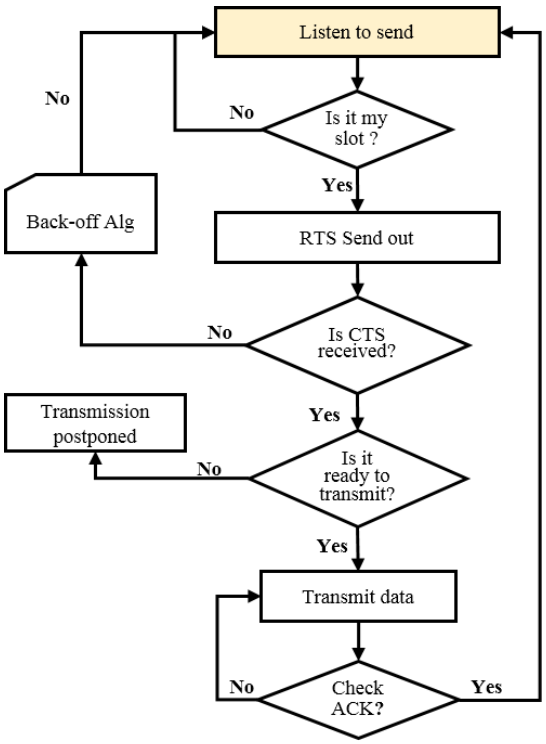

Figure 5.3: Sender behavior.

graph and every edge, where

$$\mathcal{O}(|V|+|E|). \tag{5.2}$$

5.3.2 Sender and Receiver Behavior

With the three clusters identified, each cluster is assigned a different channel, and when the cluster tags want to transmit simultaneously, the channel is checked periodically by the sensors. If sensor N_i sends an RTS control message to utilize its own time slot S_i to transmit a packet to a pre-defined receiver, and the channel is declared idle, i.e., the RTS and CTS have been communicated successfully between the tag and the receiver, then the tag sends the packet. However, if the CTS is not received by the sender, i.e., a collision occurred and transmission is inhibited to start the back-off algorithm to wait for a random number of frames, back-off delay, before the next attempt to re-transmit an RTS in the same slot. Figs 5.3 and 5.4 respectively v the sender and the receiver behaviour for a tag in a specific cluster to transmit data on an individually scheduled time slot.

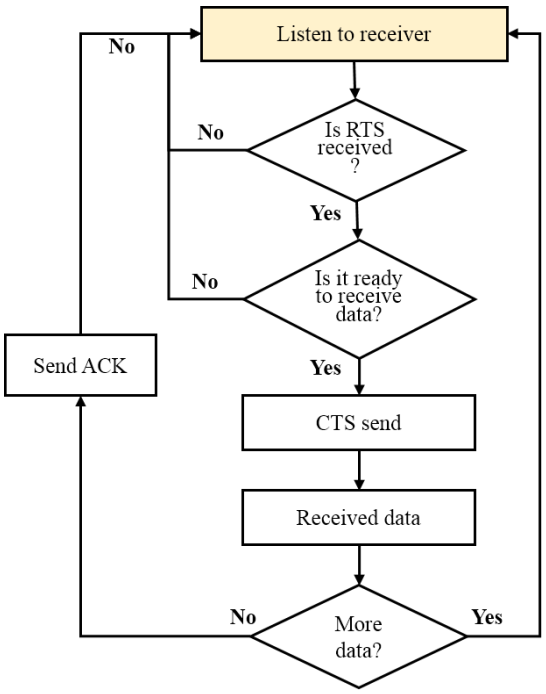

Figure 5.4: Receiver behavior.

5.3.3 Delay and Throughput of Various MAC Protocols

FDMA

The transmission delay for FDMA data data can be computed as [156]

$$D_{FDMA} = T_{Oh} + T_{ACK} + T_{GT} + T_{Ta} + T_{Fr} \tag{5.3}$$

where $T_{Oh} = N_{Oh}/R_B$, $T_{ACK} = N_{ACK}/R_B$, and $T_{Fr} = N_{Fr}/R_B$. The throughput can be computed as

$$\eta = \frac{N_T N_P}{C_L}\left[1 + \frac{Q}{2(1-Q)}\right]. \tag{5.4}$$

where the notations are given in Table 5.3.

TDMA

TDMA has three types of delays, which are transmission delay, queuing delay, and propagation delay. The transmission delay and for TDMA can be expressed as

$$D_{TDMA} = T_{Oh} + T_{ACK} + T_{GT} + T_{Sync} + T_{Ta} \tag{5.5}$$

where $T_{Sync} = N_{Synch}/R_B$. Therefore,

$$\eta = \frac{N_P}{C_L}\left[1+\frac{N_T}{2}\left(\frac{Q}{1-Q}+1\right)\right]. \tag{5.6}$$

CSMA-CA

CSMA-CA works with the standard tag detecting medium by sending packets to the receiver when it finds that the medium is free. In the unlikely chance that the medium is occupied, the tag goes to random back-off time slots waiting for the channel to be free for transmitting. With the improved CSMA-CA RTS/CTS trade system tag that senses the free channel, it sends RTS to the receiver and waits for the CTS message from receiver to start transmitting. The delay from sender to receiver is calculated as

$$D_{CSMA} = T_{Bo} + T_{Fr} + T_{Ta} + T_{ACK} + T_{ITS} + T_{RTS} + T_{CTS}. \tag{5.7}$$

where $T_{BP} = N_{Bo}T_{Bo}$. The relation between the transmission delay and throughput is given,

$$D_{CSMA} = \frac{(\kappa-1)\,(\mathrm{e}^{2\eta}-1)}{2+2D_{EtE}+1} + 1 + D_{EtE}. \tag{5.8}$$

where κ is a metric used to capture the packet loss correlation on different links [156].

Hybrid MAC protocol

For the hybrid model, the tags are divided into three clusters, and FDMA is used to assign a particular frequency band for each cluster. Within each cluster, the tags' data are multiplexed using TDMA and CSMA-CA. The delay for each of the cluster tag is given by

$$D_{Hybrid} = \frac{1}{N_{TC}}(D_{FDMA} + D_{TDMA} + D_{CSMA}). \tag{5.9}$$

The throughput of the different considered types of MAC protocols is calculated while assuming that the information is moved from the sender to receiver utilizing only one of the MAC protocol types. Because of the similarity between the sender and receiver, there is no collision or packet loss due to buffer overflow. Moreover, the channel is assumed error free. In such scenarios, the throughput can be expressed as [156],

$$\eta = 8\frac{T_{Fr}}{D} \tag{5.10}$$

where D is the total delay. Calculate throughput using (5.10) confirms that the proposed MAC protocol is preferable over other MAC protocols for BCI applications as demonstrated by the presented numerical results.

Table 5.3: Notations of equation parameters.

Parameters	**Description**
T_{Fr}	Data time to end of frame
η	Throughput
T_{Oh}	Overhead time
T_{Sync}	Synchronization time
T_{Ta}	Turnaround time
T_{ACK}	ACK time
T_{GT}	Guard time
N_{Oh}	Overhead bits (total)
N_{ACK}	ACK/NACK bits
N_{Fr}	Data bits per frame
T_{BP}	Back-off period
T_{RTS}	RTS
T_{CTS}	CTS
T_{ITS}	Inter Frame Space
N_{Bo}	Number of back-off slots
T_{Bo}	Back-off slots' time
R_B	Data rate
D	Transmission Delay
C_L	Duty-cycle length
N_P	Number of packets
N_T	Number of tags
Q	Queue length
N_{Sync}	Number of synchronization bits
D_{EtE}	End-to-end delay
N_{TC}	Number of tags per cluster

5.3.4 Model efficiency

Model efficiency can be calculated by considering transmission and propagation time for CSMA-CA by assuming

$M(t)$ is the number of full frames up to time t,

$$\sum_{i=0}^{M(t)} T_f^i \leq t \leq \sum_{i=1}^{M(t+1)} T_f^i \tag{5.11}$$

$$\frac{1}{M(t)} \sum_{i=0}^{M(t)} T_f^i \leq \frac{t}{M(t)} \leq \frac{1}{M(t)+1} \sum_{i=1}^{M(t+1)} T_f^i \cdot \frac{M(t)+1}{M(t)} \tag{5.12}$$

where T_f is the frame time and T_f^i is X_i ith time frame, where the expected value of X_i is given by

$$\frac{1}{n} \sum_{i=1}^{n} X_i \to \mathbb{E}(x_i) \tag{5.13}$$

where $\mathbb{E}(\cdot)$ denotes the expectation process. Given that $t \to \infty$ then

$$\mathbb{E}(T_f) \leq \frac{t}{M(t)} \leq \mathbb{E}(T_f) \frac{1+M(t)}{M(t)}. \tag{5.14}$$

On the other hand, the transmission efficiency can be expressed as

$$\zeta = \frac{M(t)T_t}{t} = \frac{T_t}{\mathbb{E}(T_f)} = \frac{T_t}{T_t + 2\mathbb{E}(N_{Fa})T_{Pr}} \tag{5.15}$$

where ζ is the transmission efficiency, T_t is the transmission time, and $E(N_{Fa})$ is the expected value for number of failed attempts, and T_{Pr} is the propagation time.

To calculate the expected value for number of failed attempts, we consider that the first success happens at nth transmission with probability

$$P_{S_1} = \frac{1}{\mathrm{e}} \left(1 - \frac{1}{\mathrm{e}}\right)^{n-1}. \tag{5.16}$$

Therefore, the expected value for number of failed attempts is given by

$$\begin{aligned} \mathbb{E}(N_{Fa}) &= \frac{1}{\mathrm{e}} \sum_{n=1}^{\infty} (n-1) \left(1 - \frac{1}{\mathrm{e}}\right)^{n-1} \\ &= \mathrm{e} - 1. \end{aligned} \tag{5.17}$$

By plugging (5.17) into (5.15), we obtain,

$$\zeta = \frac{T_{Tx}}{T_{Tx} + 2(\mathrm{e}-1)T_{Pr}} \tag{5.18}$$

where T_Tx is the transmission time. For $T_{Tx} \gg T_{Pr}$, it can be noted from (5.18) that $\zeta \to 1$.

Table 5.4: Parameters used for protocol simulation.

	RFID	**UWB**	**Ultrasonic**
Frequency	908 MHz 912 MHz 915 MHz	3.5 GHz 4 GHz 4.5 GHz	1.85 MHz 1.95 MHz 2.05 MHz
Bandwidth	250 KHz	499.2 MHz	30 KHz
Tx Power	0.2 mW	0.0026 mW	0.12 mW
Rx Sensitivity	-84 dBm	-85 dBm	-85 dBm
Buffer Size	5 kByte	5 kByte	5 kByte
Data Rate	2 Mbps	300 Mbps	1 Mbps

5.3.5 Numerical and Simulation Results

The network model used in this work follows the model given in [31–34], using three different RFID technologies, which are UHF, UWB, and Ultrasonic. For each technology, multiple tags are placed with parameters that mimic the implantable electrode array (MEA). For each technology, we evaluate the data dropped, network delay and traffic sent/received in each case. The considered protocols are based on Network Time Protocol [32, 33] concept, which provides synchronization and is used with both local area networks (LANs) and wide area networks (WANs).

The sensor properties are selected to match the network parameters such as the channel capacity, channel recurrence, transmit control, transmit power, receiver sensitivity, buffer size and data rate. The results for the delay and throughput are calculated after feeding OpNet [147] simulates the inter-arrival time as constant 1 ms, traffic generation parameters, start time as constant 0, on-state time as exponential with a value of 10^{-3}, and off-state time as 4×10^{-3}, packet generation arguments as uniform $(0.5, 1)$ packet size in byte and no segmentation, Beacon interval, back-off time in sec., as 2×10^{-2}, maximum receive life time as 0.5 sec., and buffer size as 5 kbyte. Further, we use the constant network model, which is more suitable for BCI applications. Table 5.4 shows the required parameters for each technology to simulate the network.

The considered and proposed protocols are evaluated using 12 and 100 tags, and using three receivers for both cases. For the 12 tags scenario, the total number of tags is divided into three clusters each of which has three tags, and assigned a unique frequency band, which can be

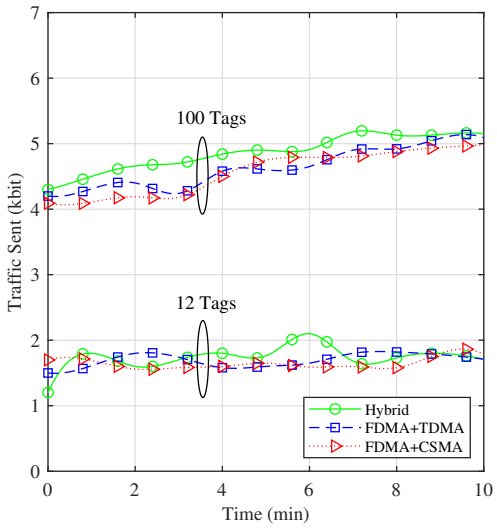

Figure 5.5: UHF-RFID traffic sent using the hybrid, FDMA+TDMA and FDMA+CSMA protocols for 12 and 100 tags.

915 MHz, 920 MHz, and 925 MHz [151]. The same argument is applied to the 100 tags, except that the three clusters contain 33, 33 and 34 tags. Then, three different protocols are applied as follows:

1. FDMA+TDMA: The tags send data over the three frequencies at different time slots to three receivers. Therefore, all the tags in a given cluster are assigned one out of available time slots, and thus, this protocol is denoted as FDMA+TDMA.

2. FDMA+CSMA: The tags in each cluster use CSMA-CA, and thus two different tags in different clusters may transmit at the same time, but at different frequency, and hence, this protocol is called FDMA+CSMA. The starting time for the tags to transmit data is 10^{-2} sec.

3. Hybrid: In this scenario, the tags in each cluster employ TDMA for multi-access, however, CSMA is applied as well to allow tags that have data to transmit to utilize the time slots of the idle tags. Therefore, this protocol effectively composed of three protocols FDMA+TDMA+CSMA.

Figs. 5.5–5.8 show traffic sent, traffic received, dropped data, and network delay for the proposed and other considered protocols using UHF. The x-axis represents the run time of the simulation. For the 12 tag scenario, it can be noted that the three considered protocols can send roughly the same amount of data, but the received data is for the hybrid is significantly larger, because it suffered less dropped data. For the network delay, the hybrid protocol offers the minimum,

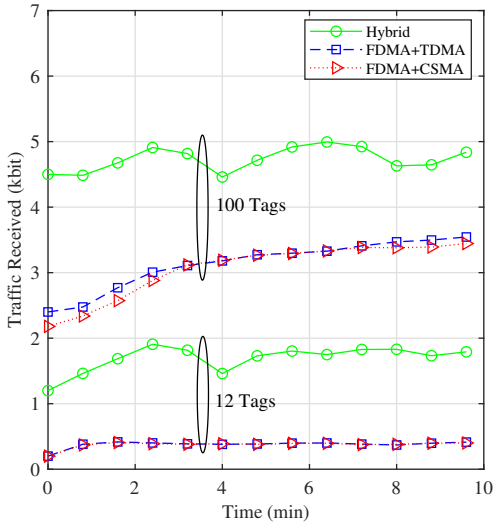

Figure 5.6: UHF-RFID traffic received using the hybrid, FDMA+TDMA and FDMA+CSMA protocols for 12 and 100 tags.

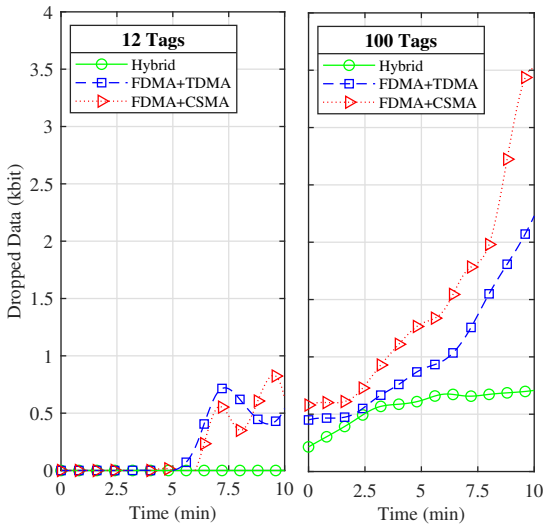

Figure 5.7: UHF-RFID data dropped for the hybrid, FDMA+TDMA and FDMA+CSMA protocols using 12 and 100 tags.

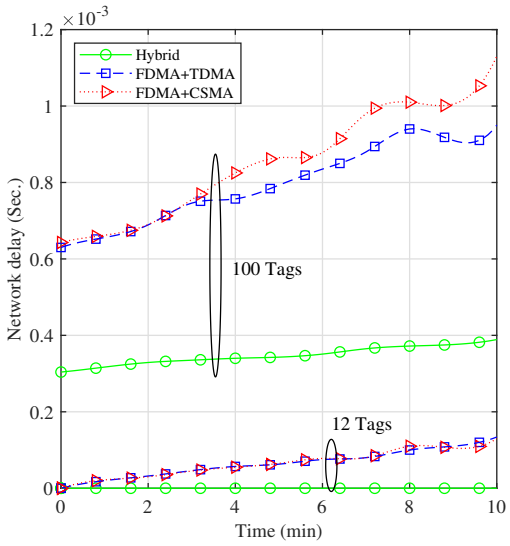

Figure 5.8: UHF-RFID network delay for the hybrid, FDMA+TDMA and FDMA+CSMA protocols using 12 tags and 100 tags.

Table 5.5: UHF-RFID Results using 12 tags at the last simulation point.

Protocol	**Tx Traffic (kbps)**	**Rx Traffic (kbps)**	**Dropped (kbps)**	**Delay (sec.)**
FDMA+CSMA	1.8	0.24-0.38	0-0.6	0.15
FDMA+TDMA	1.5-1.78	0.24-0.38	0-0.6	0.15
Hybrid	1.2-1.8	1.2-1.8	0	0

while the other two protocols perform generally the same in all aspects. For the 100 tags scenario, it can be noted that the hybrid protocol can transmit slightly higher data, but the traffic received is significantly larger because the dropped data is much less. The traffic delay of the hybrid protocol is substantially less than the other two protocols. For the 100 tags scenario, it can be noted that the data sent increases over time as the buffer fills over time. Table 5.5 shows the numerical results ranges for all the considered metrics. From these summarized results, it can be concluded that the hybrid protocol is the most compatible with brain function as observed by the previous reported research. From previous studies [18], the end-to-end time for the neural signal to travel from the action potential of the arm is nearly 60 to 90 ms. The hybrid protocol aligns with this previous knowledge as the delay is less than the BCI capturing time range and therefore suitable for BCI.

Ultra-wide-band radio technology supports micro-electromagnetic systems. Circuit fabrication [103, 152] shows that for BCI applications, in order to capture the EEG signals by electrodes from inside the brain and transmit them in wireless form with a transmitter placed on the scalp to a

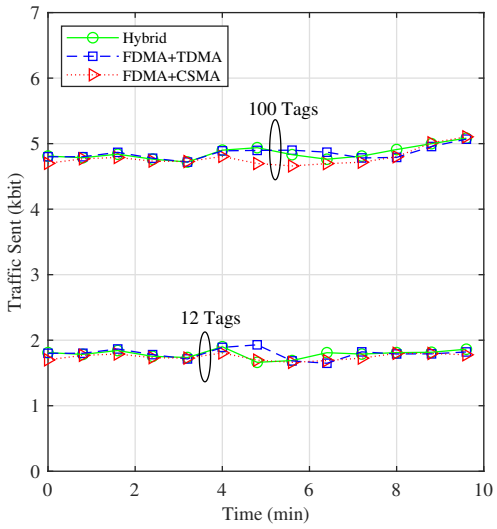

Figure 5.9: UWB-traffic sent for three scenarios; Hybrid MAC protocol, FDMA+TDMA and FDMA+CSMA using 12 tags and 100 tags.

receiver or processor located outside the skull, a transmission frequency of 3.5 GHz is used. Based on our last study, using 3.5 GHz gives better results in terms of the received signal strength, signal to noise ratio (SNR), path loss, and channel capacity [108, 141]. In Opnet, we used UWB parameters to transmit the data. We have implemented the different technologies in order to place the tags. The values for each tag were changed using edit attributes so that we can send the data packets according to the desired application. Generally speaking, for the brain space, the transmission of the data performs differently with UWB and RFID. The synchronization is performed by sending out beacon signals every 2×10^{-2} sec. The first scenario analyzes transmitting the data with different frequencies at the same time. This method is similar to the Frequency Division Multiplexing in the CSMA-CA protocol. The frequencies used in this case are 3.5, 4 and 4.5 GHz. In this scenario, the tags begin to transmit data at 1×10^{-2} sec.

Figs. 5.9–5.11 present the network parameters for each of the three scenarios: FDMA+CSMA, FDMA+TDMA, and hybrid. As can be noted from Fig. 5.9, it can be noted that the buffering time is less significant as compared to the UHF as the traffic sent increase over time is very small. For traffic received, it can be noted that the hybrid and FDMA+TDMA significantly outperform the FDMA+CSMA. For the network delay depicted in Fig. 5.11, the delay for the 12 tags is very small and comparable for the three protocols. However, for the 100 tags case, it can be noted that the hybrid noticeably outperforms the other two protocols.

It is worth noting that the dropped data is zero for all protocols and thus, the figure is not

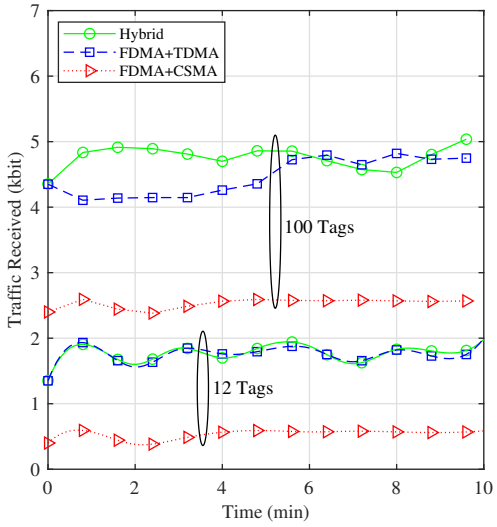

Figure 5.10: UWB-traffic received for three scenarios; Hybrid MAC protocol, FDMA+TDMA and FDMA+CSMA using 12 tags and 100 tags.

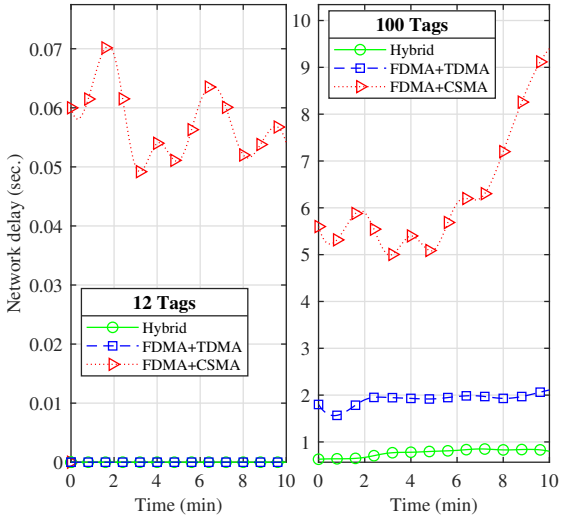

Figure 5.11: UWB-network delay for three scenarios; Hybrid MAC protocol, FDMA+TDMA and FDMA+CSMA using 12 tags and 100 tags.

included. By considering this aspect, it can be concluded that the Hybrid protocol works better for UWB technology. Table 5.6 provides a comparison of the three scenarios. It can be noted that the hybrid protocol is the most compatible with natural brain function as the delay is within this limit for several cases of interest.

While ultrasonic has been used in medicine for many decades, it has only recently taken

Table 5.6: UWB simulation Results using 12 tags.

Protocol	Tx Traffic (kbps)	Rx Traffic (kbps)	Dropped (kbps)	Delay (sec.)
FDMA+CSMA	1.8	0.5	0	6×10^{-2}
FDMA+TDMA	1.2-1.8	1.2-1.8	0	0
Hybrid	1.6	2.1	0	0

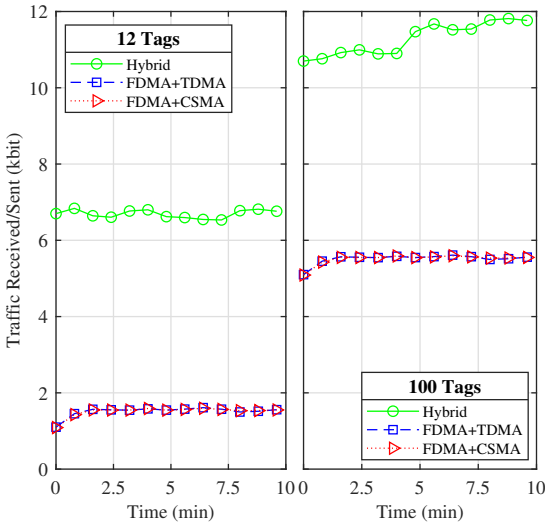

Figure 5.12: Ultrasonic traffic sent or received for the hybrid, FDMA+TDMA and FDMA+CSMA MACs using 12 and 100 tags.

specialized form in bio-electronics where promising new technology is developing. Ultrasonic has a potential for widespread use due to its ability to potently deliver power [153]. The smaller size of an ultrasonic transducer is an added advantage for applications such BCI. In Opnet, the ultrasonic technology parameters [30] were used to transmit data. The simulation is performed using the same procedure as described for the UHF and UWB. In the first scenario, the FDMA+CSMA protocol combines both FDMA and CSMA protocols. The tags transmit at different frequencies and detect the medium before transmitting data to avoid collisions. Each on of the three clusters transmits at 1.85 MHz, 1.95 MHz and 2.05 MHz, respectively [149]. The tags start transmitting data at 0 sec. In this scenario, collisions are introduced early in the network, however, CSMA-CA is used to effectively avoid collisions [154].

In the second scenario, the FDMA+TDMA protocol calls for the network to include three

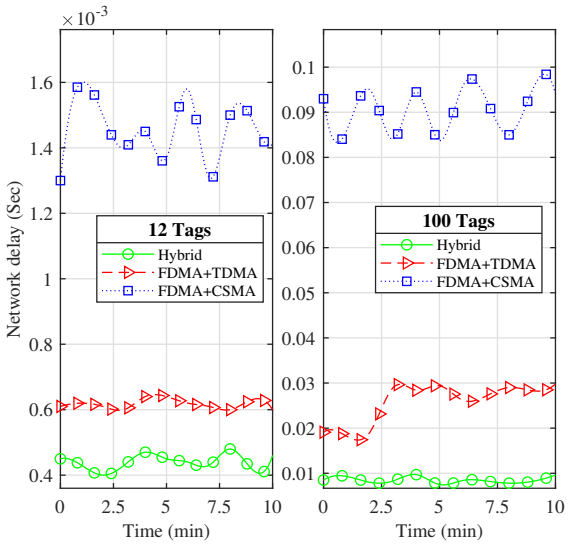

Figure 5.13: Ultrasonic network delay for the hybrid, FDMA+TDMA and FDMA+CSMA protocols using 12 and 100 tags.

clusters that use the same frequencies of the FDMA+CSMA, and different times for transmission. For each cluster, one tag is designed to transmit any any given time.

In the third scenario, the Hybrid protocol includes each cluster with different frequencies and times for each given cluster, similar to other two cases. However, each tag sends data only in a particular time slot. Three tags, one from each cluster, may send data in the same time slot. In order to prevent collision, the tag is forced to hold transmission for a random number of slots. Synchronization of all tags in each protocol is achieved by configuring the access point to broadcast beacon signals.

Figs. 5.12 and 5.13, the network parameters are presented for each protocol. As can be noted from Fig. 5.12 for the 12 tags scenario, the hybrid protocol traffic sent/received is between 6.35-6.85 Kbit, the data dropped is approximately zero and the network delay is about 4.2×10^{-4} sec. For the FDMA+TDMA protocol, traffic sent and received was between 1.4-1.6 kbps and there was no data dropped. The network delay is between 6×10^{-4} to 6.5×10^{-4} sec. For the FDMA+CSMA protocol, the traffic sent was approximately 1.50 kbps and the traffic received is about 1.45 kbps, the network delay is about 1.5×10^{3} sec. Consequently, the hybrid protocol performs very well for this technology as well. For the 100 tags case, it can be noted that the delay becomes more critical for the FDMA+CSMA scenario, while it remains below 10^{-3} for the hybrid MAC. Table 5.7 summarizes the results for each protocol in terms of traffic sent, traffic received, data dropped and delay for the ultrasonic transmission using 12 tags. From the results, it is clear

Table 5.7: Ultrasonic simulation Results using 12 tags.

Protocol	Tx Traffic (kbps)	Rx Traffic (kbps)	Dropped (kbit)	Delay (sec.)
FDMA-CSMA	1.5	1.5	0	1.6×10^{-3}
FDMA-TDMA	1.4-1.6	1.4-1.6	0	6.2×10^{-4}
Hybrid	6.35-6.85	6.35-6.85	0	4.2×10^{-4}

that the hybrid protocol performs better in terms of delay and data transmitted/received.

5.4 Proposed Protocol 2

This section explains our second proposed protocol that can reliably transmit data with minimum power and delay. Also, it reduces the number of collisions while providing scalability and throughput. Our proposed protocol does not require complex hardware or high power. The protocol is based on backoff the transmission of data from RFID tags for a random time. The protocol minimizes the energy consumption by decreasing the number of collisions as compared to the traditional anti-collision Q algorithm that used RFID tags [149].

There are several reasons that make the RFID as a very effective solution for BCI applications, such as low power, low cost, and the ability of its signal to pass the signal through several layers of the brain. Passive RFID is a great solution for medical applications because it operates with less power than other technologies. The technique used in these tags is called backscatter communication, they are powered by electromagnetic coupling. They receive power externally from the reader and send back the reflected signals that contain the data. The RFID tags showed great promise for real time monitoring of fully implantable sensors in the human body [115, 137, 138].

According to the Federal Communication Commission (FCC) of the United States of America, the power transmitted in the ISM band has to be less than 4 W (EIRP), making UHF-RFID as the best fit for BCI applications [115, 138, 158]. The reader sends out query commands to initiate the communication. The query commands inform the senders about its availability to read. The RFID tags that are available in the reader's region may reply to the reader. A collision might occur if more than one tag reply. To avoid collisions, each tag delays its transmission of data for a random

time interval. Upon a successful reception of data, the reader sends an ACK. If the reader receives multiple replies, it will send a NACK to the tags that are involved in the collision. Then, the tags will send the data again by following the same procedure. The phases involved in this process are explained in the following sections.

5.4.1 Query

The query command is a broadcast message the reader sends when it is ready to read. Every tag in the range of the reader receives this query command. If the tags have data to send, it starts transmitting the data after a random back-off time. Otherwise, it remains idle. Staying in the idle state helps the tag to save power. The time taken for the query to reach the tag is called the propagation delay.

5.4.2 Tag Reply

After receiving the query command, tags prepare themselves for sending the data. The time taken for a tag to send back the reply to the reader is called the system delay of the tag. This time includes any actual system delay and the random back-off time. The random back-off time is uniformly chosen in the interval of [0.1 to 0.5] seconds. This interval is chosen due to the fact that BCI applications are time sensitive. The overall delay with and without re-transmissions is explained in the next sections.

5.4.3 Successful Transmission

A successful transmission is defined as the transmission that does not involve any collision. The probability of a successful transmission will be high when the number of tags is low. When two tags receive the query command, they choose a random back-off time uniformly from the interval [0.1, 0.5]. If the two tags choose different times, there will be no collision and the data can be sent to the reader successfully.

5.4.4 Collision and Re-transmission

The collision occurs when two or more tags send reply the reader at the same time. The following scenario explains the event in which a collision might occur. Assume that two tags selected the same back-off time. If two tags have data to send, a collision will take place at the reader. In

Table 5.8: Parameters used for protocol simulation.

Parameters	RFID
Frequency	900 MHz 930 MHz
Bandwidth	250 KHz
Tx Power	0.2 mW
Rx Sensitivity	-84 dBm
Buffer Size	64 kb
Data Rate	2 Mbps

this case, the propagation delay and system delay are expected to be the same. If the reader detects the collision, it will send a NACK and a new query commands. The time the reader takes to send a new query after a NACK is called the system delay at the reader side. When the tags receive the new query, they will choose a random back-off time again. If the random time is different, a successful transmission will take place.

The above scenario explains the implementation of our proposed protocol with two RFID tags. However, there could be multiple tags implanted in the brain. In our model, a tag with a new packet to transmit delays the transmission for a random time after it receives the query from the reader. The behavior of a single tag is studied using a Markov model [152], and the probability of packet transmission and collision was calculated.

5.4.5 Evaluation of Protocol 2

This protocol was simulated using the NS 2 simulator [87, 109, 130]. It is a discrete-event network simulator for Internet systems. We have used 10 tags as passive RFID that work on backscatter, we used frequency hop to assign random channel frequency to each tags. The frequency ranges from 900 MHZ to 930 MHZ frequency hop. During the simulation, the delay and collisions were calculated. The parameters used in the simulation are shown Table 5.8.

The protocol was designed in a way that mimics the human brain. Ten RFID tags were used to analyze the effectiveness of the protocol, assuming that the transmitters are implanted in the brain [107]. The transmit power and receive power are kept as low as possible, which abides by the FCC recommendations [115, 138]. The bandwidth range of the RFID UHF was set from

Table 5.9: Collision Comparison - 10 Tags

Parameters	Number of collisions
Average number of collisions	530000
Collision for 6 hours	12045
Collision for 24 hours	470594
Collision for 48 hours	974269

900 to 930 MHZ [30, 107, 129].

In our previous tests, we found that the center frequency must be set to 914 MHz. Therefore, we set the frequency of operation to 914 MHz. We used a single reader to analyze the performance of multiple implantable transmitters that are communicated to it. Because of BCI systems were designed to operate without human intervention for a long time, the simulation was carried out for a duration of up to 48 hours. The following sections explain the evaluation results.

Collision

One of the most important factors for BCI applications is a collision. The purpose of developing this protocol is to minimize the number of collisions when multiple tags are used inside the brain. The collision is detected at the reader when replies from more than one tag reaches the reader at the same time. Table 5.9 shows the average number of collisions that are detected at the reader for a duration of 48 hours. The number of collisions detected is calculated as a function of the simulation time in hours.

As illustrated in the table, the total number of collisions for the duration of 6 hours is 12145 collisions. While, the number of collisions for the duration of 48 hours is 984269 collisions. The average number of collisions detected is 530000 collisions. The average number of collision is less than, by 5000, the number of collisions of the Slotted Aloha MAC protocol and 25000 less than the number of collisions of the No MAC protocol [182]. This proved that our proposed protocol enhanced the network performance by reducing the number of collisions.

Delay

BCI applications are delay sensitive. The total time taken for neuron firing to lead to a muscle activity or a reaction is called the delay. The average time taken by a human to put thoughts

Table 5.10: Delay Comparison - 10 Tags

Parameters	Average Delay
Average Delay With Re-transmissions in milliseconds	60
Delay without re-transmissions for 6 hours in hours	1.23
Delay without re-transmissions for 24 hours in hours	3.19
Delay without re-transmissions for 48 hours in hours	4.21

into action is about 150 ms [105, 135]. The auditory and visual reaction time are about 140 ms to 160 ms and 180 to 200 ms, respectively. Reflex actions are even faster (in the order of micro seconds) as they do not involve the neuron firings [30, 129, 182, 197].

The delay in our protocol can be of two types, which are: delay without re-transmissions and delay with re-transmissions. Delay without re-transmissions is the time taken to receive a successful reply in the first attempt itself, it is involved in a successful transmission. While, the delay with re transmissions is the total time taken by for the reader to read a successful reply from a tag after several attempts. Hence, this delay includes the time taken to send a NACK, and the systems delays of the tag and the reader. As shown in Table 5.10, the average delay with re-transmission is higher than the delay without re-transmission.

It is more likely to have several inventory rounds before reading a selected tag [139]. The proposed algorithm does not have multiple command exchanges which decreases the delay and overhead. As shown in the table, the average delay with re-transmission is 60 ms, which is 9 ms less than the delay time of the Slotted Aloha protocol and 17 ms less as compared to the No MAC protocol. The delay time of the Slotted Aloha protocol is 69 ms, and the delay of the No MAC algorithm is 77 ms [182]. This proved that our proposed protocol enhanced the network performance by reducing the delay time.

5.5 Discussion

BCI applications are designed to allow people with disabilities to communicate with external devices. This takes place by analyzing and translating the brain signals (e.g. ECoG an dEEG) to generate useful commands to control the external devices. BCI applications use implanted sensors inside the skull in order to read the brain signals. These sensors communicate in a wireless

manner with external readers to send and receive signals. This thesis proposed two MAC protocols that improve the communication between the implanted RFID sensors and the external readers. The first proposed MAC protocol is based on combining three conventional MAC protocols to improve the transmission efficiency and reduce the delay. The proposed hybrid protocol divides the sensors into clusters, where the tags in a particular cluster are assigned a specific frequency band. The tags within each cluster use TDMA, however, the time-slots can be accessed by other tags to reduce the average waiting time, and thus, reduce the delay and increase the throughput. The proposed hybrid protocol was compared with two other hybrid protocols, but only using a combination of two protocols. The obtained results demonstrated that the proposed hybrid MAC has several advantages in terms of the delay, throughput and dropped data. Moreover specifically, the delay was significantly less than the other considered protocols, which makes it attractive for time-sensitive applications such as BCI. The second protocol was designed for the ECoG signals, it was simulated using the NS 2 simulator. The evaluation results showed that both protocols have improved the performance of the brain network and they are suitable for BCI applications.

Acknowledgment

We thank Dr. Arafat Al-Dweik for his useful contribution.

Chapter 6

Enhancing Data Gathering in Medical Records

6.1 Overview

Brain-Computer Interfaces was developed in the 1970's. Its purpose was to study and process brain activity to convert brain processes to be used with machines and devices [157]. This concept has been researched for decades and can now not only record brain activity but also stimulate it. Fig 6.1 describes the general BCI cycle that manages recording and stimulating neurons in the brain [158, 159]. The clockwise cycle in the Fig 6.1 shows the acquiring and recording of the neural data and the counterclockwise representation shows the stimulation of the brain. In acquiring neural activity, it was found that neurons communicate with one another to produce neural activity when actions are preformed such as playing with a joystick. Neural activity is also generated when no task is performed (Phase 1, Fig 6.1). Once this neural activity is generated, it is recorded by the BCI and transformed into digital data (phase 2). Once phase 2 is completed the data is analyzed by the BCI processing system to determine the action that was intended by the person (phase 3). In the last phase, applications perform the intended action on an external device. The applications can generate new neural activity by generating optional feedback. The counterclockwise phases of 6.1 begins in the 4th phase, applications define the intended action. In phase 3 the intended action is processed to generate a neural firing pattern containing the required pattern required by the BCI to stimulate the brain. In the last phase of the counter clockwise stimulating phase the firing pattern is transferred to the BCI. The BCI stimulates the neurons belonging to the different brain regions and depends on the technology used. BCI can be communicated bidirec-

tional or unidirectional between the brain and the external computational devices. In unidirectional communication the BCI can either collect data from the brain or stimulate the brain. Bidirectional communication is when both tasks are performed [160].

Therefore, BCI's network security is particularly important. Network security usually refers to the security of the computer network, in fact, it can also refer to the security of the computer communication network. A computer communication network is a system that interconnects several computers with independent functions through communication devices and transmission media. With the support of communication software, information transmission and exchange between computers is realized. The computer network refers to a system that uses communication means to connect several relatively independent computer systems, terminal devices, and data devices in a geographically dispersed area, and exchange data under the control of a protocol. The fundamental purpose of the computer network is to share resources. The communication network is a way to achieve network resource sharing. Therefore, the computer network is safe, and the corresponding computer communication network must also be safe. It should be able to achieve information exchange and resource sharing for network users. In the following, network security refers to both computer network security and computer communication network security.

The basic meaning of security: objectively, there is no threat, and subjectively, there is no fear. That is, the object does not worry about its normal state being affected. Network security can be defined as: a network system is free from any threats and infringements, and can normally achieve resource sharing functions. To enable the network to realize the resource sharing function normally, it is necessary to ensure that the hardware and software of the network can operate normally, and then to ensure a secure data exchange. As can be seen from the previous two sections, due to the misuse of resource sharing, it has caused network security problems. Therefore, the technical approach to network security is to implement limited sharing. Network security attacks will affect every stage of the cycle, and the BCI cycle configuration is also different. We propose a new version of the five-phase BCI cycle acquisition and stimulation function.

BCI is in the early stages of cyber security development. Cyber security has not previously been considered an important aspect of BCI until very recently. Since then teams such as neuro security, neuro privacy, neuro confidentially, brain hacking and neuro ethics have developed [161–163]. There is a history of cyber security attacks on BCI affecting its integrity, privacy, availability and safety. The current literature on these attacks miss relevant information and a complete analysis [157, 164–167]. The 198 works cited by this article are organized in four categories:

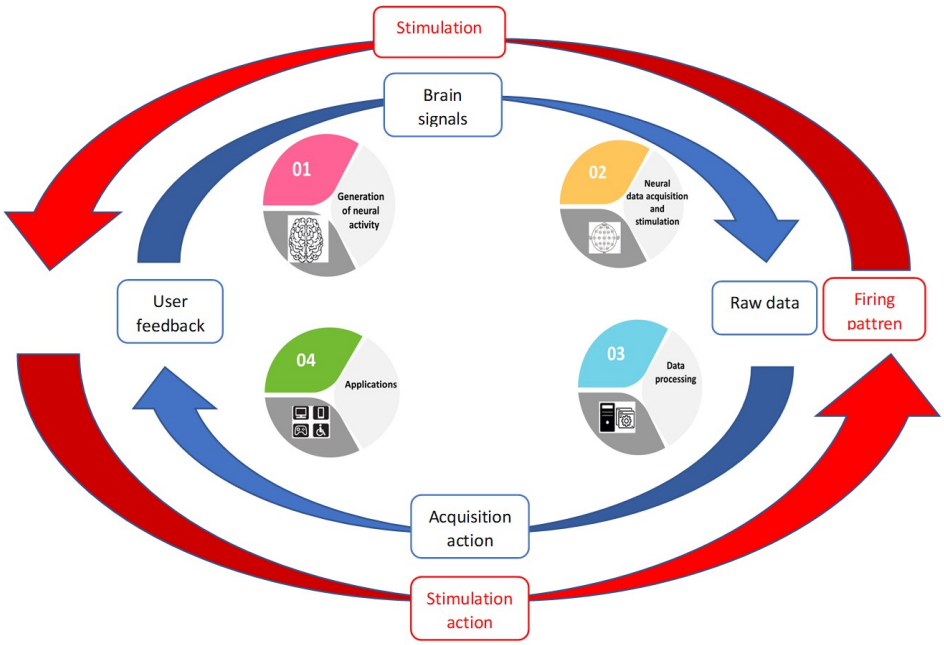

Figure 6.1: The Bidirectional BCI general functioning. The clockwise flow indicated with a blue arrow represents the neural data acquisition process, while the counterclockwise flow represented by a red arrow models the brain stimulation.

BCI, Cybersecurity, Network communications, and Internet of Things. Subsections of these categories are meant to provide a more thorough understanding. This article main focuses are on BCI, Cybersecurity and Network communications.

BCI is a non-invasive medical tool can be used to benefit people with many different medical conditions and people who are paralyzed. BCI is mostly used today as a neuro prosthesis. It helps nerves function that is damaged and do not work properly. The most common use is cochlear implants. It is a device that can help people hear. However, issues with security of retrieving information from people's brain activity must be taken into account. Researchers and companies are now looking into whether the BCI can be used to read people's thoughts. The U.S military has use of BCI and Facebook has even recently purchased a BCI company. Facebook is predicting that the future of how we interact with our devices will be through our thoughts [167, 168]. Given the critical context, it is imperative that the thoughts must be protected from an unauthenticated access in order to carry out BCI applications duties effectively. Though research on BCI network security is rare in the literature, this thesis is geared towards offering a solution to the looming problem via the use of radio frequency identification (RFID) technology. The choice of RFID technology is that it has been known as one of the pervasive computing technologies that offers support for

both practical and real-time implementations with reference to item identification, monitoring and tracking [162]. The integrity of the BCI applications will be protected against impersonation vulnerability and consequently, if the RFID based system is properly implemented. .

6.2 Cybersecurity in BCI

RFID technology is gaining an extensive consideration lately more than other technologies in the automatic identification and data capture (AIDC) group. Today, the innovation has discovered application in different fields going from an object and human or animal identification, tracing, tracking to monitor [175].
Researches in the literature have shown that where RFID has been effectively applied, it yields positive effects. Some of the successful applications of RFID are featured in this part: One significant use of RFID is in object observing. In this pattern, an RFID-based domesticated animals, observing framework was created by [176]. The framework screens each livestock movement and furthermore gives data about them utilizing the RFID tag implanted in the animals.

Also, in another investigation [177], a Cold Chain observing framework utilizing RFID was created and used to track the product movements in the supply chain. The system operates in a real-time manner where location is tracked, temperature monitored to ensure product quality during delivery. Moreover, a project called FARMA was developed by [178]. It uses the RFID technology alongside wireless mobile network to track animals as well as access their information stored in a data repository. With this type of system, animals were being tracked and identified in the case it gets lost. Additionally, in a similar work by [179], a context-aware notification system based on RFID was designed and developed for university students. The notification system was developed with the objective of conveying urgent notifications to expected students instantly where there were at the moment according [178, 179].

Moreover, [179, 180] designed a student tracking system that track students' location in a live-in school utilizing a combination of RFID and biometric sensor. In the same vein, Christopher et al [169] additionally built up a framework that robotize the drawn out mice conduct viewing in socially or structurally complex caged environments via RFID. The framework precisely represents the locations of all the mice as well as each mouse's location information over the long run,.

In associated work by [182], an RFID-based framework was created to distinguish patients in the emergency clinic. The point was to animate patients' recognizable proof cycle particularly on account of oblivious patients or those who can't communicate thereby delaying treatments. Likewise, Catarinucci et al [183] built up an RFID-based computerized framework that tracks and examinations conduct of rodents in an ultra-high frequency bandwidth. However, we have discussed just a few of RFID application successes in this thesis. Based on these successes in tracking, monitoring and identifying, we strongly support that the application of RFID BCI systems will assist people who are suffering from spinal cord injuries to protect their thoughts and brain activities..

6.3 BCI challenges

The history of BCI can be traced back to the 1990s, when the nerve repair device made it possible to control artificial limbs and wheelchairs through nerves [169]. In the 21st century, this device has been further developed, which can help patients regain their motion ability by establishing communication links between severely paralyzed patients and various external prosthesis [170]. This new trend of BCI became the normal form at the beginning of the 20th century and this concept has been developed continuously, which thus defines bi-directional BCIs. Brain−net is a kind of brain network that can create correlations. It can not only contact other users, but also establish cooperative relationships with them, so that knowledge sharing can be realized [170].

The importance of BCI has been recognized by more and more people, and even different governments have promoted the proposal of BCI. Different countries have started to explore it as a new technology, and an increasing number of participants have joined in it [171]. As a result, the standards of this industry are better refined, and new usage scenarios are constantly developed. At the same time, the research of BCI equipment has also brought opportunities to manufacturers, who have managed to improve their competitiveness by establishing their respective services. With the continuous development of products, BCI's use scenarios are extending to all walks of life, and it is expected that the development of BCI equipment is very promising [172]. The development of BCI devices aims at specific scenarios and demand, but the interoperability between BCI and the emerging cloud computing is not taken into account. In recent years, the development of cloud computing is greatly emphasized by various enterprises and countries, so cloud computing will be the core of the following industry. If interoperability is not achieved in BCI devices, its scalability in the future will not be quite optimistic, and it will also lead to some functional issues

such as network security [167]. Hence, a uniform standard is required for different BCI devices, which will also be of positive significance for its progressive development. Therefore, different companies have tried to solve the security issues and functional design problems by using common standards.

The inability to alter or add functions as required is also a disadvantage of BCI devices [165–167, 173]. How to make BCI devices applicable to different scenarios, changing from the single application to a fixed scenario with the capability of adding different functions as required is one of the challenges for the further development of BCI devices. Therefore, the trend of a global BCI will require new processing methods and framework construction. All aspects mentioned above affect the solutions to the applicable network security. This is because the BCI system only considers the defense mechanism of possible threats, but for some other known threats, expansion can't be realized by adding the threat defense function, which, to a certain extent, will cause many unpredictable security problems in the BCI system [166, 173]. A possible solution to this problem is a BCI modular design, that is, adding different modules to improve the overall function according to different needs. User privacy is another important issue, because the current BCI framework doesn't take the protection of user information into account, especially when the users' neural information is again accessed externally, it is uncertain whether it will be used for other purposes. In order to improve this situation, it is urgent to develop some user-friendly systems to help them deal with the rick of privacy problems. At the same time, every country should enact relevant laws to restrict the companies providing external services and related applications, so that users' privacy can be better protected.

We need also consider some problem such as the safety of human life and social fairness and justice. The invasive or semi-invasive brain computer interface needs to be embedded with chips and other hardware in the brain, which will damage the natural physical protection of the brain. If the relevant hardware and software facilities are illegally used (such as inputting malicious signals, changing signal thresholds), it may cause brain disorder, in serious cases, it will cause brain damage, it will also endanger people's life. The digital divide has brought more and more serious problems of fairness and justice, leading to essential differences among different groups in information acquisition, resource possession, wealth accumulation and many other aspects. With the application of brain computer interface technology, especially after the deep integration of brain and artificial intelligence, the digital gap between people will be further expanded. Brain computer interface technology can greatly improve human cognitive ability, so it has obvious advantages in learning, work and other activities, however, limited by technology, politics, economy and other

reasons, only few people have the conditions and costs to evolve themselves so they can be better than average people. This huge digital divide will undoubtedly lead to the loss of fairness and justice in human society, and lead to sharp social contradictions, so it is very important for government and relevant industry organization to establish relevant laws to strengthen management.

Of course, there will be many potential network security problems in the future. Manufacturers should evaluate the risk of network attacks from different perspectives. For example, aimed at different network threats, such as firmware attacks, password attacks, social engineering and phishing attacks, blackmail based malware attacks, botnet based malware attacks, sniffer attacks and other risks, we are supposed to adopt different standards as to different types of data information exchanges, for example, adopting the well-known standards for medical system information [173].

6.4 Cybersecurity risks associated with BCI classifications

6.4.1 Design of BCIs

The design of the BCIs determines who initiates the neural data acquisition process and how the process is performed, i.e. the process can be performed by the user or the BCI, and how the interaction can be performed the expected operation. [185–189]. Resulting in four BCI series: active, passive, reactive, and hybrid. From a cybersecurity perspective, the main risk of the four BCI series is adversarial attacks, which are described in more detail below.

Active BCIs (also known as independent [188] or spontaneous [185]) is a type of the BCI system in which the user controls external devices through direct and conscious brain activity. This type of BCI can be completely independent of external stimuli, that is, active BCI does not require external stimulation such as vision, listening, body induction. Therefore, finding an effective and stable physiological signal caused by subjective consciousness is the key to establish ingenuity BCI system. An example of the active BCIs is the imagination of limb movement [186–191]. Gilja et al. [186] used an active BCI to control the computer cursor of the rhesus monkey. Currently, the most commonly used physiological signal in active BCI systems is event-related desynchronization/synchronization (ERD/ERS) signals, which reflect the brain's motor intent. In addition, there is a slow cortex potential signal. Passive BCIs refers to a class of BCI systems that can read changes in the user's cognitive state and are used in human-machine interaction systems, which do not require active user control. Most scholars believe that passive BCIs is an extension of tradi-

tional BCI. Traditional BCI systems require users to actively send the required instructions to the outside world. In the use of passive BCIs system, users do not need to deliberately control their own brain activities, the system will read the user's emotional state, task-related psychological activities, error-related psychological activities, user mental load, fatigue and other non-user active control of the psychological activity state, so as to achieve interaction with peripheral. For example, adjust environmental elements based on the user's emotional state to maintain normal emotional activity. Therefore, passive BCI is a kind of strengthening and auxiliary way of traditional interaction, and its application scope is no longer limited to providing new communication channels for special groups of people, but can be monitored and feedbacked by the user's emotion, mental load, alertness, fatigue and other state changes in the daily work environment, as well as applied to human error detection and correction. Reactive BCIs (also identified as dependent [185, 186] or evoked [187]) is a type of BCI system that indirectly expresses the brain's intentions by decoding the brain's specific response to external stimuli. Thus, the reactive BCIs system needs to pre-produce specific patterns of stimuli to guide the brain to induce patterns of activity associated with its own intentions, and then determine the brain's instructions for intent by comparing the degree of correlation between brain activity patterns and pre-set patterns. Therefore, the coding and decoding of instructions is an important part of the reactive BCIs system.

At present, the main coding methods of reactive BCIs are sometimes multi-access, frequency-divided multi-access, code-sharing multi-access, empty multi-access and mixed mode. Either way, a certain type of stimulus is required to act on the body's sensory channels. Therefore, according to the function of the sensory channel division, the reactive BCIs can be divided into visual dependence, auditory dependence, body sense dependence and so on. At present, the typical reactive BCIs system mainly has SSVEP system and P300 system. Finally, hybrid BCIs is a system that combines the brain-computer interface with other physiological or technical signals. The purpose of the hybrid BCIs is to improve the performance of the brain interface by integrating multiple input signals, thereby expanding the end-user population. In the hybrid BCIs, there is at least one brain signal as the brain interface intended input for real-time communication or control, in addition to the combination of brain electrical signals, can also use other types of brain signals to build pure hybrid BCIs. For example, the brain-machine interface, which combines NIRS and brain power, can significantly improve the precision of the classification of imaginary motion.

Malicious external stimuli are the most damaging of the previous BCI family's cyber security risks. It can be considered that hybrid BCIs is the most risky one, followed by reactive BCIs, passive BCIs, and finally active BCIs.

6.4.2 BCI technology

BCIs are also differentiated according to their technique, which produces two additional subcategories, depending on whether they are used to obtain neural data or brain stimulation. Considering the collection of brain waves, the most representative techniques are EEG, Functional Magnetic Resonance imaging (fMRI), Magnetoencephalography (MEG), Electrocorticography (EC0G), and neural dust [185–189]. On the other hand, the most relevant brain stimulation techniques are Transcranial Magnetic Stimulation (TMS), Transcranial Electrical Stimulation (tES), Transcranial Focused Ultrasound (tFUS), Deep Brain Stimulation (DBS), and neural dust [181–186], [178]. All of these families pose a cyber security risk.

Electroencephalogram (EEG) is a method of recording brain activity using electrophysiological indicators, which are formed after a large number of neurons occur simultaneously after the synapse has combined. It records changes in electrical waves during brain activity and is an overall reflection of the electrophysiological activity of brain nerve cells in the cerebral cortex or on the surface of the scalp. Functional Magnetic Resonance Imaging (fMRI) is a non-invasive imaging technique used to study brain function and cognition in healthy individuals and groups with abnormal brain states. MEG is a completely invasive, injury-free brain function detection technology, which can be widely used in the development of brain function and clinical brain disease diagnosis. The process of detecting MEG directly measures the very weak bio-magnetic field signals emitted by the brain's neural currents, and the measurement system itself does not release any harmful rays, energy, or machine noise. Electro spectral (ECoG) is a partially intrusive method that provides a signal-to-noise ratio (SNR) that is superior to non-intrusive systems, such as EEG, and higher spatial and temporal resolution [186]. However, ECoG cannot be used to detect single neuronal spikes, and using these devices outside the operating room is challenging [185–187].

The current DBS system requires the surgical implantation of the electrode leads into the brain, usually in deep brain structures or near the thalamus, while an implantable pulse generator (IPG) is implanted in the chest cavity. DBS is also used in the treatment of epilepsy to reduce seizures by stimulating the prenuclear or hippocampus of the thalamus. Many non-invasive neuro regulation methods have been developed to regulate nerve tissue without invasive surgical treatment, including transcranial magnetic stimulation (TMS), transcranial current stimulation (TCS), and transcranial focused ultrasound stimulation (tFUS). Although the spatial resolution of the non-intrusive method is lower than that of the intrusive method, the risk is lower due to the non-intrusive nature. TMS uses electromagnetic induction to generate sensing currents in the brain, and since

its introduction in 1985, TMS has become a neuroregulatory therapy for many neurological disorders. Applications of TMS include depression treatment, stroke recovery and Parkinson's disease treatment. TCS is generally considered a stimulation technique under the threshold because it only regulates excitability and does not directly generate action potentials. TFUS is still in the early stages of clinical application, but in theory, tFUS with focused energy has higher spatial resolution and precision than other non-invasive technologies. Neural dust technology is a neural remote sensing technology developed from the perspective of wireless energy supply. The basic strategy is to supply energy to the neural signal amplifier implanted in the body using the energy transmitted wirelessly from the outside, and the amplified signal can be transmitted in reverse. Thus, both time and spatial resolution pose important network security risks. BCI technologies such as neural dust, ECoG, or MEG in particular have higher risks for data confidentiality and security, while lower-resolution technologies such as EEG, fMRI, or TMS are higher.

6.5 The Proposal

In order to help protect the integrity of the BCI system, this thesis proposes the design of a security system that is based on RFID technology, which utilizes EPCglobal Network [192–196] to secure patient brain activities. The overall requirements that need to be satisfied by the system is the identification of the device controller (control device) as real or not real. Details about the system architecture is discussed in the sub-sections that follows.

6.5.1 System Architecture

The system architecture consists of the following components: (1) RFID tag and reader, the (2) Clinic database, (3)The Clinic Electronic Product Code Global Network (EPC global Network) and the clinic computer. The overall structure of the system in terms of identification and authentication as well as their interactions are shown in Fig. 6.2 As shown, the system requires the clinic to maintain a central database where information of all patients identification are collected and stored. Fig. 6.2 shows the relational diagram of the database containing information to be collected.

For the RFID tags we used Wireless Identification Sensing Platform (WISP5). Considering

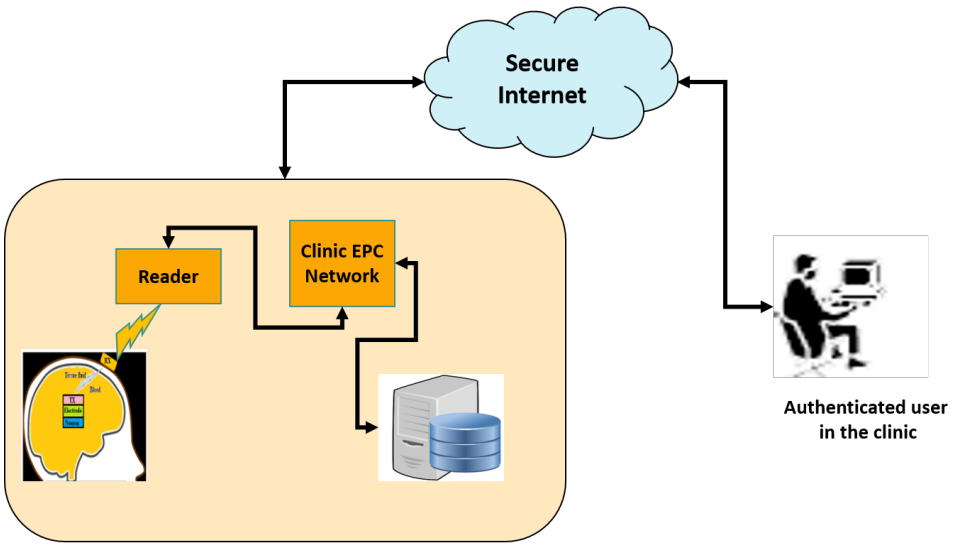

Figure 6.2: Proposed system architecture

a sample rate of 8KHz which is more practical in case of WISP, continuous action potential signals are sampled at 8K samples/second. When we consider each sample to be 8 bits, we get 64 K bits/second, which is the raw data without headers, error correcting codes, synchronization bits, etc. Including all the above overhead it can go up to 100KHz. If we use a grid of 512 electrodes it rises to 51.2Mbps, we need around 50 RFID tags because the maximum data rate transmission for each RFID tag is around 1Mbps [29, 196].

Although the data rates for certain BCI applications such as the P300-based BCI can be very low [195], there are other applications that is currently being investigated were much higher data rates might be required. For example, Kaplan et al. [196] considered adapting the P300-BCI for gaming applications. Furthermore, it is shown in [47] that an EEG signal might require about 85 kbps in particular scenarios. Therefore, the need for high data rate support for BCI systems is a key enabler for future BCI applications.

For different BCI paradigms such as movement imagery (MI) we need to use more tags because we need more information. For our scenario we considered just the upper limp. The motor cortex comprises three different areas of the frontal lobe, immediately anterior to the central sulcus. These areas are the primary motor cortex, the premotor cortex, and the supplementary motor area. The primary motor cortex, or M1, is located on the precentral gyrus and on the anterior paracentral lobule on the medial surface of the brain. The stimulation of the primary motor cortex requires the least amount of electrical current to elicit a movement. Stimulation of premotor cortex or the supplementary motor area requires higher levels of current to elicit movements, and often results in

more complex movements than stimulation of primary motor cortex. Stimulation for longer time periods (500 msec) in monkeys results in the movement of a particular body part to a stereotyped posture or position, regardless of the initial starting point of the body part. The tags positions are fixed outside the brain on the scalp where the primary motor cortex of cerebellum is located, because the cerebellum responsible in generating neuron signals for the upper limp.

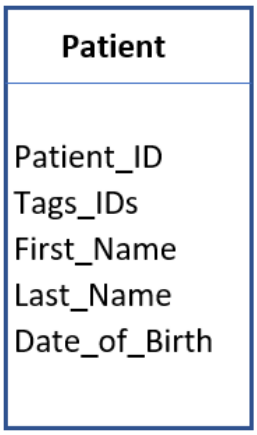

Figure 6.3: Relational diagram for Patient class

To facilitate the identification process, each patient will be assigned a unique identifier called PatientID In the same vein, each Patient will be given an electronic device as mini reader. The tags are semi-active RFID tags placed on outside the brain on the scalp which contain the EPC code. The electronic device that has the mini reader called scanner controller which will be wirelessly used to read the tag data to identify and authenticate if a patient data is real or not. This process will be made effective in a real-time mode by utilizing the EPCglobal Network [183].

6.5.2 RFID Tag and Reader

For effective communication and in line with patients' operations, the design of the scanner controller contains both the tags IDs' and the associated reader beside GPS to update the patient location. That is, a semi-active RFID tags and a mobile RFID reader. The mobile RFID reader will have the capability to scan and wirelessly send tags information via the EPC network for processing and receives the results that identify if a patient is real or not. In addition, the structure of the RFID tag will be in line with the EPCglobal specification which is shown in Fig. 6.4 .

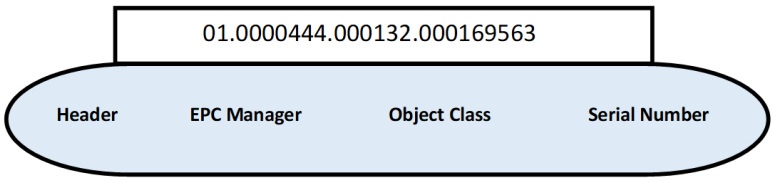

Figure 6.4: RFID tag structure

- Header: In the device, the header will identify the type, length, structure, version that these tags will take, which could be 64bits, 96bits, 256 bits, and 512 bits as needed.
- EPC Manager: will contain the number that identifies an organizational entity. In this case, the clinic administrator ID which will have a code that represents the patient ID who has the semi active RFID placed tags on his brain outside the skull and the EPC is embedded into.
- bject Class: It identifies the semi-active RFID tags ID's. In this case, the object class will identify the tags.
- Serial Number: This is a unique number of items within each object class. The serial number will be the unique identification number of each patient. The number will be used to query the central databases through the secured Internet to retrieve, update, and identify the authenticated patient information.

6.5.3 RFID Reader and Central Database Interactions

Based on the recommended design that incorporates both the semi active RFID tags and the scanner controller, care must be taken to ensure that each of the RFID readers do not read the same tag data every time it senses a brain activity. In this case, each scanner controller will be embedded with the intelligence of identifying its own tag data with timer that can be triggered whenever the tag sense new brain activities using backscatter technique (reference shams). That is, the scanner controller must store the same serial number and timer for each tag. The algorithm represented by the flowchart captured in Fig.6.5 can be followed to design the device that contains the tags and the reader. With the algorithm, anytime the reader senses or reads a tag data, it gets the tag data first and compares it with its own data. If they are the same, it does nothing, otherwise it uses the tag data to identify whether the tag information is real or not. In the same vein, the scanner controller device must be able to communicate with the clinic central database on a real-time mode at least 24

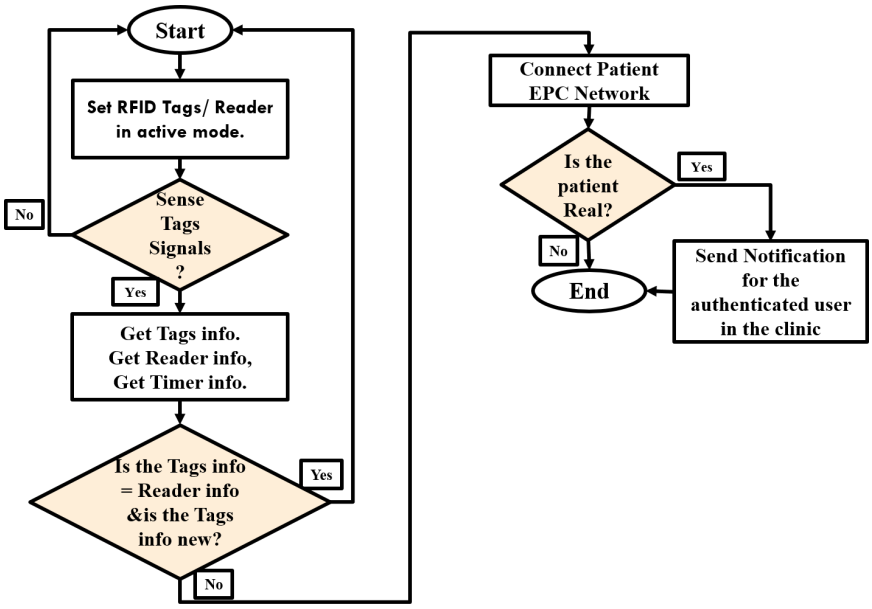

Figure 6.5: The RFID reader and tag communication

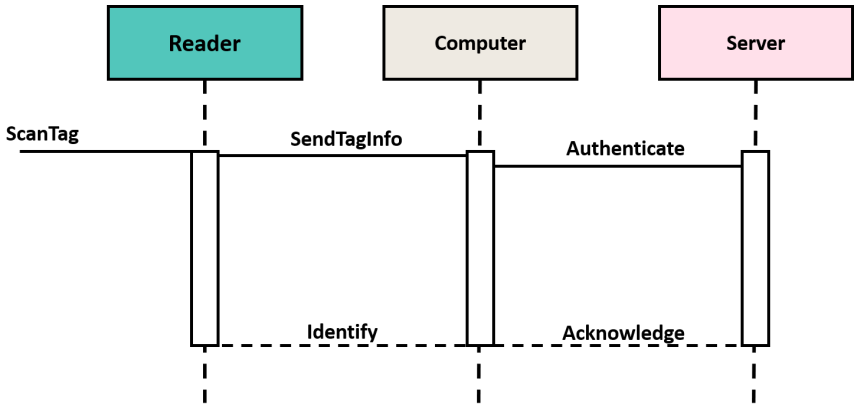

Figure 6.6: RFID scanner/Central database sequence diagram

times per a day to carry out the task of identification and authentication effectively and efficiently. The communication is represented using the sequence diagram shown in Fig.6.6 .

As represented in Fig. 6.6, to identity and authenticate a Patient brain signals as real or not, the RFID scanner would read the device, transmit tag data which is the PatientID via the EPCglobal Network. The PatientID is then automatically used as a primary key to query the central database. If the PatientID matches information stored in the database, an acknowledgement is sent in the form of vibration or information display on the computer screen. Otherwise, they are not real. (See Fig. 6.2)

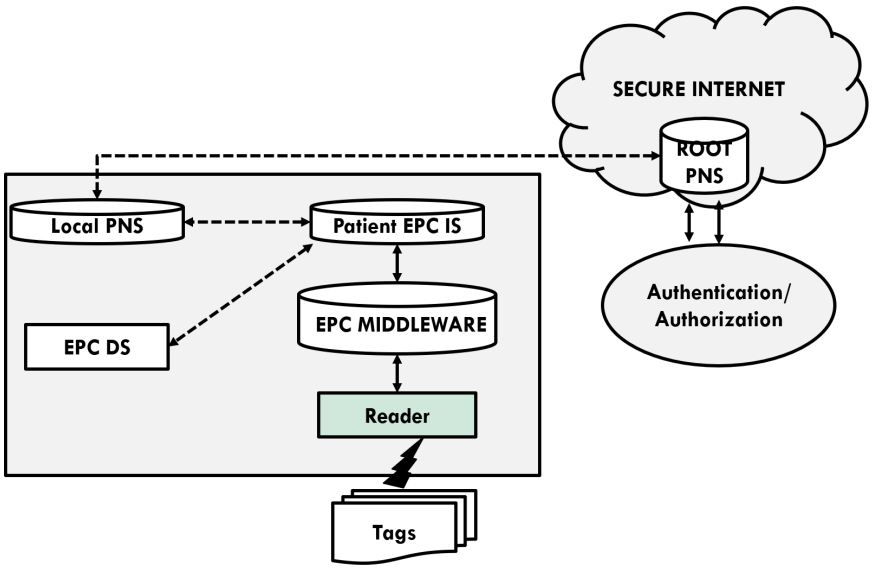

Figure 6.7: Patient EPCglobal network architecture

6.5.4 Patient EPCglobal Network

EPC global Network provides several benefits which forms a part of the motivation of its applicability in this work. Some of the benefits are: (1) the network is designed to provide a link for all EPC tag-oriented physical objects, (2) scale to support the huge volume of data generated by RFID-enabled activities between readers and tags, and (3) to proffer a data format that is universal for transferring information specific to a particular object [22, 29, 195, 196]. The EPCglobal Network architecture is captured in Fig. 6.7. With the EPCglobal architecture shown in Fig.6.7, the contribution of each component to the operation of the proposed system is given as follows:

Given the electronic device having a timer and a mini-reader, if an RFID reader senses or reads an RFID tag data, the data which is the EPC will then be transmitted by the reader through the EPCglobal Network to the middleware. The RFID savant, which has the capability to process, filter, aggregate the tag data will in turn, use the processed EPC to query the root object Patient Naming Service (PNS) over the secured Internet for the Patient local PNS. At this point, the root PNS queries the local PNS for the patient data which is in the EPC Information Service (EPCIS). To access the data for a particular patient, the EPCIS is queried using the EPC-related data and if a matched is found in the database maintained by EPCIS, the result of the request is sent back to the device in the form of a vibration or screen display, confirming the patient is realistic. Lastly, the EPC Discovery Services (EPCDS) will keep track or record of all patient's tags and patient ID

identified by EPCIS.

6.6 Results and Discussions

BCI applications are designed to allow people with disabilities to communicate with external devices. This takes place by analyzing and translating the brain signals (e.g. ECoG and EEG) to generate useful commands to control the external devices. BCI applications use implanted sensors inside the skull in order to read the brain signals. These sensors communicate in a wireless manner with external readers to send and receive signals. This thesis proposed the design of a security system that is based on RFID technology, which utilizes EPCglobal Network that improve the communication between the implanted RFID sensors and the external readers to secure patient brain activities. The overall requirements that need to be satisfied by the system is the identification of the device controller (control device) as real or not real. This novel proposed system is very crucial for Bidirectional BCI applications. For the Bidirectional BCI applications, we can program the patient's brain by sending back different instructions, so it is very important to secure the BCI channel as it is Bi− directional channel. Our future work includes investigating the use of different sensing devices (e.g. WUB) and test our proposed algorithms with more sensors than the sensors we used in this work.

Chapter 7

Conclusions and Future Work

7.1 Conclusion

The series of experiments and analyses in this thesis were intended to address the feasibility of BCI system using ECoG and EEG signals for possible use in many applications such as the P300-based BCI [44], other applications that is currently being investigated were much higher data rates might be required. For example, Kaplan et al. [45] considered adapting the P300-BCI for gaming applications. Furthermore, it is shown in [46] that an EEG signal might require about 85 kbps in particular scenarios.

The general approach to this goal was to investigate it from three different research avenues: Signal acquisitions, Signal transmission and cyber security aspects for BCI applications. Our first avenue to this primary goal was to propose a novel machine-learning algorithm called *HRFE* to increase the classification accuracy on time of the ECoG signals for BCI applications. HRFE utilizes one classifier to pick the significant features and uses different classifiers to optimize the detection of signal features objectively. We use noise to model the ecological presence in signals and determine features more resistant to noise. In order to make the final model robust, we assume features with large coefficients in logistic regression. The results confirm the accuracy improvements to reach the optimal level. We test the HRFE algorithm on two real datasets, namely dataset I and BCI competition III, and achieve about 93% accuracy in 5 minutes and by mimicking the brain environment and collecting signals at 4 cm depth as ECoG signal. We also show that the testbed experiments can classify two signals with 95% accuracy.

Additionally, Developing BCI systems is vital to help individuals with motor disabilities. BCI systems detect brain activities using signals extraction and classification algorithms, and con-

verts them into useful commands that can be used to control external devices. Designing and developing BCI systems requires accurate extraction and classification algorithms to detect brain activities in a timely manner. In this thesis, we presented an accurate ECoG signals extraction and classification approach. The FAWT was used to extract three entropy features (i.e. log energy entropy, SURE entropy, and cross corr-entropy), and the LS-SVM was utilized to classify the extracted features. Testbed experiment and the dataset I of the BCI competition III was used to evaluate our proposed approach. The evaluation result has proved the validity of our proposed approach. Our LS-SVM classifier has achieved 93.02%, and 95% classification accuracy, using the dataset I of BCI competition III and the testbed experiment, respectively. Our future work includes investigating other features, developing a data mining technique to classify the ECoG signals, and implementing the other features extraction technique.

Finally, at the receiver side the basic adaptive algorithm, Least Mean Square Algorithm can be used to cancel the distortion produced in Communication Systems .Choice of μ plays key role in operating adaptive cancellers using LMS Algorithm. To increase the sampling rate of Analog to Digital conversion,time interleaved ADC system is a good option. Even if ADC's made at the same place and same time are used they are not identical. When interleaving, since ADC's are not identical, mismatch errors in time, gain and offset occurs.

These errors result in distortion of signal, which need to be corrected for better performance. Calibration of ADCs is costly and time consuming. Further more, the mismatch errors may slowly change with temperature and aging. Therefore, it is preferable to continuously estimate the mismatch errors while using ADC. Adaptive methods are preferred for estimating and correcting time mismatch errors. An adaptive process which uses LMS Algorithm is proposed which is cost effective and fast.A real sinusoid is used as a probe to test the adaptive model.In this project we have used pair of ADC's. We can use a similar method for multiple ADC's along with multiple probes to cancel the artifacts.

There is another method blind equalization which is also an adaptive process but is much more complicated than our method. Our method is much simpler and faster.

For our second avenue which is signal transmissions, We have found that passive UHF-RFID is a viable wireless technology for many BCI applications. This technology can support stable transmissions for at least a hundred electrodes in the depths and configurations we have measured. We studied the impact of tissue fluid, blood viscosity and implant depth on signal transmission (e.g. ECoG signals) using multiple UHF passive RFID transmitters. Also we present a comparative study between single, two and three transmitters at different implant depth. Our

study is the first step in modelling multiple channels for BCI applications. We specifically studied system parameters, which are imperative to the design of any wireless communication system. These were received signal strength, channel capacity, path loss, Maximum number of electrodes, power delay and frequency response for varying implant depths from 1cm to 4 cm. These results have been showcased in tables and graphical representation for varying implant depth. We find that passive UHF RFID do not work accurately when the implant depth of the transmitter is greater than 3 cm. Using multiple transmitters can improve the bandwidth transmission even though the transmission data rate could be reduced. Furthermore, implantable chips should be ultra-low power devices to avoid any deleterious effects of high power on the neural tissue within the cranium and the spinal cord. In conclusion, the appropriate requirements for WBAN sensor devices are small, lightweight and low maintenance. These devices are achieved by using a promising communication technology which is backscatter RFID in the UHF range. Backscatter sensor tags have low power consumption and thus make it suitable for WBAN systems.

As we are going to use many transmitters, developing MAC protocol using RFID-UHF for BCI applications becomes vital and essential. This thesis presented a new MAC protocol for BCI applications. The proposed two MAC protocols, Hybrid MAC based on combining three conventional MAC protocols to improve the transmission efficiency and reduce the delay. The proposed hybrid protocol divides the sensors into clusters, where the tags in a particular cluster are assigned a specific frequency band. The tags within each cluster use TDMA, however, the time slots can be accessed by other tags to reduce the average waiting time, and thus, reduce the delay and increase the throughput. The proposed hybrid protocol was compared with two other hybrid protocols, but only using a combination of two protocols. The obtained results demonstrated that the proposed hybrid MAC has several advantages in terms if the delay, throughput and dropped data. Moreover specifically, the delay was significantly less than the other considered protocols, which makes it attractive for time-sensitive applications such as BCI. The second protocol was designed for the ECoG signals, it was simulated using the NS 2 simulator. The evaluation results showed that both protocols have improved the performance of the brain network and they are suitable for BCI applications.

Final research avenue states BCI applications are designed to allow people with disabilities to communicate with external devices. This takes place by analyzing and translating the brain signals to generate useful commands to control the external devices. BCI applications use implanted sensors inside the skull in order to read the brain signals. These sensors communicate in a wireless manner with external readers to send and receive signals. This thesis proposed the design of a

security system that is based on RFID technology, which utilizes EPCglobal Network that improve the communication between the implanted RFID sensors and the external readers to secure patient brain activities. The overall requirements that need to be satisfied by the system is the identification of the device controller (control device) as real or not real. This novel proposed system is very crucial for Bidirectional BCI applications. For the Bidirectional BCI applications, we can program the patient's brain by sending back different instructions, so it is very important to secure the BCI channel as it is Bi− directional channel.

7.2 Future Work

Finally, as mentioned in Chapter 2, we developed and tested the HRFE and FAWT algorithms on binary class data sets to distinguish between just two types of brain activities. In the future we are planning to investigate multiple class data sets considering different features and machine learning metrics. For Noise cancellation future work in chapter 3 , the blind equalization technique will be used to demonstrate the complexity-performance trade-off. Besides, performance analysis and evaluation over the actual human brain environment will be considered.

A second objective in chapter 4 for signal transmission, we are planning to investigate the ultrasonic transmission not just UWB, and RFID-UHF to compare the transmission parameters such as RSS,SNR, Path loss and maximum number of electrodes. While, the future work for chapter 5 considering the performance of the proposed system as it is evaluated in terms of throughput, data rate and time delay. The hybrid system is evaluated using three different combinations FDMA+TDMA, FDMA+CSMA, and FDMA+TDMA+CSMA, for three technologies, which are UHF-RFID, UWB, and ultrasonic. The obtained results show that the proposed hybrid MAC outperforms all the individual MACs and can satisfy the requirements of BCI applications. The results are presented for several cases of using 12 and 100 tags. The results are obtained using Opent [147], which is a highly reliable simulation tool that is used by several industrial giants such as Cisco and AT&T. Nevertheless, developing a test-bed will be targeted in our future work to capture all practical aspects. The main obstacle in developing a test bed in the time-being is the lack of reliable development kits that can support such a system.

As demonstrated in this thesis, the brain is quite capable of applying signals from a relatively limited area of cortex to a variety of output functions. It may be well in the future, but brain-assisted technologies may very well revolutionize how we drive our vehicle to work or oper-

ate complicated machinery while leaving our hands available for other tasks and vice versa. It may seem far-fetched now, but it is exciting to think of the seemingly limitless possibilities along those lines. In the future, BCI devices may not only be thought of as medical devices intended for those with debilitating diseases, but devices made to change the way we proceed with our everyday life, similar to the way many of us wonder how we ever lived without being able to check our e-mail and surf the internet on our smart phones. The author is excited to be a part of the research that may one day lead to those exciting technologies.

Bibliography

[1] B.Blankertz et al, "The BCI competition III: Validating alternative approaches to actual BCI problems," *IEEE T NEUR SYS REH*, vol 14, 2006.

[2] B. J. Edelman, B. Baxter and B. He,"EEG Source Imaging Enhances the Decoding of Complex Right-Hand Motor Imagery Tasks," *IEEE Trans. Biomed. Eng*, vol. 63, no. 1, pp. 4-14, Jan. 2016.

[3] A. S. Aghaei, M. Mahanta and K. N. Plataniotis, "Separable Common Spatio-Spectral Patterns for Motor Imagery BCI Systems," *IEEE Trans. Biomed. Eng*, vol. 63, no. 1, pp. 15-29, Jan. 2016.

[4] J. Meng et al, "Effects of Soft Drinks on Resting State EEG and Brain–Computer Interface Performance," *Access IEEE*, vol. 5, pp. 18756-18764, 2017.

[5] D. McFarland, J.Wolpaw, "EEG-Based Brain-Computer Interfaces," *Current Opinion in Biomedical Engineering*, 2017.

[6] P. Shenoy, K. J. Miller, J. G. Ojemann, and R. P. N. Rao, "Generalized Features for Electrocorticographic BCIs," *IEEE Trans. Biomed. Eng*, vol. 55, no. 1, pp. 273-280, Jan. 2008.

[7] X. Li, c. Guan, H. Zhang and K. Ang, "Discriminative Ocular Artifact Correction for Feature Learning in EEG Analysis," *IEEE Trans. Biomed. Eng*, vol. 64, no. 8, pp. 1906-1913, 2017.

[8] D. Rathee, H. Raza, G. Prasad, and H. Cecotti,"Current Source Density Estimation Enhances the Performance of Motor-Imagery-Related Brain–Computer Interface," *IEEE T NEUR SYS REH*, Vol. 25, no. 12, pp. 2461-2471, 2017.

[9] B. Edelman, J. Meng, N. Gulachek, C. Cline, and B. He, "Exploring Cognitive Flexibility With a Noninvasive BCI Using Simultaneous Steady-State Visual Evoked Potentials and Sensorimotor Rhythms," *IEEE T NEUR SYS REH*, vol. 26, no. 5, pp. 936-947, 2018.

[10] A. Nourmohammadi, M. Jafari, and T. Zander,"A Survey on Unmanned Aerial Vehicle Remote Control Using Brain–Computer Interface," *IEEE T HUM-MACH SYST*, vol. 48, no. 4, pp. 337-348, 2018.

[11] M. Tavakolan, Z. Frehlick, X. Yong, and C. Menon, B. He, "Classifying three imaginary states of the same upper extremity using time-domain features," *PLOS ONE*, vol. 12, pp. e0174161, 2017.

[12] O. Özdenizci, F. Quivira, and D. Erdoğmuş,"Information theoretic feature projection for single-trial brain-computer interfaces," *MLSP* 2017 IEEE 27th International Workshop on, pp. 1-6, 2017

[13] R. Jenke, A. Peer, and M. Buss, "Feature extraction and selection for emotion recognition from EEG," *IEEE T AFFECT COMPUT*, vol. 5, no. 3, pp. 327–339, 2014.

[14] M. Grosse-Wentrup and M. Buss,"Multiclass common spatial patterns and information theoretic feature extraction," *IEEE Trans. Biomed. Eng*, vol. 55, no. 8, pp. 1991–2000, 2008.

[15] A.Salazar-Ramirez, JI.Martin, R.Martinez, A.Arruti, and J.Muguerza,"A hierarchical architecture for recognizing intentionally in mental tasks on a brain-computer interface," *PLOS ONE*, Vol.14, 2019.

[16] L.Wenyu et al,"A Human-Vehicle Collaborative Simulated Driving System Based on Hybrid Brain–Computer Interfaces and Computer Vision," *IEEE Trans. Cogn. Develop. Syst*, vol. 10, no. 3, pp. 810-822, 2018.

[17] C. Liu, H. Zhao, C. Li and H. Wang,"Classification of ECoG motor imagery tasks based on CSP and SVM," *International Conference on Biomedical Engineering and Informatics, Yantai*, pp. 804-807, 2010.

[18] A.Bablani, D.Reddy-Edla, D.Tripathi, and R.Cheruku, "Survey on Brain-Computer Interface: An Emerging Computational Intelligence Paradigm," *ACM Comput Suerv*, Vol.52, 2019.

[19] P. Shenoy, K. Miller, J. Ojemann and R. Rao, "Generalized Features for Electrocorticographic BCIs," *IEEE Trans. Biomed. Eng*, vol. 55, no. 1, pp. 273-280, Jan. 2008.

[20] J. Wilson, E. Felton, P. Garell, G. Schalk and J. Williams,"ECoG factors underlying multimodal control of a brain-computer interface," *IEEE Trans. Biomed. Eng*, vol. 14, no. 2, pp. 246-250, June 2006.

[21] A.Barachant, S.Bonnet, M.Congedo, and C.Jutten, "Multiclass brain-computer interface classification by Riemannian geometry," *IEEE Trans Biomed Eng*, Vol. 59, 2011.

[22] T. Lal et al, "Methods towards invasive human brain computer interfaces," *NIPS*, pp. 737–744, 2005.

[23] Q. Wei and Wei Tu, "Channel selection by genetic algorithms for classifying single-trial ECoG during motor imagery," *IEMBS*, pp. 624-627, 2008.

[24] P. Hammon and V. R. de Sa, "Preprocessing and Meta-Classification for Brain-Computer Interfaces," *IEEE Trans. Biomed. Eng*, vol. 54, no. 3, pp. 518-525, March 2007.

[25] K.Yelamarthi, S.Aman, and A.Abdelgawad,"An Application-Driven Modular IoT Architecture," *WIREL COMMUN MOB COM*, PP.16, 2017.

[26] F. Huang, C. Hsieh, K. Chang, and C. Lin, "Iterative scaling and coordinate descent methods for maximum entropy," *Journal of Machine Learning Research*, vol. 11, pp. 815–848, 2010.

[27] G. Yuan, K. Chang, C. Hsieh, and C. Lin,“A comparison of optimization methods and software for large-scale l1-regularized linear classification," *Journal of Machine Learning Research*, vol. 11, pp. 3183–3234, 2010.

[28] O. Mangasarian, “A finite Newton method for classification," *Optimization Methods and Software*, vol. 17, no. 5, pp. 913–929, 2002.

[29] S. Al Ajrawi et al "Investigating feasibility of multiple UHF passive RFID transmitters using backscatter modulation," *SPECTS*, vol. 54, no. s9, 9 Jul 2017.

[30] S. Al Ajrawi, H. Bialek, M. Sarkar, R. Rao, and S. Ahmed, “Bi-directional channel modeling for implantable UHF-RFID transceivers in BCI applications,” *Future Gener. Comp. Syst.*, vol. 88, pp. 683-692, 2018.

[31] M. Lebedev and M. Nicolelis, “Brain-Machine Interfaces: Past, Present and Future," *TRENDS NEUROSCI*, vol. 29, pp.536—546, 2006.

[32] L. Hochberg et al., “Neuronal Ensemble Control of Prosthetic Devices by a Human with Tetraplegia," *Nature*, vol. 442, pp. 164–171, 2006.

[33] J.R. Wolpaw et al., “Brain-Computer Interface Technology: A Review of the First International Meeting," *IEEE Trans Rehabil Eng*, vol. 8, pp.164—173, 2000.

[34] M.H. Alomari, A. Samaha, and K. Al Kamha,“Automated Classification of L/R Hand Movement EEG Signals using Advanced Feature Extraction and Machine Learning," *IJACSA*, vol. 4, pp. 207-212, 2013.

[35] A. Schloegl, C. Neuper, and G. Pfurtscheller, “Subject Specific EEG Patterns During Motor Imaginary,"*IEMBS* ,Nineteenth Annual International, 1997, pp. 1530-1532.

[36] E. Costa and E. Cabral Jr., “EEG-Based Discrimination Between Imagination of Left and Right Hand Movements Using Adaptive Gaussian Representation," *MED ENG PHYS*, vol. 22, pp. 345-348, 2000.

[37] F. Wang, K. Kim, S. Wen, Y. Zhang, and C. Wu, “EEG Based Automatic Left-Right Hand Movement Classification," *Proc IEEE Conf Decis Control*, 2012. CCDC 2012 .I , 2012, pp. 1469 – 1472.

[38] F. Quandt et al., “Single Trial Discrimination of Individual Finger Movements on One Hand: A Combined MEG and EEG Study," *NEUROIMAGE*, vol. 59, pp. 3316–3324, 2012.

[39] P. Hammon, V. de Sa,"Preprocessing and Meta-Classification for Brain-Computer Interfaces," *IEEE Trans.Biomed. Eng*,v. 54, pp. 518 - 525, 2007.

[40] A. Mittal, A. Zisserman, and P. H. Torr,"Hand detection using multiple proposals.," *in BMVC*, vol. 40, pp. 75–1, Citeseer, 2011.

[41] G. Schalk, J. R. Wolpaw, D. J. McFarland, and G. Pfurtscheller,"Eeg-based communication: presence of an error potential," Clinical neurophysiology, vol. 111, no. 12, pp. 2138–2144, 2000.

[42] D. J. Yeager, A. P. Sample, and J. R. Smith, "Wisp: A passively powered uhf rfid tag with sensing and computation," *in RFID Handbook*, pp. 261–276, CRC Press, 2017.

[43] D. L. Donoho and I. M. Johnstone,"Adapting to unknown smoothness via wavelet shrinkage," Journal of the american statistical association, vol. 90, no. 432, pp. 1200–1224, 1995.

[44] J. Han, F. Dong, and Y. Xu,"Entropy feature extraction on flow pattern of gas/liquid two-phase flow based on cross-section measurement," *in Journal of Physics: Conference Series*, vol. 147, p. 012041, IOP Publishing, 2009.

[45] R. J. Hyndman and G. Athanasopoulos, Forecasting: principles and practice. OTexts, 2018.

[46] Y. Geerts, M. Steyaert, and W. M. Sansen, Design of multi-bit delta-sigma A/D converters, vol. 686. Springer Science & Business Media, 2006.

[47] D. Donnoho, "On minimum entropy segmentation in wavelets: theory, algorithms and applications," 1994.

[48] İ. Bayram, "An analytic wavelet transform with a flexible time-frequency covering," IEEE Transactions on Signal Processing, vol. 61, no. 5, pp. 1131–1142, 2012.

[49] W. Liu, P. P. Pokharel, and J. C. Príncipe, "Correntropy: Properties and applications in non-gaussian signal processing," IEEE Transactions on Signal Processing, vol. 55, no. 11, pp. 5286–5298, 2007.

[50] H. Moore, MATLAB for Engineers. Pearson, 2017.

[51] R. G. Andrzejak, K. Schindler, and C. Rummel, "Nonrandomness, nonlinear dependence, and nonstationarity of electroencephalographic recordings from epilepsy patients," Physical Review E, vol. 86, no. 4, p. 046206, 2012.

[52] A. B. Das and M. I. H. Bhuiyan,"Discrimination and classification of focal and non-focal eeg signals using entropy-based features in the emd-dwt domain," biomedical signal processing and control, vol. 29, pp. 11–21, 2016.

[53] M. Kumar, R. B. Pachori, and U. R. Acharya,"Characterization of coronary artery disease using flexible analytic wavelet transform applied on ecg signals," Biomedical signal processing and control, vol. 31, pp. 301–308, 2017.

[54] M. Kumar, R. B. Pachori, and U. R. Acharya,"Use of accumulated entropies for automated detection of congestive heart failure in flexible analytic wavelet transform framework based on short-term hrv signals," Entropy, vol. 19, no. 3, p. 92, 2017.

[55] M. Kumar, R. B. Pachori, and U. R. Acharya, "An efficient automated technique for cad diagnosis using flexible analytic wavelet transform and entropy features extracted from hrv signals," Expert Systems with Applications, vol. 63, pp. 165–172, 2016.

[56] D. Avci, "An expert system for speaker identification using adaptive wavelet sure entropy," Expert Systems with Applications, vol. 36, no. 3, pp. 6295–6300, 2009.

[57] E. Fields, R. F. Cleveland, and J. L. Ulcek, "Questions and answers about biological effects and potential hazards of radiofrequency electromagnetic fields," *in Oet Bulletin*, Citeseer, 1999.

[58] M. Mark, T. Björninen, Y. D. Chen, S. Venkatraman, L. Ukkonen, L. Sydänheimo, J. M. Carmena, and J. M. Rabaey,"Wireless channel characterization for mm-size neural implants," *in 2010 Annual International Conference of the IEEE Engineering in Medicine and Biology*, pp. 1565–1568, IEEE, 2010.

[59] S. Roundy, P. K. Wright, and J. M. Rabaey, "Energy scavenging for wireless sensor networks," *in Norwell*, pp. 45–47, Springer, 2003.

[60] J. A. Sweet, A. M. Hdeib, A. Sloan, and J. P. Miller,"Depths and grids in brain tumors: Implantation strategies, techniques, and complications," Epilepsia, vol. 54, pp. 66–71, 2013.

[61] V. Talla and J. R. Smith,"Hybrid analog-digital backscatter: A new approach for battery-free sensing," *in 2013 IEEE International Conference on RFID (RFID)*, pp. 74–81, IEEE, 2013.

[62] L. A. Burdet,"Rfid multiple access methods," ETH Zurich, 2004.

[63] K. Finkenzeller, RFID handbook: fundamentals and applications in contactless smart cards, radio frequency identification and near-field communication. John wiley & sons, 2010.

[64] D. J. Yeager, P. S. Powledge, R. Prasad, D. Wetherall, and J. R. Smith, "Wirelessly-charged uhf tags for sensor data collection," *in 2008 IEEE International Conference on RFID*, pp. 320–327, IEEE, 2008.

[65] J. R. Wolpaw, N. Birbaumer, D. J. McFarland, G. Pfurtscheller, and T. M. Vaughan, "Brain–computer interfaces for communication and control," Clinical neurophysiology, vol. 113, no. 6, pp. 767–791, 2002.

[66] A. Fort, C. Desset, P. De Doncker, P. Wambacq, and L. Van Biesen, "An ultra-wideband body area propagation channel model-from statistics to implementation," IEEE Transactions on Microwave Theory and Techniques, vol. 54, no. 4, pp. 1820–1826, 2006.

[67] K. Koski, T. Björninen, L. Sydänheimo, L. Ukkonen, and Y. Rahmat-Samii, "A new approach and analysis of modeling the human body in rfid-enabled body-centric wireless systems," International Journal of Antennas and Propagation, vol. 2014, 2014.

[68] M. Marciani, F. Stefanini, N. Stefani, M. Maschio, G. Gigli, S. Roncacci, C. Caltagirone, and G. Bernardi, "Lateralization of the epileptogenic focus by computerized eeg study and neuropsychological evaluation," International journal of neuroscience, vol. 66, no. 1-2, pp. 53–60, 1992.

[69] T. Instruments,"Code composer studio ide getting started guide," User's Guide, 2005.

[70] J. Meng, T. Streitz, N. Gulachek, D. Suma, and B. He,"Three-dimentional brian-computer interface control through simultaneous overt spatial attentional and motor imagery tasks," *IEEE Trans. Biomedical Eng.*, vol. 65, no. 11, pp. 2417–2427, Nov. 2018.

[71] A. Belkacem, S. Nishio, T. Suzuki, H. Ishiguro, and M. Hirata, "Neuromagnetic decoding of simultaneous bilateral hand movements for multidimensional brain-machine interfaces," *IEEE Trans. Neural Systems and Rehabi. Eng.*, vol. 26, no. 6, pp. 1301–1310, Jun. 2018.

[72] H. Ando, K. Takizawa, T. Yoshida, K. Matsushita, M. Hirata, and T. Suzuki, "Wireless multicannel neural recording with a 128-Mbps UWB transmitter for an implantable brain-machine interfaces," *IEEE Trans. Biomedical Circuits and Systems* , vol. 10, no. 6, pp. 1068–1078, Dec. 2016.

[73] S. Nagaraj, and F. Rassam,"Improved non-coherent UWB receiver for implantable biomedical devices," *IEEE Trans. Biomedical Eng.*, vol. 63, no. 10, pp. 2220–2225, Oct. 2016.

[74] K. Yelamarthi, Md. S. Aman, and A. Abdelgawad,"An application-driven modular IoT architecture," *Wireless Communications and Mobile Computing*, vol. 2017, ID. 1350929, 16 pages, May 2017.

[75] J. Andreu-Perez., D. Leff, H. Ip, and G.-Z. Yang, "From wearable sensors to smart implants–toward pervasive and personalized healthcare," *IEEE Trans. Biomed. Eng.*, vol. 62, no. 12, pp. 2750–2762, Dec. 2015.

[76] X. Zhang, L. Yao, S. Zhang, S. Kanhere, M. Sheng, and Y. Liu, "Internet of things meets brain-computer interface: a unified deep learning framework for enabling human-thing cognitive interactivity," *IEEE Internet of Things Journal*, vol. 6, no. 2, pp. 2084–2092, Apr. 2019.

[77] P. Yong, and E. Ho,"Streaming brain and physiological signal acquisition system for IoT neuroscience application," *IEEE EMBS Conference on Biomedical Engineering and Sciences, Kuala Lumpur, Malaysia*,4-8 Dec. 2016.

[78] A. Teles, M. Cagy, F. Silva, M. Endler, V. Bastos, and S. Teixeira, "Using brain-computer interface and internet of things to improve healthcare for wheelchair users," *The Eleventh International Conference on Mobile Ubiquitous Computing, Systems, Services and Technologies*, 2017.

[79] F. Harris, S. Parekh, and I. Gurantz, "I-Q balancing techniques for broad-band receivers," *Proceeding of the Software Defined Radio Technical Conference, 6 pages*, 2005.

[80] W. Al-Hussaibi, "Signal design for higher capacity correlated fading signature multiple access," *Wireless Networks*, vol. 20, no. 8, pp. 2275-2285, Nov. 2014.

[81] F. Harris, "Artifact-corrected time-interleaved ADC," *U.S. Patents, US8957798B1, 17 pages*, Feb. 2015.

[82] T. Tsai, P. Hurst, and S. Lewis, "Time-interleaved analog-to-di gital converters for digital communications," *i*n Proc. IASTED Conf. Circuits, Signals Syst., 2004, pp. 193

[83] C.-L. Liu,"Impacts of i/q imbalance on qpsk-ofdm-qam detection," *IEEE Trans. Consum. Electron*, vol.44, no.3, pp.984-989, Aug. 1998.

[84] H. Tsou, “The effect of phase and amplitude imbalance on the performance of offset quadrature phase-shift-keyed (OQPSK) communication systems,” The Telecommunications and Mission Operations Progress Report, pp.1-15, Sep. 1998.

[85] C. Vogel, and S. Mendel, “A flexible and scalable structure to compensate frequency response mismatches in time-interleaved ADCs,” *IEEE Trans. Circuits Syst. I*, vol. 56, no. 11, pp. 2463–2475, Nov. 2009

[86] H. Johansson, “A polynomial-based time-varying filter structure for the compensation of frequency-response mismatch errors in time-interleaved ADCs,” *IEEE J. Sel. Topics Signal Process.*, vol. 3, no. 3, pp. 384–396, Jun. 2009.

[87] K. M. Tsui, and S. C. Chan,“New iterative framework for frequency response mismatch correction in time-interleaved ADCs: Design and performance analysis,” *IEEE Trans. Instrum. Measurments*, vol. 60, no. 12, pp. 3792–3805, Dec. 2011

[88] M. Soudan and C. Vogel, “Correction structures for linear weakly time varying systems,” *IEEE Trans. Circuits Syst. I*, vol. 59, no. 9, pp. 2075–2084, Sep. 2012.

[89] K. M. Tsui, and S. C. Chan,“A novel iterative structure for online calibration of M-channel time-interleaved ADCs,” *IEEE Trans. Instrum. Measurments*, vol. 63, no. 2, pp. 312–325, Feb. 2014.

[90] W. Al-Hussaibi, “Effect of filtering on the synchronization and performance of chaos-based secure communication over Rayleigh fading channel,” *Communications in Nonlinear Science and Numerical Simulation*, vol. 26, no. 1-3, pp. 87-97, Sep. 2015.

[91] W. Al-Hussaibi, and F. Ali, “Generation of correlated Rayleigh fading channels for accurate simulation of promising wireless communication systems,” *Simulation Modelling Practice and Theory*, vol. 25, no. 4, pp. 56-72, Jun. 2012.

[92] A. Sample, D. Yeager, P. Powledge, A. Mamishev, and J. Smith, “Design of an RFID-based battery-free programmable sensing platform,” *IEEE Trans. Instrum. Measurments*, vol. 57, no. 11, pp. 2608–2615, Nov. 2008.

[93] IMPINJ, Speedway R420 RAIN RFID Reader.

[94] Monson H. Hayes, Statistical Digital Signal Processing and Modeling, Wiley, 1st Ed., 1996.

[95] Yeager, Daniel J., Jeremy Holleman, Richa Prasad, Joshua R. Smith, and Brian P. Otis. "Neuralwisp: A wirelessly powered neural interface with 1-m range." *IEEE Transactions on Biomedical Circuits and Systems 3*, no. 6 (2009): 379-387.

[96] Buettner, Michael, Richa Prasad, Matthai Philipose, and David Wetherall. "Recognizing daily activities with RFID-based sensors." *In Proceedings of the 11th international conference on Ubiquitous computing*, pp. 51-60. ACM, 2009.

[97] Harrison, Reid R., Paul T. Watkins, Ryan J. Kier, Robert O. Lovejoy, Daniel J. Black, Bradley Greger, and Florian Solzbacher. "A low-power integrated circuit for a wireless 100-electrode neural recording system." *IEEE Journal of Solid-State Circuits 42*, no. 1 (2007): 123-133.

[98] Taylor, Dawn M., Stephen I. Helms Tillery, and Andrew B. Schwartz. "Direct cortical control of 3D neuroprosthetic devices." *Science 296*, no. 5574 (2002): 1829-1832. 3.

[99] Olsson, Roy H., and Kensall D. Wise. "A three-dimensional neural recording microsystem with implantable data compression circuitry." *IEEE Journal of Solid-State Circuits 40*, no. 12 (2005): 2796-2804.

[100] Sample, Alanson Paul. "Design of a battery free wireless identification and sensing platform." *PhD diss., University of Washington*, 2008.

[101] Al Ameen, Moshaddique, Niamat Ullah, M. Sanaullah Chowdhury, SM Riazul Islam, and Kyungsup Kwak. "A power efficient MAC protocol for wireless body area networks." *EURASIP Journal on Wireless Communications and Networking 2012*, no. 1 (2012): 33.

[102] S. Marinkovic, C. Spagnol, E. Popovici, "Energy-efficient "TDMA-based MAC protocol for wireless body area networks," *SENSORCOMM*, June 2009, pp. 604-609.

[103] P. Park, P. Di Marco, C. Fischione and K. Johansson, "Modeling and optimization of the IEEE 802.15. 4 protocol for reliable and timely communications," *IEEE Trans. Parallel Distrib. Syst.*, vol. 24, no. 3, 2013.

[104] Davidson, Donald W., and Robert H. Cole. "Dielectric relaxation in glycerol, propylene glycol, and n-propanol." *The Journal of Chemical Physics 19*, no. 12 (1951): 1484-1490.

[105] Finkenzeller, Klaus. RFID handbook: fundamentals and applications in contactless smart cards, radio frequency identification and near-field communication. *John Wiley, Sons*, 2010.

[106] geophree. WISP5, http://wisp5.wikispaces.com/ Getting+Started.

[107] Patel, Pragnesh V., Mahasweta Sarkar, Santosh Nagaraj, and Kiran Kushalad. "Channel modelling based on statistical analysis for brain-computer-interface (BCI) applications." *In Computer Communications Workshops (INFOCOM WKSHPS), 2016 IEEE Conference on*, pp. 320-321. IEEE, 2016.

[108] P. Patel, J. Lalwani, A. Kumar, M. Sarkar, and S. Nagaraj, "Tracking the behavior of UWB transmissions in invasive BCI applications," *IEEE 13th Int. Conf. on Wearable and Implantable Body Sensor Networks (BSN)*, 2016, pp. 205-210.

[109] P. Rutul, P. Patel, J. Lalwani, M. Sarkar, and S. Nagaraj, "Investigating the feasibility of multiple UWB transmitters in brain computer interface (BCI) applications," *BSN: San Francisco*, CA, USA, pp. 236-241, 2016.

[110] John Smith. IMPINJ, http://www.impinj.com/ products/readers/speedway-revolution/.

[111] Talla, Vamsi, and Joshua R. Smith. "Hybrid analog-digital backscatter: A new approach for battery-free sensing." *In RFID (RFID), 2013 IEEE International Conference on*, pp. 74-81. IEEE, 2013. Harvard

[112] Yeager, Daniel James. "Development and application of wirelessly-powered sensor nodes." *PhD diss., University of Washington*, 2009.

[113] Sweet, Jennifer A., Alia M. Hdeib, Andrew Sloan, and Jonathan P. Miller. "Depths and grids in brain tumors: implantation strategies, techniques, and complications." *Epilepsia 54, no. s9 (2013)*: 66-71.

[114] http://www.opensourceinstruments.com/Electronics /A3019/Electrodes.html.

[115] J. Lalwani, A. Kumar, M. Sarkar, S. Mohanty, S. Ahmed, "A comparative study of MAC protocols in brain-computer interface (BCI) applications," *IWCMC*, pp. 1522-1527, 2017.

[116] M.S.Hossain, G. Muhammad, A. Alamri "Smart healthcare monitoring: a voice pathology detection paradigm for smart cities" *Multimedia Systems (2017)*. DOI: 10.1007/s00530-017-0561-x.

[117] M. S. Hossain, "Cloud-Supported Cyber–Physical Localization Framework for Patients Monitoring," *IEEE Systems Journal*, vol. 11, no. 1, pp. 118-127, March 2017.

[118] M. S. Hossain and G. Muhammad,"Emotion-Aware Connected Healthcare Big Data Towards 5G," IEEE Internet of Things Journal, vol. PP, no. 99, pp. 1-1. doi: 10.1109/JIOT.2017.2772959.

[119] M. S. Hossain," Patient State Recognition System for Healthcare Using Speech and Facial Expressions". *J Med Syst (2016)*; 40: 272. doi: 10.1007/s10916-016-0627-x.

[120] M. S. Hossain, G. Muhammad, "Cloud-assisted Industrial Internet of Things (IIoT) – Enabled framework for health monitoring". *Computer Networks*, vol.101, no. 2016, pp.192-202.

[121] A. Fort, J. Ryckaert, C. Desset, P. Doncker, P. Wambacq, and L. Van Biesen, "Ultra-wideband channel model for communication around the human body," *IEEE J. Sel. Areas Commun.*, vol. 24, no. 4, 2006.

[122] Fort, Andrew, Claude Desset, Julien Ryckaert, Philippe De Doncker, Leo Van Biesen, and Piet Wambacq. "Characterization of the ultra wideband body area propagation channel." In Ultra-Wideband, 2005. ICU 2005. *2005 IEEE International Conference on*, pp. 6-pp. IEEE, 2005.

[123] Alomainy, A., Y. Hao, Y. Yuan, and Y. Liu. "Modelling and characterisation of radio propagation from wireless implants at different frequencies." *InWireless Technology, 2006. The 9th European Conference on*, pp. 119-122. IEEE, 2006.

[124] Wang, Jianqing, and Donglin Su. "Design of an ultra wideband system for in-body wireless communications." *In Environmental Electromagnetics, The 2006 4th Asia-Pacific Conference on*, pp. 565-568. IEEE, 2006.

[125] Taparugssanagorn, A & Rabbachin, Alberto & Hämäläinen, Matti & Saloranta, Jani & Iinatti, Jari. (2008). "A Review of Channel Modelling for Wireless Body Area Network in Wireless Medical Communications".

[126] Y. Cui *et al*., "Identifying brain networks at multiple time scales via deep recurrent neural network," *IEEE J. Biomed Health*, 2018.

[127] J. Wolpaw and E. Wolpaw, *Brain–Computer Interfaces: Principles and Practice*, Oxford University Press; 2012.

[128] S. Katsigiannis and N. Ramzan, “DREAMER: A database for emotion recognition through EEG and ECG signals from wireless low-cost Off-the-Shelf devices," *IEEE J. Biomed Health*, vol. 22, no. 1, pp. 98-107, Jan. 2018.

[129] E. Hodkin, Y. Lei, J. Humby, and I. Glover, “Automated FES for upper limb rehabilitation following stroke and spinal cord injury", *IEEE Trans. Neural Syst. Rehabil. Eng.*, vol. 26, no. 5, pp. 1067–1074, 2018.

[130] A. Javier, D. Leff, H. Yang, and G. Yang, “From wearable sensors to smart implants-–toward pervasive and personalized healthcare," *IEEE Trans. Biomed. Eng.,* vol. 62, no. 12, pp. 2750-2762, Dec. 2015.

[131] A. Waziri, A. Schevon, J. Cappell, R. Emerson, G. McKhann, and R. Goodman, “Initial surgical experience with a dense cortical microarray in epileptic patients undergoing craniotomy for subdural electrode implantation," *J. Neurosurg*, vol. 64, no. 3 2009.

[132] Cleveland Clinic, “Invasive EEG Monitoring". Online. Available at: https://my.clevelandclinic.org/health/diagnostics/17144-invasive-eeg-monitoring.

[133] Y. Zhang and G. Dolmans, “A New priority-guaranteed MAC protocol for emerging body area networks," *ICWMC*, pp. 140-145, 2009.

[134] H. Harikrishnan, M. Sarkar, S. Nagaraj and A. Mihovska, “An experimental study of a novel MAC protocol using UHF- RFID passive backscatter modulation for brain computer interface (BCI) applications," *IEEE Int. Black Sea Conf. Commun. and Networking (BlackSeaCom)*, Sochi, Russia, 2019, pp. 1-5.

[135] H. Harikrishnan, A. Sarkar, C. Paolini and A. Mihovska, “Design and evaluation of a novel MAC protocol for multi implantable UHF-RFID transmitters in brain computer interface Applications," *Wireless Telecommunications Symposium (WTS)*, New York City, NY, USA, 2019, pp. 1-7.

[136] N. Jain, S. R. Das and A. Nasipuri, “A multichannel CSMA MAC protocol with receiver-based channel selection for multihop wireless networks," *ICCCN*, 2001, pp. 432-439.

[137] D. Seo, H. Tang, J. Carmena, J. Rabaey, E. Alon, B. Boser, and M. Maharbiz, “Ultrasonic beamforming system for interrogating multiple implantable sensors”, *EMBC*, pp. 2673-2676, Aug. 2015

[138] S. Ullah, H. Higgins, B. Shen, K. Kwak, “On the implant communication and MAC protocols for WBAN,” *Int. J. Commun. Syst.*, vol. 23.8, pp. 982-999, July 2010.

[139] R. Chávez-Santiago *et al.*, “Propagation models for IEEE 802.15.6 standardization of implant communication in body area networks," *IEEE Commun. Mag*., vol. 51, no. 8, 2013.

[140] P. Park, P. Di Marco, C. Fischione, K.H. Johansson, “Modeling and optimization of the IEEE 802.15.4 protocol for reliable and timely communications," *IEEE Trans. Parallel Distrib. Syst.,* vol. 24, no. 3, pp. 550-564, Mar. 2013.

[141] V. B. Mišić and J. Mišić, “A polling MAC for wireless sensor networks with RF recharging of sensor tags," *QBSC*, Kingston, 2014, pp. 76-80.

[142] A. Tzamaloukas and J. Garcia-Luna-Aceves, “A receiver-initiated collision-avoidance protocol for multi-channel networks," *IEEE Infocom*, vol. 1, 2001, pp. 189-198.

[143] S. Ganeriwal, R. Kumar, and M. B. Srivastava, “Timing-sync protocol for sensor networks," *in Proc. 1st Int. conf. on Embedded networked sensor systems*, 2003, pp. 138-149.

[144] T. Castermans *et al*., “Optimizing the performances of a P300-based brain–computer interface in ambulatory conditions," *IEEE Trans. Emerg. Sel. Topics Circuits Syst.*, vol. 1, no. 4, pp. 566-577, Dec. 2011.

[145] A. Y. Kaplan, S. L. Shishkin, I. P. Ganin, I. A. Basyul and A. Y. Zhigalov, “Adapting the P300-Based brain–computer interface for gaming: A review," *IEEE Trans. Comput. Intell. and AI in Games*," vol. 5, no. 2, pp. 141-149, June 2013.

[146] S. Movassaghi, M. Abolhasan, J. Lipman, D. Smith and A. Jamalipour, “Wireless body area networks: A survey," *IEEE Commun. Surveys & Tuts.*, vol. 16, no. 3, pp. 1658-1686, Third Quarter 2014.

[147] OPNET Network simulator. [Online]. Available: https://opnetprojects.com/opnet-network-simulator. Accessed: 13*th* Aug. 2020.

[148] P. Patel, M. Sarkar, S. Nagaraj, and K. Kushalad, “Channel modeling based on statistical analysis for brain-computer-interface (BCI) applications," *IEEE INFOCOM WKSHPS*, 2016, pp. 320-321.

[149] D. Seo, J. Carmena, J. Rabaey, E. Alon, M. Maharbiz, “Neural dust: An ultrasonic, low power solution for chronic brain machine interfaces”, *arXiv preprint arXiv*, pp. 1307-2196, 2013.

[150] D. Seo, R. Neely, K. Shen, U. Singhal, E. Alon, J. Carmena, M. Maharbiz, “Wireless recording in the peripheral nervous system with ultrasonic neural dust”, *Neuron*, vol. 91, pp. 529–539, Aug. 2016.

[151] J. Elson, L. Girod, D. Estrin, “Fine-grained networked time synchronization using reference broadcast,” *OSDI Symposia*, vol. 36, 2002, pp. 147-163.

[152] J. Zhao, R. Govindan, “Understanding packet delivery performance in dense wireless sensor networks,” *SenSys*, 2003, pp. 1-13,

[153] G. Zhou, C. Huang, T. Yan, T. He, J. A. Stankovic and T. Abdelzaher, “MMSN: Multi-frequency media access control for wireless sensor networks,” *ICCCN*, 2006, pp. 1-13.

[154] H. Balakrishnan, C. Barrett, V. Kumar, M. Marathe, and S. Thite, “The distance-2 matching problem and its relationship to the MAC-layer capacity of ad hoc wireless networks,” *IEEE J. Sel. Areas Commun.*, vol. 22, no. 6, pp 1069-1079, Aug. 2004.

[155] N. Meghanathan, “A greedy algorithm for neighborhood overlap-based community detection,” *Algorithms*, v. 9, n. 1, p. 8, 2016.

[156] N. Javaid *et al.*, “Analyzing medium access techniques in wireless body area networks," *Research Journal of Applied Sciences, Engineering and Technology*, vol. 7, no. 3, pp. 603-613, 2014.

[157] Q. Li, D. Ding, and M. Conti, “Brain-Computer Interface applications: Security and privacy challenges,” in 2015 IEEE Conference on Communications and Network Security (CNS). IEEE, Sep 2015, pp. 663–666.

[158] D. Mills, “Network time protocol (version 3) specification, implementation and analysis", RFC 1305, 1992. Available: https://tools.ietf.org/html/rfc1305.

[159] L. Lamport, “Time, clocks and the ordering of events in a distributed system", *Commun ACM*, vol. 7, pp. 558-565, July 1978.

[160] A. Sample and J. Smith, “Experimental results with two wireless power transfer systems,"*IEEE Radio and Wireless Symposium*, 2009, pp. 16-18.

[161] P. Patel, M. Sarkar, and S. Nagaraj, “Ultra wideband channel characterization for invasive biomedical applications," *IEEE 17th Ann. Wireless and Microwave Technology Conf. (WAMICON)*, 2016, pp. 1-6.

[162] Y. Zhao, Y. Hao, A. Alomainy, and Clive Parini, “UWB on-body radio channel modeling using ray theory and subband FDTD method, “ *IEEE Trans. Microw. Theory Tech.*, vol. 54, no. 4, 2006.

[163] F. Bouabdallah, C. Zidi, R. Boutaba, and M. Mehaoua, “Collision avoidance energy efficient multi-channel MAC protocol for underwater acoustic sensor networks," *IEEE Trans. Mobile Comput.*, 2018.

[164] Q. Li, D. Ding, and M. Conti,“Brain-Computer Interface applications: Security and privacy challenges,” in 2015 IEEE Conference on Communications and Network Security (CNS). *IEEE, Sep 2015*, pp. 663–666.

[165] E. Khabarova, N. Denisova, A. Dmitriev, K. Slavin, L. Verhagen Metman, E. A. Khabarova, N. P. Denisova, A. B. Dmitriev, K. V. Slavin, and L. Verhagen Metman, “Deep Brain Stimulation of the Subthalamic Nucleus in Patients with Parkinson Disease with Prior Pallidotomy or Thalamotomy,” *Brain Sciences*, vol. 8, no. 4, p. 66, apr 2018.

[166] W. J. Tyler, J. L. Sanguinetti, M. Fini, and N. Hool, “Non-invasive neural stimulation,” *in Proc.SPIE, T. George, A. K. Dutta, and M. S. Islam, Eds.*, vol. 10194. International Society for Optics and Photonics, may 2017, p. 101941L.

[167] R. P. Rao, "Towards neural co-processors for the brain: combining decoding and encoding in brain–computer interfaces," *Current Opinion in Neurobiology*, vol. 55, pp. 142–151, 2019.03.008.

[168] T. Denning, Y. Matsuoka, and T. Kohno, "Neurosecurity: security and privacy for neural devices," *Neurosurgical Focus*, vol. 27, no. 1, p. E7, 2009.

[169] M. Ienca, "Neuroprivacy, neurosecurity and brain-hacking: Emerging issues in neural engineering," *Bioethica Forum*, vol. 8, no. 2, pp. 51–53, 2015. [Online]. Available: http://www.bioethica-forum.ch/docs/15f g2/05f gIencaf gBF8f g2.pdf.

[170] M. Ienca and P. Haselager,"Hacking the brain: brain–computer interfacing technology and the ethics of neurosecurity," *Ethics and Information Technology*, vol. 18, no. 2, pp. 117–129, jun 2016.

[171] I. Martinovic, D. Davies, and M. Frank, "On the feasibility of side channel attacks with brain-computer interfaces," *in Proceedings of the 21st USENIX Security Symposium. Bellevue, WA: USENIX, 2012*, pp. 143–158.

[172] T. Bonaci, R. Calo, and H. J. Chizeck, "App Stores for the Brain : Privacy and Security in Brain-Computer Interfaces," *IEEE Technology and Society Magazine*, vol. 34, no. 2, pp. 32–39, jun 2015.

[173] H. Takabi, A. Bhalotiya, and M. Alohaly, "Brain computer interface (BCI) applications: Privacy threats and countermeasures," *in Proceedings - 2016 IEEE 2nd International Conference on Collaboration and Internet Computing, IEEE CIC 2016. IEEE, nov 2016*, pp. 102–111.

[174] K. Sundararajan, "Privacy and security issues in Brain Computer Interface," *Master's thesis, Auckland University of Technology*, 2017.

[175] Best, J. (2019, November 13). What is a brain-computer interface? Everything you need to know about BCIs, neural interfaces and the future of mind-reading computers. Retrieved May 05, 2020, from https://www.zdnet.com/article.

[176] M. A. L. Nicolelis,"Actions from thoughts," *Nature*, vol. 409, no. 6818, pp. 403–407, 2001, doi: 10.1038/35053191

[177] M. A. Lebedev and M. A. L. Nicolelis, "Brain-Machine Interfaces: From Basic Science to Neuroprostheses and Neurorehabilitation," *Physiological Reviews*, vol. 97, no. 2, pp. 767–837, apr 2017, doi: 10.1152/physrev.00027.2016

[178] M. Pais-Vieira, G. Chiuffa, M. Lebedev, A. Yadav, and M. A. L. Nicolelis, "Building an organic computing device with multiple interconnected brains," *Scientific Reports*, vol. 5, no. 1, p. 11869, dec 2015, doi: 10.1038/srep11869.

[179] "The BRAIN Initiative." [Online]. Available: https://braininitiative.nih.gov/

[180] Cybersecurity in Brain-Computer Interfaces: State of the art, opportunities, and future challenges, Sergio L´opez Bernal, Alberto Huertas Celdr´any, Gregorio Mart´ınez P´erez , Michael Taynnan Barros y, Sasitharan Balasubramaniam Available: https://arxiv.org/pdf/1908.03536.pdf.

[181] HL7 International, “Health Level Seven.” [Online]. Available: https://www.hl7.org/

[182] Lewis S. Basic Introduction to RFID and its Uses in the Chain Supply, LARAN RFID, TECH white paper publication, May 2004.

[183] Bakery, N.S., Johari, A., Wahab, MHA and Danial, N. RFID "Application in Farming Management System". *In Proceeding of 3rd International Conference on Robotics, Vision, Information and Signal Processing 2007 (ROVISP2007), Penang, 28 – 30 November 2007*

[184] Yan, B. and Lee, D. Application of RFID in Cold Chain Temperature Monitoring System. *2009 ISECS International Colloqium on Computing, Communication, Control, and Management. Aug. 8 – 9, 2009. Sanya, China.*

[185] Voulodimos, A. S. et al. "A Complete Farm Management System based on Animal Identification using RFID Technology". *Computers and Electronics in Agriculture*. Vol. 70. Pp. 380 – 388, 2010.

[186] Haron, N. S., Saleem, N. S., Hassan, M. H., Ariffin, M. M. and Aziz, I. A.A RID-based Campus Context-Aware Notification System. *Journal of Computing*. Vol. 2. Issue 3, 2010.

[187] Herdawatie et al. Fusion of Radio Frequency Identification (RFID) and Fingerprint in Boarding School Monitoring System (BoSs), Sustainable Radio Frequency Identification Solutions, Cristina Turcu (Ed.), *InTech, 2010.*

[188] Christopher L. Howertona, Joseph P. Garner b, Joy A. Mencha.A system utilizing radio frequency identification (RFID) technology to monitor individual rodent behavior in complex social settings. *Journal of Neuroscience Methods 209 (2012) 74–78*

[189] Rama, N.S., Prasad, K. and Rajesh, A. RFID-Based Hospital Real Time Patient Management System. *International Journal of Computer Trends and Technology*- volume 3, Issue 3- pp.509, 2012 ISSN: 2231-2803.

[190] Catarinucci, L. et al. An animal tracking system for behavior analysis using radio frequency identification. *Lab Anim (NY)*. 2014 Sep, 43(9):321-7.

[191] R. A. Ramadan and A. V. Vasilakos, "Brain computer interface: control signals review," Neurocomputing, vol. 223, pp. 26—44, feb 2017, doi: 10.1016/J.NEUCOM.2016.10.024.

[192] K. Wahlstrom, N. B. Fairweather, and H. Ashman,"Privacy and Brain- computer Interfaces: Identifying Potential Privacy Disruptions," *ACM SIGCAS Computers and Society*, vol. 46, no. l, pp. 41—53, mar 2016, doi: 10.1145/2908216.2908223.

[193] T. O. Zander, C. Kothe, S. Jatzev, and M. Gaertner, "Enhancing Human- Computer Interaction with Input from Active and Passive Brain- Computer Interfaces," *in Brain-Computer Interfaces. Human-Computer Interaction Series., D. Tan and A. Nijholt, Eds. Springer, London, 2010, ch. Il*, pp. 181-199, doi: 10.1007/978-1-84996-272-8-1 1.

[194] K. S. Hong and M. J. Khan, "Hybrid brain-computer interface techniques for improved classification accuracy and increased number of commands: A review," vol. 11, no. JUL, p. 35, jul 2017, doi: 10.3389/fnbot.2017.00035.

[195] V. Gilja, P. Nuyujukian, C. A. Chestek, J. P. Cunningham, B. M. Yu, J. M. Fan, M. M. Churchland, M. T. Kaufman, J. C. Kao, S. 1. Ryu, and K. V. Shenoy, "A high-performance neural prosthesis enabled by control algorithm design," *Nature Neuroscience*, vol. 15, no. 12, pp. 1752-1757, dec 2012, doi: 10.1038/nn.3265.

[196] M. van Gerven, J. Farquhar, R. Schaefer, R. V lek, J. Geuze, A. Nijholt, N. Ramsey, P. Haselager, L. Vuurpijl, S. Gielen, and P. Desain,"The brain—computer interface cycle," *Journal of Neural Engineering*, vol. 6, no. 4, p. 041001, aug 2009, doi: 10.1088/1741-2560/6/4/041001.

[197] M. Aim, M. Lee, J. Choi, S. Jun, M. Ahn, M. Lee, J. Choi, and S. C. Jun, "A Review of Brain-Computer Interface Games and an Opinion Survey from Researchers, Developers and Users," *Sensors*, vol. 14, no. 8, pp. 14601-14633, aug 2014, doi: 10.3390/040814601.

[198] R. Polanfa, M. A. Nitsche, and C. C. Ruff,"Studying and modifying brain function with non-invasive brain stimulation," *Nature Neuro- science*, vol. 21, no. 2, pp. 174-187, feb 2018, doi: 10.1038/s41593- 017-0054-4. https://www.emotiv.com/bci-guide/ online resource

[199] Auto-ID Center. Technology Guide, Auto-ID Center, 2002, www.autoidcenter.org, 27/08/2015

[200] Wikipedia. EPCglobal Network, https://en.wikipedia.org/wiki/EPCglobal$_N$*etwork*.02/09/2015.

[201] Wikipedia. Auto-ID Labs, https://en.wikipedia.org/wiki/Auto-ID$_L$*abs*.02/09/2015.

[202] T. Castermans *et al*., “Optimizing the performances of a P300-based brain–computer interface in ambulatory conditions," *IEEE Trans. Emerg. Sel. Topics Circuits Syst.*, vol. 1, no. 4, pp. 566-577, Dec. 2011.

[203] A. Y. Kaplan, S. L. Shishkin, I. P. Ganin, I. A. Basyul and A. Y. Zhigalov, “Adapting the P300-Based brain–computer interface for gaming: A review," *IEEE Trans. Comput. Intell. and AI in Games*," vol. 5, no. 2, pp. 141-149, June 2013.

AppendixA

.1 List of Abbreviations

ECoG - **E**lectro **C**ortico **G**raphy

BCI - **B**rain **C**omputer **I**nterface

MAC - **M**edium **A**ccess **C**ontrol

HRFE - **H**ierarchical **R**ecursive **F**eature **E**limination

FAWT - **F**lexible **A**nalytic **W**avelet **T**ransformation

LS-SVM - **L**east **S**Squares **S**Support **V**ector **M**achines

I/Q - **I**n-phase **Q**uadrature

ADC - **A**nalog-to **D**igital **C**onverters

LMS - **L**east **M**ean **S**quare

BBCI - **B**i-directional **B**rain **C**omputer **I**nterfacing

UHF-RFID - **U**ltra- **H**igh **F**requency **R**adio **F**requency **I**dentification

RSSI - **R**eceived **S**ignal **S**trength **I**ndication

UWB - **U**ltra - **W**ide **B**and

SC - **S**canner **C**ontroller

WINC - **Wi**reless **N**etworks and **C**ommunication Lab

CSNE - **C**enter for **S**ensorimotor **N**euro **E**ngineering

WHO - **W**orld **H**ealth **O**rganization **EPDA** - **E**uropean **P**arkinson's **D**isease **A**ssociation

EEG - **E**lectro **E**ncaphalo **G**raphy

FMRI - **F**unctional **M**agnetic **R**esonance **I**maging

PET- **P**ositron **E**mission **T**omography

MEG - **M**agneto **E**ncephalo **G**raphy

DC - **D**irect **C**urrent **TI-ADC** - **T**exas **I**nstruments **A**nalog-to **D**igital **C**onverters

BCIIS - **B**rain **C**omputer **I**nterface **I**dentification **S**ystem

QPSK - **Q**uadrature **P**hase **S**hift **K**eying

PCA - **P**rincipal **C**omponent **A**nalysis

ICA - **I**ndependent **C**omponent **A**nalysis

LDA - **L**inear **D**iscriminant **A**nalysis

AR - **A**uto **R**egressive

MA - **M**oving **A**verage

ConvNets - Shallow **C**onvolutional neural **Net**works

ML - **M**achine **L**earning

SVM - **S**upport **V**ector **M**achine

CSSD - **C**entral **S**terile **S**upply **D**epartment

CWT - **C**ontinuous **W**avelet **T**ransform

CSP - **C**ontent **S**ecurity **P**olicy

PSD - **P**ower **S**pectral **D**ensity

LR - **L**ogistic **R**egression

RFID - **R**adio- **F**requency **Id**entification

UHF - **U**ltra- **H**igh **F**requency

WBAN - **W**ireless **B**ody **A**rea **N**etwork

RSS - **R**eceived **S**ignal **S**trength

WISP - **W**ireless **I**dentification and **S**ensing **P**latform

EPC - **E**lectronic **P**roduct **C**ode

ASK - **A**mplitude **S**hift **K**eyed

FM0 - Bi-phase space encoding

NS2 - **N**etwork **S**imulator Version **2**

QF - **Q**uality **F**actor

RBF - **R**adial **B**asis **F**unction

SVC - **S**upport **V**ector **C**lassifier

VAR- **V**ector **A**uto - **R**egressive

ARIMA - Understanding **A**uto- **R**egressive **I**ntegrated **M**oving **A**verage

IoT - **I**nternet **o**f **T**hings

LPF - **L**ow **P**ass **F**ilters

FCC - **F**ederal **C**ommunication **C**ommission

EIRP - **E**quivalent **I**sotropically **R**adiated **P**ower

ISM - **I**ndustrial, **S**cientific **M**edical

IEEE 802.15.6 - Wireless Body Area Network **WBAN**

TDMA - **T**ime **D**ivision **M**ultiple **A**ccess

OPNET - **Op**timized **N**etwork **E**ngineering **T**ools

CRFID - **C**omputational **R**adio- **F**requency **Id**entification

FDMA - **F**requency **D**ivision **M**ultiple **A**ccess

CDMA - **C**ode **D**ivision **M**ultiple **A**ccess

CSMA - **C**arrier **S**ense **M**ultiple **A**ccess

CSMA-CD - **C**arrier **S**ense **M**ultiple **A**ccess with **C**ollision **D**etection

CSMA-CA - **C**arrier **S**ense **M**ultiple **A**ccess with **C**ollision **A**voidance

WSN - **W**ireless **S**ensor **N**etworks

WPAN - **W**ireless **P**ersonal **A**rea **N**etworks

BT - **Bluet**ooth

ZB - **Z**ig**B**ee

MEA - **M**ulti -**E**lectrode **A**rray

RTS - **R**equest -**T**o -**S**end

CTS - **C**lear -**T**o -**S**end

ACK - **Ack**nowledgement

BFS - **B**readth-**F**irst **S**earch

LAN - **L**ocal **A**rea **N**etwork

WAN - **W**ide **A**rea **N**etwork

NACK - ACK/NACK bits

dEEG - **d**ifferential **E**lectroencaphalo**G**raphy

AIDC - **A**utomatic **I**dentification and **D**ata **C**apture

ERD/ERS- **E**vent-**R**elated**D**esynchronization/ **E**vent-**R**elated**S**ynchronization

SSVEP - **S**teady-**S**tate **V**isually **E**voked **P**otential

TMS - **T**ranscranial **M**agnetic **S**timulation

TES - **T**ranscranial **E**lectrical **S**timulation

TFUS - **T**ranscranial**F**ocused **U**ltra**S**ound

DBS - **D**eep **B**rain **S**timulation

EPCIS - **E**lectronic **P**roduct **C**ode **I**nformation **S**ervice

EPCDS - **E**lectronic **P**roduct **C**ode **D**iscovery **S**ervice

FNS - **F**ood and **N**utrition **S**ervices

.2 Symbols

a distance m

P power W ($\mathrm{J\,s^{-1}}$)

D Dataset

X_i feature set

Y_i label set

B bias term

W weight vector

F_s Set of ranked features which =

R_f Remaining features set = 1,2,3,4,....,N

A Accuracy of k-fold cross validation

T_x Transmission power mW

R_x Receiving power mW

f frequency Hz

e positive threshold value

x_i ith sample of signal

X_i sample observation

u_i ith input vector

b bias

α_i Lagrange multiplier

(x, xi) mapping function

loss function

E_s MSE

y_i^k desired output

e_i^k neural network's output

α learning rate

$E(r)$ expectation error for r samples

C Co-variance matrix

$\mu 1$ mean of class 1

$\mu 2$ mean of class 2

$sin()$ amplitude element of distortion signal

$cos()$ phase element of distortion signal

$|V|$ number of vertices

$|E|$ number of edges

Throughput

$M(t)$ number of full frames

υ Transmission efficiency

ω angular frequency rad